ISBN 978-82-326-1396-0 (printed version)
ISBN 978-82-326-1397-7 (electronic version)
ISSN 1503-8181

NTNU
Norwegian University of
Science and Technology

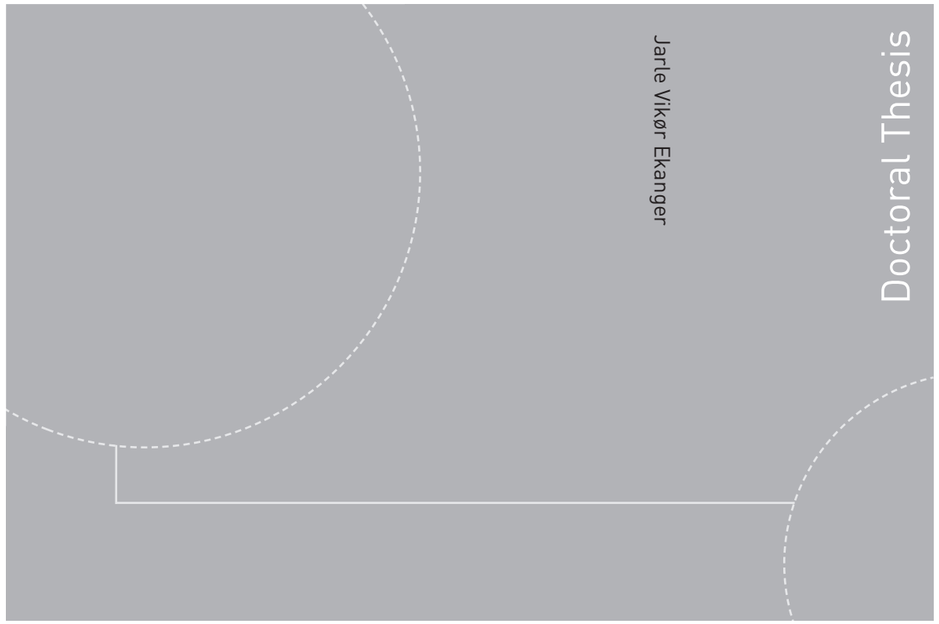

Doctoral theses at NTNU, 2016:26

Jarle Vikør Ekanger

Investigation of the relationship between water quality variations and cavitation occurence in power plants

Doctoral theses at NTNU, 2016:26

NTNU

NTNU
Norwegian University of
Science and Technology
Faculty of Engineering
Science and Technology
Department of Energy and Process Engineering

NTNU
Norwegian University of
Science and Technology

Jarle Vikør Ekanger

Investigation of the relationship between water quality variations and cavitation occurence in power plants

Thesis for the degree of Philosophiae Doctor

Trondheim, January 2016

Norwegian University of Science and Technology
Faculty of Engineering
Science and Technology
Department of Energy and Process Engineering

NTNU
Norwegian University of
Science and Technology

NTNU
Norwegian University of Science and Technology

Thesis for the degree of Philosophiae Doctor

Faculty of Engineering
Science and Technology
Department of Energy and Process Engineering

ISBN 978-82-326-1396-0 (printed version
ISBN 978-82-326-1397-7 (electronic version
ISSN 1503-8181

Doctoral theses at NTNU, 2016:26

Printed by Skipnes Kommunikasjon as

Dedication

For Haldis

Abstract

Lab experiments on clean water samples have revealed that water may withstand large tension; a state which could be explained as negative pressure, without occurrence of cavitation. At the same time, one struggles to design hydro power plants that are less susceptible to cavitation; since it limits the range of operation of the power plant. The author has investigated possible effects of water quality variations on cavitation risk, in order to provide better planning of production limits, as well as documenting cavitation events.

Hydro power production planning is aimed at maximizing revenue earned from the available water resources, and utilize e.g. weather and power consumption predictions to estimate the current value of water versus its future value. Furthermore, maintenance divisions aim to minimize unnecessary wear on the turbine units, to minimize risk of both unexpected down time and necessary maintenance time. Increased knowledge of the effect of water quality on the maintenance cost of operating a power plant has been one of several motivations for this project. As well as providing data on the presumed effect of water quality on cavitation characteristics, the project is expected to provide useful monitoring tools that may be applied for a wider scope of measurements.

The work presented within the thesis consists of experiments in a closed cycle cavitating flow tunnel, as well as long and short term monitoring studies on the medium head Francis turbine at Svorka Power Plant. Methodology is based on and spins further on work done by colleagues in the research group.

Main findings are that dissolved gas content has little effect on cavitation inception, but it alters the characteristics of cavitation when other factors are unchanged. The experiments at Svorka also imply that increased suspended particle content may in fact increase risk of cavitation in the sense that cavitation may occur at higher pressures than in clean water cases.

We have classified the work in this thesis within three main themes:

- Investigate variations of water quality in hydro power plants; across both seasons and due to weather.
- Further development of existing cavitation detection algorithms, with special focus on continuous monitoring.
- Development of hardware-software integration for cavitation detection and recording.

The main contributions are:

- Cavitation monitoring knowledge that is important for further studies, and add provided commercial assets for candidate employer
- Publication of work on measuring and assessing cavitation risk and operation limits in working hydro power plants.
- Increased focus on power plant monitoring, and new advances in less intrusive experimental methods.

Preface

This thesis is submitted to the Norwegian University of Science and Technology (NTNU) for partial fulfillment of the requirements for the degree of philosophiae doctor.

This doctoral work has been performed at the Department of Energy and Process Engineering, NTNU, Trondheim, with Prof. Torbjørn Kristian Nielsen as main supervisor and with co-supervisor Morten Kjeldsen, Dr. Ing.

The thesis was financed by my employer; Flow Design Bureau AS and the Norwegian Research Council through the PhD in Industry program, project number 214814/O30.

Acknowledgements

I was given the opportunity to do the work I am about to present thanks to my employer; Flow Design Bureau AS (FDB), and the Norwegian Research Council, both of whom sponsored the work through the "PhD in Industry" program.

First and foremost I would like to thank my co-supervisor Morten Kjeldsen for the cooperation that has produced this work, and for his trust in me when he gave me a position in Flow Design Bureau AS and the opportunity to do this PhD work.

I would also like to thank Prof. Torbjørn Nielsen, NTNU, for his role as supervisor and facilitator in my dealings with NTNU.

Xavier Escaler, UPC, has been a key support figure in the process of developing a standalone cavitation detection algorithm, and a keen and attentive colleague through work with several articles.

My colleague Håkon Hjort Francke brought me quickly up to par with regards to data acquisition, and has been my go-to-guy in terms of figuring out the software-hardware setups used throughout the experimental work.

Statkraft AS, represented by Erik Jacques Wiborg and Kjell-Tore Fjærvold, has granted us access to the Svorka HPP, allowing us to install the cavitation and water quality monitor, as well as allowing us to perform several cavitation mappings.

Last, but not the least, my wife Haldis has supported me when inspiration fled and helped me to the finish line of this project.

Tank you all!

Contents

List of Tables

List of Figures

Nomenclature

Abbreviations

AoA	Angle of Attack	
FFT	The Fast Fourier Transform (for digitalized signals)	
$NPSH$	Net Positive Suction Height	[m]
[EU]	Engineering Unit - Used were the units of the source is valid for the processed value (e.g. filtered signals)	
BEP	Best Efficiency Point; design load/head of turbine	
DO	Dissolved Oxygen	[PPM]
FDB	Flow Design Bureau AS	
GVO	Guide Vane Opening	[%]
GVO	Guide Vane Opening; a measure of turbine throttling	
SAFL	Saint Anthony Falls Laboratory, University of Minnesota	
TDGP	Total Dissolved Gas Pressure - partial pressure of gas dissolved in a liquid	[Pa]

Constants

α	Angle of attack of a hydrofoil or turbine blade	degrees
σ	Cavitation Number	[1]
j	The imaginary unit	[1]
T_c	Critical Temperature	
T_m	Threshold Temperature, used by Temperley [28]	

Variables

σ_v	Vaporous Cavitation Number	[-]
σ_{Thoma}	Thoma Number; normalization of the NPSH	[-]
dh	Head difference across a hydraulic unit	[m]

h_s	Height of submergence	[m]
h_v	Vapour pressure, converted to meters (of water column)	[m]
h_{atm}	Atmospheric pressure, converted to meters (of water column)	[m]
$NPSH_A$	Available NPSH	[m]
$NPSH_R$	Required NPSH	[m]
$x(t)$	General symbol for a time-variable measurand	[EU]
x_{AE}	The amplitude envelope of x	[EU]
$x_{analytical}$	The complex analytical signal of a real signal x	[EU]
x_{BPF}	A band pass filtered time signal	[EU]
x_{raw}	Raw signal as measured, but having applied calibration correction	[EU]

1

Introduction

Norway's favorable geography has allowed us to cover more or less our entire electrical energy consumption through large hydro power schemes. Eventually we have reached a point where there are no more river systems of significant size open for development. The rate of construction of large hydro power projects has decreased, while small scale hydro power has emerged. Consequently the assignments and challenges one meets in the hydro-power engineering community has also changed. The author was once advised by a senior engineer to avoid the small hydro-power industry if any scientific or innovative ambitions were to be had. The soundness of that advise would, and should, probably be challenged. Nevertheless it was after this the author found that smart refurbishment and optimization are the technological fields that most vividly kindle his engagement. This dissertation concerns the use of water quality measurements, and predictions, as an additional production planning aid, chiefly focusing on prediction of cavitation risk.

Chapter Summary

This first chapter outlines the motivation, context and structure of the scientific work, and provides a reading guide for the following chapters. It is a useful tool to gain an overview of the text, and should be used to quickly locate the sections most useful/interesting to you. It is the author's sincere hope that this text will thoroughly illustrate the potential of condition monitoring, as well as bring new planning tools to the table.

Reading Guide

While a PhD dissertation should be a work of academic excellence it is the author's opinion that the work should also be available to the curious outsider, whose area of expertise might not overlap with hydro-power machinery. Look for *smaller text* that attempts to provide explanations using everyday terms of important phenomenons or topics of this work.

1.1 Work Context

This doctoral work has been possible thanks to cooperative effort between the Norwegian University of Science and Technology; as the degree-awarding institution, Flow Design Bureau AS (FDB); which employs the author, and the Norwegian Research Council's Nærings-PhD-program (PhD in Industry). The program provides the support needed for a business to sponsor one of their employees through a doctoral work. However, the support does not extend to experimental equipment. The experiments were conducted at Saint Anthony Falls Laboratory (SAFL) at the University of Minnesota, and at Svorka HPP in Surnadal. Statkraft AS provided near limitless access to the power plant at Svorka, a courtesy that has been a very valuable contribution to the experimental work.

1.2 Motivation; Research and Personal

It is challenging to ask what can be done with reasonable investments to even more effectively utilize a source of electrical energy that is already effective, clean and flexible compared to other "old renewable" energy sources. What can possibly be gained when turbines are already capable of operating at 95% efficiency? Even factoring in losses in long conduit systems hydro-power converts stored energy to torque/electricity at a far higher efficiency than most other methods. However, one should not forget that large hydro power plants are not without an ecological footprint. Thus, it is eventually in everyone's interest to utilize their potential to the fullest. This can be done by avoiding unfavorable conditions that reduce the efficiency of the turbine, and by minimizing operation time at conditions that accelerate turbine degradation.

Through the work on his project and master theses the author found working with methods which quantitatively describe the condition of flow regimes in hydro-turbine machines inspiring. First by analyzing the nature of swirling flows, and then by evaluating the effects of flow control devices both in simulated and real flows. This spurred his interest in experimental work, which in turn kindled the desire to continue along this track for the doctoral work. The personal hope of the author has been to provide at least the initial steps towards better knowledge of some of the factors that determine the operation restrictions

of hydro-power machinery, to provide better foundation for the higher level considerations that govern the production planning strategies of the power plant owners.

1.2.1 Research Goal and Benefit

The main research is focused towards an assumption of variations in cavitation behavior originating from water quality variations. As will be covered in the next chapter, it is known that presence of microscopic gas bubbles and suspended particles in the water greatly affects inception pressures in controlled experiments. Higher concentrations of gas and particles have proven to ensure cavitation to take place at or near the vapour pressure of the water, while reduced concentrations have proven to significantly increase the tensional strength of the water. Variation of gas and particle content can be logically assumed to occur due both to changing weather and seasons. It is feasible to perform controlled and repeatable experiments in a lab, where the effect of water quality is certain. It has been the aim of the present work to demonstrate the presence of these effects in real applications; here represented by hydraulic turbines, as well as closed loop systems using untreated river water.

Demonstration of these effects during normal operation of turbines provides increased quality definitions of operation restrictions based on real-time (current) conditions. One should expect to be able to set restrictions less strictly in periods of very clean water, but add further restrictions during periods of very bad water quality. One can see a potential for increased flexibility in some periods, and/or achieve reduced cavitation related maintenance. The experiments provide tools that allows a power plant owner to make operation decisions based on currently measured conditions.

1.2.2 Cavitation in Francis Turbines - Background

Cavitation is a phenomenon in water (or any other liquid) that normally occurs when flow-induced reduction of pressure causes the water to start evaporating in to the tiny air bubbles that normally are present in the water. The pressure at which this process starts is called the cavitation inception pressure. Visually, the process would appear relatively similar to boiling, where the bubbles form due to addition of heat. However, unlike most cases of boiling, the bubbles usually experience rapid reentry to regions of higher pressure in which they cannot exist. When that happens the bubbles collapse quickly. Erosion may occur if the bubbles collapse at or near a solid surface.

Cavitation occurs in hydraulic reaction turbines, like the Francis turbine, when adverse flow conditions cause low pressure zones to develop. This is typically related to operation far from the design load of the turbine. Cavitation erosion in the turbine can be found where the cavities left a low pressure zone and collapsed close to the blade surface.

It is well known that developed cavitation has the potential to severely damage hydraulic reaction turbines[1] through pitting and erosion, thus increasing maintenance cost and down time. Furthermore, efficiency loss is associated with reduction of lift on cascaded blades experiencing developed cavitation [11]. At present erosion is most commonly detected by visual inspection of the turbine during maintenance. Cavitation is often audible when one is near the turbine, allowing crude definitions of cavitation conditions in the machine in question. The combination of these methodologies confirms that cavitation erosion has taken place, but does not consistently identify the operation conditions at which it occurred. This must be contributed to the knowledge that the intensity must reach a normally unknown threshold for erosion to occur. Evidently detailed knowledge of when and under what conditions cavitation takes place is of high value. At the initiation of this thesis, the author had only been able to find documented examples of one-day experiment type mappings of a turbine's cavitation behavior. Such methods are presented by e.g. Escaler [13] and Bajic [7].

It has been the intention of the work described herein to supply additional information through long term experiments in order to detect changes in cavitation behavior affected by such variable quantities as power plant head[2] and water quality properties. Herein the most novel theme is monitoring water properties, or water quality as it is commonly termed. Water quality in the current context is introduced in chapter 1.2.3, below.

1.2.3 Water as a Medium for Cavitation

Water Quality is a term that is being used across a wide variety of scientific fields that relate to water in some way or other, to describe the physical properties of the water that is important within that field. Just consider the different requirements of water being used in food, and water being used to mix concrete. In the context of cavitation it has been found, in laboratory experiments, that content of microscopic gas bubbles and solid matter particles affects the cavitation inception pressure.

It is a routine design feature to submerge the turbine below the tail race water level to provide sufficient back-pressure to prevent cavitation. One choses submergence level such that the added pressure and the atmospheric pressure ensure sufficient absolute pressure in the runner outlet, i.e. static pressure that is higher than the inception pressure. It is commonly assumed that cavitation inception occurs at the vapour pressure of water [10]. Were one to consult reports from controlled laboratory experiments investigating inception pressures one would find that this is not the case; extensive research has been performed in this field and is summarized by e.g. Trevena [29]. On the contrary, it is found that the tensional strength of water, i.e. its ability to withstand low pressure without cavitation, is strongly affected by the water quality, which in this context is presumed to

[1] A particular problem in the Francis turbine, due to its fixed geometry.

[2] A typical power plant in Norway might experience significant variation in head as reservoir levels rise and sink.

be characterized mainly by presence of microscopic water bubbles and solid matter particles in the water sample. It has been shown that sufficiently clean water samples exhibit considerable tensional strength, i.e. a pressure well below the vapour pressure is required for cavitation to take place. One has to conclude that the vapour pressure of water is in fact the highest pressure at which cavitation can occur. From this arises the question whether the laboratory experience is valid in field applications, or if the vapor pressure assumption is always valid in the hydro-power context. It is our belief that complex upstream water sources, which include both reservoirs and creek intakes, renders variations of water quality possible, either as seasonal or weather induced variations. Such complex water ways are commonly found in Norwegian hydro-power schemes. It is not uncommon that a power plant's catchment area not only collects water in large reservoirs, but in periods of high precipitation feeds water directly into the head race tunnel through so-called creek intakes. Such intakes are characterized by funneling river/creek surface flows directly in to the tunnel or piping system, without any form of settling basin. Logically, one must expect that the amount of particulate matter and free gas in such flows is higher than that of flows from (more) settled reservoirs.

1.3 Research Topics

Research Topic 1: The relationship between water quality and cavitation inception has been extensively studied in laboratory experiments, as can seen in e.g. Trevena [29] or Mørch [24]. The general observation in these studies is that water quality, quantified by the presence of so-called cavitation nuclei, has a significant impact on the inception pressure of cavitation bubbles. In fact it is common to use the term tensional strength because the water is able to withstand tension (pressures below zero), if sufficiently cleaned from what is generically called cavitation nuclei. These are foreign bodies in the water; either small, rough particles, or microscopic gas bubbles, that provide a phase boundary at which evaporation can occur, thus allowing vapour cavities to form. Given that studies of the nature mentioned above routinely use filtering of ordinary tap water to achieve large variations in tensional strength, there is reason to investigate if the same observations can be made during presumed variations of the same type found in production water at hydro power plants.

Furthermore it is evident that water quality must vary due to seasonal changes and weather conditions in the power plant water system. To be able to determine the nature of the variation, an experimental setup that samples the water and quantifies the water quality needs to be designed, tested and utilized in parallel with a cavitation detection scheme (see RT2).

Summary: Investigate variations of water quality in hydro power plants; across both seasons and due to weather.

Research Topic 2: The trivial solution to cavitation erosion detection is visual inspection during maintenance. This is probably the most common method today. It holds merit as a late-stage maintenance planning observation, and confirms or disproves suspected cavitation erosion. Using experience, audibly detecting cavitation, and frequently inspecting the runner, one can postulate under which conditions the cavitation takes place. However it is hard to estimate variations of intensity at the various operating conditions, which is necessary to more accurately pinpoint conditions that cause harmful cavitation. Methods have been developed by e.g. Xavier Escaler [13] and Branko Bajic[7] to accurately describe the cavitation behavior of a turbine. To achieve the goals of the current project, the methods needs to be further developed to allow continuous monitoring of cavitation activity in a turbine for an extended (e.g. a year) period of time. One would thus need to forfeit some of the details of the raw data that is normally acquired for cavitation diagnostics, in order to store continuously generated results from a properly designed analysis algorithm.

An existing academic relationship to Xavier Escaler caused his work to be most influential to the algorithm development herein. The method utilizes knowledge of the main hydrodynamic frequencies of the machine, to identify cavitation signatures in measured vibrations and acoustic emissions. At the initiation of this doctoral work it was however heavily based on post-processing and "manual" analysis of the measurements. It has been

a goal to use the experimental work herein to develop an algorithm based on Escaler's work, that does not require manual intervention, but still provides reliable data. Accordingly, time was, and will, be invested in developing an autonomous hardware-software system capable of recording and analyzing measurements, and store results, for extended periods of time without supervision.

Summary: Further development of existing cavitation detection algortihms, with special focus on continuous monitoring.

Research Topic 3: By properly addressing Research Topic 1 and Research Topic 2 one will be in a position to investigate effects of water quality variations on turbine cavitation characteristics. Water quality monitoring, and prediction, could then become an interesting tool during production planning, allowing the power plant owner to actively take cavitation damage into account. While it is expected that the most interesting results will originate from this topic it is clear that initial efforts will also contain significant character of product development, which could cause the total data record to be smaller than the time alloted would imply.

Summary: Development of hardware-software integration for cavitation detection and recording.

Additional Topics: Confirmation of the postulations of the research topics imply added factors in production planning, that may increase or release operation restrictions. Opportunity to operate at previously restricted loads may emerge. However, this could require a flexibility in power production that is not necessarily available. It is therefore interesting to use the tools developed to evaluate the cavitation mitigation abilities of various flow control technologies. In particular, a draft tube water injection system designed to reduce flow effects of part load operation, will be evaluated.

1.3.1 Research Design

The work has been focused around a string of partial goals, with the aim of answering Research Topic 1 and Research Topic 2. These partial goals have been chosen in order to successfully migrate the cavitation inception research from laboratory environments to prototype hydro turbines. Eventually[3] the work should provide a tool that predicts cavitation risk as well as recording actual cavitation activity. The work flow has been as follows:

1. Experiments in closed-loop cavitation tunnel, with gradual de-gassing through cavitation, to familiarize with analysis methods.

2. Field measurements for mapping of cavitation characteristics of a Francis turbine.

[3]Given the nature of the PhD in Industry-program the author expects to be able to continue his work in this field as part of his duties to his employer, FDB AS.

3. Field measurements to identify effect of draft water injection on cavitation characteristics of a Francis turbine.
4. Experiments in closed-loop cavitation tunnel, with active degassing through misting in vacuum pipe, to build on results from point one.
5. Continuous monitoring of cavitation activity in Francis turbine over a period of 8 months.

1.4 Publication of work

Results and a full discussion of the work is presented within the scope of this dissertation. Additionally articles and conference papers that has been produced during the work are attached in the appendix. A short chronological summary of published articles and conference papers follows below.

Co1	*Jarle Vikør Ekanger, et al: "Cavitation Intensity Measured on a NACA0015 Hydrofoil with Various Gas Contents", Proceedings of the 8th International Symposium on Cavitation, Abstract No. 265, Singapore, 2012* **Relevance to this thesis:** Investigation of the effect of gas and particle content in water on the intensity of cavitation vibration on a hydrofoil in a high speed water tunnel. The experiments were performed in the lab at SAFL[4], but using water tapped directly from the Mississippi River. It was found that air content mainly had an effect on transitions between types of developed cavitation. **My contribution:** I personally executed the experiments, in cooperation with Morten Kjeldsen. I performed all post-processing as well as writing the conference article, while receiving feedback from Xavier Escaler.

[4]St. Anthony Falls Laboratory, University of Minnesota, Minneapolis, USA

P1	*Xavier Escaler; Jarle Vikør Ekanger; Morten Kjeldsen; et al: "Experimental Investigation of Draft Tube Surge and Erosive Blade Cavitation in a Full Scale Francis Turbine", Journal of Fluids Engineering, Proceedings of the ASME, Vol. 137, January 2015* **Relevance to this thesis:** In this experiment we mapped the cavitation behavior of the (full scale) Francis runner at Svorka Kraftverk, near Surnadal, Norway. The paper demonstrates how a complete cavitation mapping of a turbine is performed, and has been invaluable in the parametrization of the algorithm. **My contribution:** I was i charge of the measurements at the power plant, and contributed to the post-processing of the data, as well as the article sections describing the palnt and the experimental setup. I also contributed to the discussion and conclusion.
P2	*Jarle Vikør Ekanger; Xavier Escaler; Morten Kjeldsen; et al: "Influence of Draft Tube Flow Control System on Cavitation Behavior in a Medium Pressure Francis Turbine", Submitted for Cavitation 2015 (Lausanne), 2015* **Relevance to this thesis:** The cavitation mapping methodology described in P1 is used to investigate the impact of a draft tube flow control mechanism installed at Svorka Kraftverk on the cavitation behavior of the turbine. Algorithms with potential for autonomous operation are employed to investigate if the cavitation intensity is mitigated by the flow control mechanism. **My contribution:** I was in charge of the cavitation detection measurements during this experiment. I also performed the post-processing of the collected data and wrote the full first draft of the paper. Finalization of the paper was done in cooperation with Morten Kjeldsen and Xavier Escaler.
P3	*Jarle Vikør Ekanger, Morten Kjeldsen, Roger Arndt, et al: "Experimental investigation of dissolved oxygen and turbidity influence on cavitation inception, intensity and super cavitation inception on a NACA0015 hydrofoil", "In progress", 2015-2016* **Relevance to this thesis:** Intended to compensate for reduced amount of field measurements, compared to original plan. Improved instrumentation compared to experiments referenced in C1. **My contribution:** I executed experiments, did post-processing and analysis, and drafted the paper.

Table 1.1: *Overview of publications during the doctoral work, their relevance to the research, and my contributions to each of them.*

1.5 Contributions

A list of contributions to the thesis work:

1. Collecting and analyzing data for Co1, as well as writing and presenting conference paper. Experiments at SAFL in November 2011.
2. Collecting data and parallel analysis of data for P1. Writing first part of article, contributing to discussion and conclusion.
3. Performing data collection and analysis for P2. Writing first draft of paper.
4. Development of autonomous data collection and analysis hardware system. Installed for continuous monitoring at Svorka HPP.
5. Post-processing of results from C4, which is published within the thesis.

1.6 Thesis Structure

The orientation on state of the art in chapter 2 is for practical reasons split into two sections, of which the first will concern cavitation and tensional strength in water, and the current understanding of the impact of water quality on cavitation. The second section covers cavitation in hydraulic turbines and detection of said cavitation.

Furthermore, chapter 3 covers the different experimental methods employed when data was collected, and the compromises which had to be made before setting up equipment to continuously monitor a process over a long period. As a result the analysis methods concerning cavitation detection will be discussed.

Chapters 4, 5 and 6 will finally conclude the thesis, by respectively presenting results, discussion of the findings and provide some conclusions.

It has been a goal to publish articles/papers on most of the results provided by the experiments. However, a thorough discussion of the individual and collective results of this work will be provided within the thesis. Additionally, the results of the long-term continuous monitoring effort is initially only published here. This is intended to draw the long lines that can be found in the sum of the experimental work.

2

Scientific Foundation for this Work

Chapter Summary

The existing scientific foundation for the present work is detailed in this chapter. The reader will find references and introductions to tensile strength of water, cavitation nuclei, cavitation in hydraulic machinery, cavitation detection methods and some insights in to the previous work by scientists within the author's work group.

Cavitation in water is a phenomenon that is encountered in many situations. It is a common factor to consider when designing hydraulic turbines and pumps, and is also often encountered in marine propellers. However one can logically argue that fluid conditions, which is termed water quality in this work, might also affect cavitation inception and intensity. For instance, Alfayez [2] writes:

> It is generally accepted that the critical pressure for inception of cavitation is not constant and varies with operation fluid physical properties and the surface roughness of the hydraulic equipment.

Indeed, Ceccio and Brennen [27] and e.g. Keller [17] reports to have found a significant reduction of the cavitation number at inception of cavitation on test specimens in a water tunnel after de-aeration.

Trevena [29] draws the historical overview of scientific interest in tension of liquids. From the Bernoulli equation, the relation between pressure and velocity that was in fact first derived by Leonhard Euler, one found that a liquid could be subject to negative pressures and possibly fracture. Initial experiments were performed by Donny (1846), using a U-tube filled with sulphuric acid. It is pointed out that although the tension achieved was merely 25kPa, Donny introduced important terms: the cohesion between individual molecules

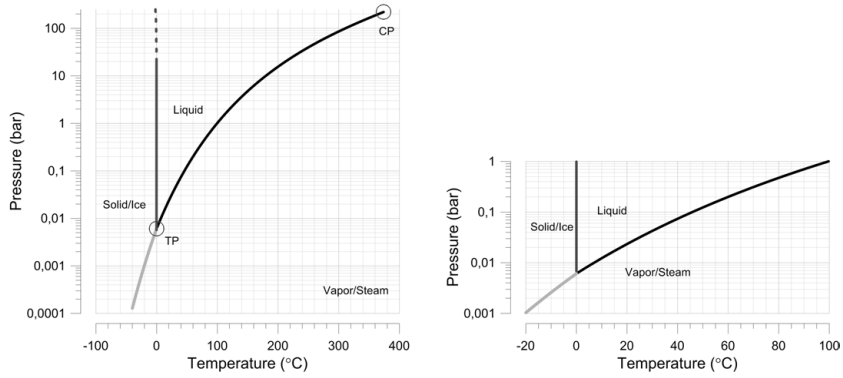

Figure 2.1: *The phase diagram is useful to aid understanding the concept of tension in water. On the left is a wide view of the three phases of water, while the area of interest around the triple point is highlighted to the right. In events of cavitation the liquid water is de-pressurized and cavitation takes place when the state enters the vapor domain. The case-in-point of water exhibiting tensile strength is that with the right conditions pressure and temperature will place the water in the vapor phase of the diagram, when the water is in fact still a liquid. In cases of extreme tensile strength of water, the pressure is reduced below zero and enters a state in which vapor is an incomprehensible state. This metastable phase occurs when the physical conditions does not allow water vapor to form, e.g. when there is no gas phase for the vapor to form in.*

and adhesion between the liquid and container wall. Donny was also the first to report that the amount of dissolved gas in the fluid affected the attainable negative pressure level. Berthelot (1850) used a sealed tube, now known as a Berthelot-tube, to achieve tension of several tens of bars. Reynolds then demonstrated cavitation in a throttled glass tube connected to a water tap. Later, Parsons (1895) pioneered propeller cavitation by building a closed-loop water tunnel, in which the static pressure could be artificially reduced.

2.1 Tensile Strength of Water and the Effect of Cavitation Nuclei

Consider a phase diagram illustrating the liquid's state as a function of temperature and pressure, fig. 2.1. As is well known, it is possible to cross the liquid-vapor phase boundary while still keeping either pressure or temperature constant. The prior is of course boiling, and not relevant here, whereas the latter consists of two forms of vaporisation. The most commonly known of the two is vaporisation across a flat boundary, which finally leaves cavitation; where vapor cavities expand (and implode) within the liquid body.

Applying tensile stress to water potentially puts it in a metastable phase[1] in which the pressure and temperature is such that it should be in a vaporous state, but it remains liquid

[1]The tensioned state is in many ways similar to superheating, also a metastable phase. Superheating is however perhaps better known, and a search for "superheated water explosion" on Youtube would readily provide examples of the effects of disrupting the metastability.

[29]. The tension required to achieve vaporization of the liquid is consequently termed the tensile strength of that water sample.

Theoretical investigations have been used to complement the experimental work associated with determining the tensional strength of water. Temperley [28] used the van der Waals equations to show that a liquid at temperature below the threshold temperature T_m, defined by

$$T_m = \frac{27T_c}{32} \tag{2.1}$$

, where T_c is the critical temperature, is theoretically capable of withstanding tension. Temperley reports that $T_m = 270\,^{\circ}\mathrm{C}$ for water. Using proper values for the van der Waals constants, Temperley estimated the theoretical tensional strength of water to be between 500 and 1000 bar. Furthermore, Trevena reports that Fürth [16] and Fisher [14] found the theoretical values to be 3000bar and 1300bar respectively.

It is evident that there is a large discrepancy when comparing theoretical values of tensional strength to experimental values, as well when more recent experiments; Andersen and Mørch [3], are considered. Andersen and Mørch used ordinary tap water in a device that focuses a tensile stress wave from a curved surface to induce cavitation in the bulk of water. Mean values in the order of one third of a bar illustrates that ordinary water does not compare to the idealized water of the theoretical models. This discrepancy is attributed to presence of what is known as *cavitation nuclei*. The apparatus developed by Andersen and Mørch focuses a tensile wave in the focal point of a parabolic surface, and the tensional strength is calculated from observations of bubble growth rates based off a high speed camera.

The large discrepancy is strong evidence that real world applications are affected by more factors than those belonging to the water itself. It is easy to assume that the cavitation bubbles come into being by tearing apart the liquid, and thus forming a cavity within it. However, one needs to consider that breaking the bonds that exist between neighboring molecules in a liquid requires a significant amount of work. It is indeed pointed out by Trevena [29] and others it is very unlikely that the formation of a cavitation bubble actually involves the creation of such a liquid-vapor interface within the liquid. There is a common consensus that presence of a gas bubble is required, as it provides the necessary phase boundary. These bubbles are commonly referred to as cavitation nuclei.

The internal pressure of a bubble is slightly higher than in the surrounding liquid, due to the surface tension. As a result, a bubble that does not rise to a surface and disappear would quickly dissolve in to the liquid. Consequently, it has been a concern of scientist to explain the persistence of cavitation nuclei in water. Fox and Herzfeld [15] suggested that bubbles are stabilized by an organic skin that hinders diffusion when the bubbles have become sufficiently small, thus rendering persistent presence of cavitation nuclei possible. The concept of bubble skins has also been addressed by Yount [31], who proposed that skins consist of surface active particles and are initially permeable. Yount reports to have found that a rapid increase of static pressure renders the skins impermeable and thus stabilizes the bubbles. Additionally, there are many who support the idea of gas cavities

trapped in crevices in either particles suspended in the free-stream or in walls. When such gas pockets are subjected to negative pressures, bubbles may break free and enter the free stream. See e.g. [24].

Considering first the skin theory, one sees that the prerequisites are "large" air bubbles and presence of organic matter that could adhere to the bubble boundary. Even assuming that the initial bubble is not entirely covered by organic particles, it is evident that diffusion would eventually lead to a situation were the organic matter covers the entire bubble. At this point the bubble skin is presumed impermeable to gas, and thus rendered stable. Subsequent exposure to tension will tear the skin apart and allow water to vaporize in to the bubble, causing cavitation. Note that the matter forming the skin must be of a kind that does not dissolve in the liquid [29].

In concave recessions and crevices surface tension tends to oppose diffusion of the gas pocket, unless very large pressures are applied for extended periods. Trevena reports that it is "common knowledge" that applying pressures in the order of 1000 bar for periods of at least 30 minutes has a prolonged effect in allowing the liquid to withstand higher tension than normally. When gas pockets are subjected to pressure from the liquid side, gas may diffuse and subsequently a higher tension is required to "pull" the bubble interface out of the crevice. Thus prolonged existence of cavitation nuclei is ensured.

2.2 Cavitation and Water Quality in Hydraulic Machinery

Water Quality

Water quality is a term that is implicitly or explicitly important within a wide range of scientific fields. It is a common term that denotes all qualities or properties one could ascribe to water, that each may have varying importance within a field. In the current setting one would employ the term to describe cavitation nuclei concentrations, as well particle content (which we have seen is tightly linked to nuclei concentration).

It is common to refer to cavitation erosion simply as cavitation, which leaves out that cavitation can take place without causing erosion. An example is cavitating draft tube flows, and cavitation that is not sufficiently intense to cause metal fatigue and erosion. So, while erosion is a visible detrimental effect of cavitation, there are others that could be as costly. However, all cavitation problems in a reaction turbine will normally be related to far-from-design operation of the machinery.

2.2.1 Characteristics of Cavitation in Hydraulic Machinery

Escaler et al [13] gives a good introduction to the concept of cavitation in hydro turbines. While the basic phenomenon; formation of gas cavities caused by sufficient reduction of dynamic pressure, is the same in real and ideal laboratory situations, some added characteristics needs to be mentioned with regard to cavitation in turbines. Because the cavitation takes place in a moving flow, cavitation bubbles may experience mitigation by re-entry to high pressure zones, and thus collapse. The effect of the cavity collapse is dependent on the location in which it happens. While some modes of cavitation often cause bubble collapse to occur at the machine surface and thus cause (risk of) pitting, cavitation may also occur in the free stream where the collapse is not erosive.

Bubbles traveling freely in the flow or on the blade surface are normally not associated with erosion, and will collapse when encountering adverse pressure gradients. This is normally associated with insufficient available submergence of the turbine.

More aggressive forms of cavitation are found to be attached to walls in the flow, e.g. cavitation attached to the turbine leading edge. Several mechanisms may occur, ranging from stable and clear sheet cavitation that steadily sheds vortices with relatively small impact energies associated. An unstable form with turbulent cavity interfaces, known as cloud cavitation, is known to hold more erosive potential. This is caused by the unsteady cavity, with aperiodic shedding.

Inter-blade vortex cavitation occur when vortices caused by varying incidence angle across the leading edge cause rotation of the flow. The vortices may attach to the blade-to-crown intersection. This kind of cavitation is mainly occurring in the free stream, but may cause erosion if the vortex tip hits the blade. At full load, the vortex cavitation may also cause strong vibration.

$NPSH$ - Net Positive Suction Head - is a commonly used term, when discussing cavitation in hydraulic machinery. In terms of engineering applications it is also common to distinguish between available and required suction head; $NPSH_A$ and $NPSH_R$, where

$$NPSH_A = h_s + h_{atm} - h_v[mWc] \tag{2.2}$$

describes the available suction height, caused by the submergence h_s, the atmospheric pressure h_{atm} and the vapour pressure h_v, i.e. plant specific parameters. Design of machinery, including brand, rim-speed and number of blades, as well as operation point, determine the required NPSH to avoid cavitation. One can easily see that $NPSH_A \geq NPSH_R$ must be fulfilled to achieve cavitation free conditions. When scaling this measure, e.g. for model testing, it is common to use the Thoma number;

$$\sigma_{Thoma} = \frac{NPSH}{dh} \tag{2.3}$$

using dh for the head difference across the machine.

One sees that the $NPSH_A$ is representing the local absolute pressure availability at the runner outlet, furthermore the vaporous cavitation number;

$$\sigma_v = \frac{P_{local} - P_v}{0.5 \cdot \rho \cdot U^2} \tag{2.4}$$

is used in cavitation tunnel experiments such as the herein described SAFL experiments. Its usefulness in conjunction with $NPSH$ and Thoma numbers is clear. The use of these dimensionless numbers allow us to compare relatively simple laboratory experiments to hydraulic machinery flows.

See also e.g. [20].

2.2.2 Expected Effect of Water Quality

It is stated in chapter 2.1 that proper degassing and filtering increases the tensile strength of water considerably, thus cavitation is less likely to happen. However, it should also be questioned whether water quality affects the severity of cavitation after inception. Amblard et al [6] reports to have investigated the effect of dissolved air on cavitation erosion, and have found that the saturation level had no effect on the erosion intensity of attached sheet cavities in a venturi nozzle. This result is attributed to the volume of entrained air in the cavities being negligible. However, the authors point out the obvious "bias" of the experiment. IF the experiment had been designed with a longer zone of relatively low pressure upstream from the nozzle, the authors expect the results would be different. It is pointed out that the level of free, not the total or dissolved, gas content at the point of cavitation is the key factor.

2.2.3 Characteristics of Cavitation Vibrations

Cavitation bubble implosions induce high frequency vibrations in the runner, in nature associated with the natural frequencies of the runner/shaft assembly [13]. However, due to rotor-stator interaction (RSI) the cavitation intensity may fluctuate at the hydrodynamic frequencies associated with the RSI. Consequently one often observes amplitude modulation of cavitation at the guide vane passing frequency on the runner, and on the blade passing frequency in the wicket gate.

2.3 Non-Intrusive Detection of Cavitation in Hydraulic Machines

Non-intrusive cavitation detection in reaction turbines has been described by e.g. Escaler [13] and Bajic [7]. The various methods have in common that they employ sensors that do

not intrude on the flow, and thus do not physically affect the flow. Instead, one measures vibrations that are secondary effects of cavitation bubble collapse. As shown in chapter 2.2.1, cavitation takes place in well known zones in the turbine machinery. This is exploited when one aims to detect signs of cavitation in the machine. While the cavitation takes place in inaccessible places, the induced vibrations propagate to more accessible areas. Escaler [13] reports four likely points of access, which through correspondence and collective work with the author has been determined to be in the following prioritized order:

1. The turbine shaft
2. The turbine shaft's guide bearing pedestal
3. The guide vane shafts
4. The draft tube wall (esp. for cavitating draft tube flow)

Likewise, Bajic [7] reports to have instrumented all 20 guide vane shafts of a 17MW double-runner Francis turbine, covering the frequency range from the runner frequency and up to 1 MHz. He also points out in [8] that such resource-heavy experiments are important to provide spatial/angular resolution to the measurements. Contrary to the practices of Escaler and Bajic, Rus [25] reports to have performed measurements in a Kaplan test rig, mounting acoustic emission sensors and high frequency accelerometers on the draft tube inlet flange only. In his experiments, the only sensor associated with the turbine shaft was a trigger for the imaging system. The authors provide various detail levels about instrumentation, but emphasize on use of high frequency accelerometers (high cut-off range varies from 15kHz to 25kHz) as well as acoustic emission sensors (ranges 50kHz to 1000kHz) to record (cavitation induced) vibrations in the turbine. The author notes that physical restraints on pivoted-mass accelerometers reduce their sensitivity as the frequency range is increased.

It is also noticeable that use of dynamic pressure measurements are widely employed to detect draft tube cavitation swirls, which are commonly expected at part load and full load. E.g. Francke [19] has worked extensively with this topic, and Escaler reports to have used pressure measurements in conjunction with vibration measurements.

2.3.1 Analysis Methods

Frequency Content

It has been observed, and widely utilized for detection, that cavitation causes increased energy levels in certain high frequency bands of the recorded vibration. Escaler [13] does not explicitly mention a range, only that high frequency content is important. Range is increased by complementing vibration measurements with acoustic emission measurements. This is supported by Bajic in [8], who however also points out that the frequency

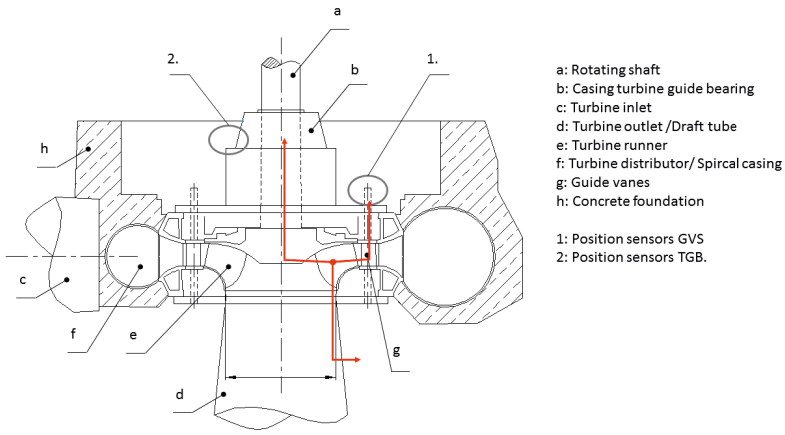

Figure 2.2: *Vibrations induced by cavitation may propagate through the machinery to surface points where it may be measured. These propagation routes include through the shaft and shaft bearing to the shaft bearing pedestal, through seals to the guide vane shaft bearings and through seals to the draft tube flange and draft tube. Also indicated in the figure are two possible sensor mounting positions, both of which were used during the experiments reported here.*

range to investigate must be selected carefully. It is a prime argument from Bajic that different cavitation mechanisms, here interpreted as types or forms of cavitation, has different characteristics. Thus, investigation of several frequency ranges is necessary to cover the possible forms of cavitation present in the turbine. Bajic propose use of total power and total spectrum of the vibro-acoustic signals to counter this problem. It is the observation of the author that the continuously increasing computing power available in PLC equipment allows the scientist to check several frequency bands, and thus be able to write algorithms that identify the frequency characteristics of several cavitation mechanisms.

Amplitude Demodulation

Modulated cavitation is identified using a method called amplitude demodulation, in which an amplitude envelope is determined and subsequently subjected to a frequency analysis. From this point, it is a matter of investigating vibration modulation levels at the known RSI frequencies; namely the blade passing frequency, guide vane passing frequency and the runner frequency. The validity of the amplitude demodulation method seems sound. It has been successfully employed by Escaler [13], however Bajic [8][9] reports examples of severe cavitation erosion with no blade passing frequency modulated vibrations. It seems as such that the method holds good merit, but is not universally valid as a cavitation detector.

To retrieve the amplitude envelope of the (presumed) amplitude modulated cavitation induced vibrations that was measured, one first needs to find the analytical signal of the

filtered raw signal.

$$x_{analytical}(t) = x_{BPF}(t) + j \cdot Hilbert(x_{BPF}(t)) \tag{2.5}$$

The Hilbert transform is defined as follows [13]:

$$Hilbert(x(t)) = \frac{a}{\pi} \int_{-\infty}^{\infty} x(\tau) \frac{1}{t-\tau} d\tau \tag{2.6}$$

Mathematically, the Hilbert transform may be determined using Fourier transformation. This is documented e.g. in the documentation of the native LabVIEW Hilbert transform function. The Hilbert transform of a signal $X(t)$ is may be determined by:

1. Forward FFT
2. Setting DC component and Nyquist component to zero.
3. Multiplying positive harmonics by $-j$ and negative harmonics by j.
4. Reverse FFT

Finally, the amplitude envelope is determined by determining the absolute value of the analytical signal. One obtains a curve that envelopes the original signal at its amplitude maxima, thus describing the amplitude variation of the signal.

$$x_{AE}(t) = \left| x_{analytical}(t) \right| \tag{2.7}$$

Escaler reports to have averaged the auto-power specta of several consecutive amplitude envelopes to amplify the signs of cavitation. It is also pointed out that by synchronizing the signals with respect to the angular position of the shaft a better demodulation can be achieved while reducing data storage requirements. The concept is further elaborated by Bajic in [7] and [8], who reports use of high spatial resolution and angular synchronization has allowed detection of specific runner blade-guide vane pairs that exhibit higher levels of cavitation.

2.3.2 Sensor Position Effects

Bajic [8] emphasizes importance of spatial resolution of measurements. Specifically, it is proposed that measuring vibrations at several angular positions around the turbine has proven to return large variations in recorded noise and modulation levels. Additionally, it becomes possible to determine specific blade-guide vane pairs that experience cavitation. These techniques are said to allow earlier detection of cavitation caused by machine degradation.

2.4 Determination of Water Quality

The quality of water that we consider in this context is its ability to withstand cavitation inducing forces; its tensional strength. Furthermore it has been established that presence of cavitation nuclei adversely affects the tensional strength of water (which is otherwise, i.e. under ideal conditions, found to be considerable). Thus the water quality parameter relevant is argued to be the presence of both particulates and dissolved air/gas in the water. In the context of field measurements the challenge is to obtain high quality data of said parameters.

2.4.1 Cavitation Nuclei Content

The Springer Handbook of Experimental Fluid Mechanics[1] describes several ways to quantify the cavitation nuclei in a flow. Using the description of cavitation nuclei from chapter 2.1 one can also easily form a clear picture of what needs to be quantified. Ideally, one should determine the quantity and size distribution of the nuclei, as well as distinguishing between bubbles and particles. The simplest approach simply involves careful analysis of a correctly lit photo of the flow cross section. While this method is dependable it is neither efficient nor easily implemented in practical conduit flows. O'Hern [**?**] is reported to have successfully examined oceanic waters using a holographic imaging approach, but this method is also suffering from large work requirements before any useful information is available. It is further mentioned that Keller [18] used scattering of laser light to determine size and incidence rate of particles in a passing flow. This method is interesting because it demonstrates that monitoring secondary effects of phenomena, in this case the scattering of light, can be used to quantify them. Knowing natural water flows, one recognizes the light scattering when considering the varying opacity of water stemming from e.g. addition of particulate matter. Additionally the Handbook refers to work using phase Doppler anemometry to accurately determine flow velocity and additionally the size of the particles that provide the measurement.

It is noted that the non-imaging methods all utilize scattering of light by the particles entrained in the flow for determination of particle quantities and size distributions. They are not capable of distinguishing solid matter from gas bubbles. By use of lasers one manages to add information about nuclei size, but is only capable of sampling a small cross section of the flow. The general quantification of opacity is however called turbidity. Turbidity can be linked to commonly comprehensible terms, such as Secchi depth[2]. In terms of solid matter content, these methods could hardly be expected to distinguish between particles that carry air in crevices and bio-particles that could be expected to manipulate the surface tension characteristics of bubbles. However, a general measure of turbidity appears to provide an indication of the content of cavitation enhancing matter in the flow, and is readily measurable using light scattering analysis.

[2](No.) Siktedyp

2.4.2 Gas Content

The Springer Handbook [1] also contains a comprehensive summary of work on gas content measurements. Notwithstanding the issues raised by its use of mercury, the van Slyke apparatus is found to be accurate, "quick" and easy to use. It uses cavitation and a Torricelian vacuum to extract the dissolved gas from a water sample, and subsequently measure the pressure of the released gas thus producing the total dissolved gas pressure of the sample. The vapor pressure is corrected for using a known relation. The process is manual, or at best expensive to automate. In fact, [1] reports that modernized versions (by e.g. Brandt, or Heller)are not widely used or known outside their labs of origin. For the purposes of the current context one would most likely have to resort to other methods to determine gas content. The effort to replace the mercury-dependent van Slyke meter has resulted in widespread use of dissolved oxygen measurement as an indicator of total gas/air content. DO probes are based on oxygen permeable membranes and electrolytic reactions, and regularly require maintenance and calibration. The term indication is used to emphasize the point that exchange rates and dissolution ratios are different in air and water. E.g. the relationship between DO and dissolved nitrogen in water and air is not the same. Oxygen is of course also more likely to be consumed in processes in the waterway than nitrogen. However, seeing that DO measurements are used in laboratory environments, it is relatively safe to argue that DO probes are also the most likely candidate in engineering applications.

2.5 Relation to Previous Work in the Research Group

The research group includes the supervisors and the contributing collaborators in relevant projects. The following is a summary of related work by members of my research group that lead up to the present efforts.

Kjeldsen's interest in water quality was originally kindled by a newspaper article concerning DynoSpheres, also known as "Ugelstadkuler", in Adresseavisen. The production technique is such that extremely narrow size distributions are possible even for sub-micron sized particles. The article also revealed that there existed a possibility of controlling the wetting properties of the sphere surface. With the knowledge that the hydrophilic properties of surfaces is an important parameter in cavitation inception Kjeldsen launched a project, as part of a larger project at Sintef/NTNU and funded by the Norwegian Research Council. The project also included Andreas Keller at the Versuchsanstalt fur Wasserbau, TUM and Knud Aage Mørch, DTU. Keller used a vortex nozzle for determining cavitation tensile strength, the device ensuring a minimum pressure in the bulk of the fluid and not at the bounding walls. Professor Mørch contributed with solid-liquid interface physics considerations. Mørch's approach of the highest relevance as SEM photographies made at DTU revealed that the spheres had a very homogeneous topology. Eventually Marschall, a student at TUM, completed a number of studies revealing that physics

at interfaces explained the experienced cavitation. The work was published Physics of Fluids by Marschall et al [22].

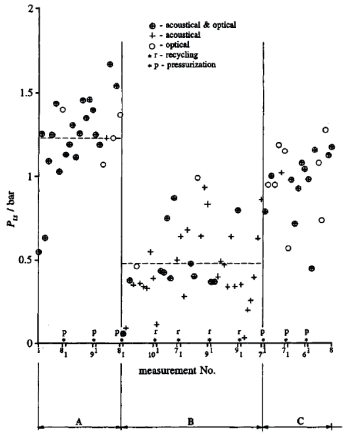

FIG. 8. Measurements of tensile strength P_{th} made with the 76-μm-diam EXP-SS-78.1-RXG/71 Dynospheres. (A) Filtration to clear the water of particles. (B) Recycling of water containing Dynospheres. (C) Filtration to clear the water of particles.

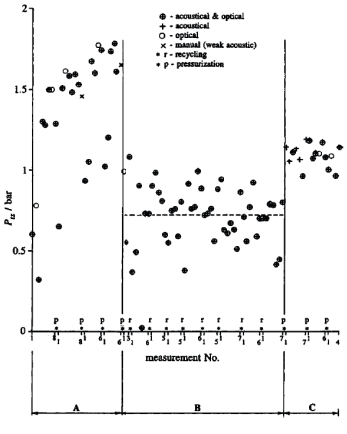

FIG. 9. Measurements of tensile strength P_{th} made with the 20-μm-diam EXP-SS-20.3-RXG Dynospheres. (A) Filtration to clear the water of particles. (B) Recycling of water containing Dynospheres. (C) Filtration to clear the water of particles.

Figure 2.3: *Facsimile from Marschall et al [22], illustrating the effect of particles on the tensional strength of water. Both graphs show chronologically sorted tests, in which the middle section had Dynospheres added to otherwise filtered water.*

Kjeldsen participated with Professor Roger Arndt, the primary researcher at St. Anthony Falls Laboratory, UMN, in work on shedding dynamics from cavitating hydrofoils. Extensive observations, using different imaging technologies, revealed that the hydrofoil would intermittently become fully wetted during a shedding cycle. The observations triggered a hypothesis that water quality can affect shedding dynamics by delaying the formation of the subsequent cycle's cavity. Professors Arndt and Keller performed a number of lift-oscillation studies for various gas contents at the water tunnel in Obernach during the summer of 1999. A collection of results are shown in 2.4. It was found that, if anything, the amplitude of the lift oscillations appeared higher for lower values of gas content. A number of publications by Arndt include discussions on these data, see e.g. [5] or [4].

A comparison between gaseous shedding and cavitation shedding was eventually made, based on the idea that a similarity exists for the two causes of shedding. Included were a study at SAFL, and a pump study at NTNU. The SAFL study aimed at establishing the link between the two phenomena. Figure 2.5 shows that this link exists. However, the results from Kjeldsen and Arndt bring to light that the lift spectrum fingerprint differ between the two causes for shedding oscillation.

A precursor to the cavitation-ventilated cavity study also evaluated the erosion potential of liquids containing free gas. This study relied heavily on the solution of the Rayleigh-Plesset bubble dynamics equation. Figure 2.6 shows the solution for two different bubbles. When submitted to collapse pressures of $100kPa$ the maximum interior pressure

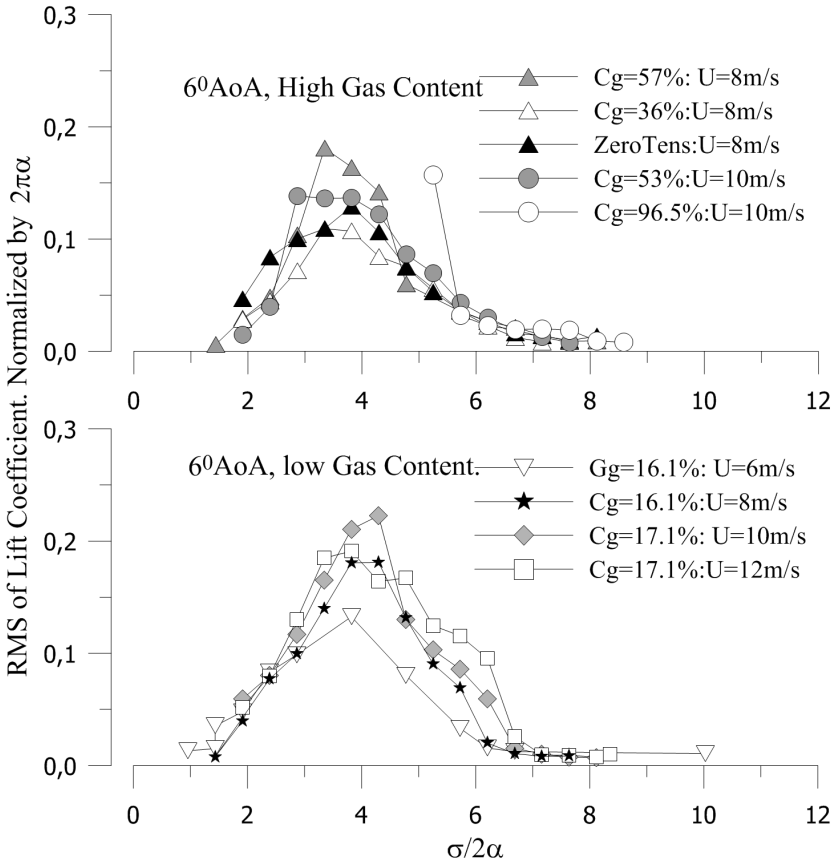

Figure 2.4: *Data from Versuchsanstalt fur Wasserbau, Obernach. Data from measurements performed by Andreas Keller and Prof. Arndt the summer of 1999 [4].*

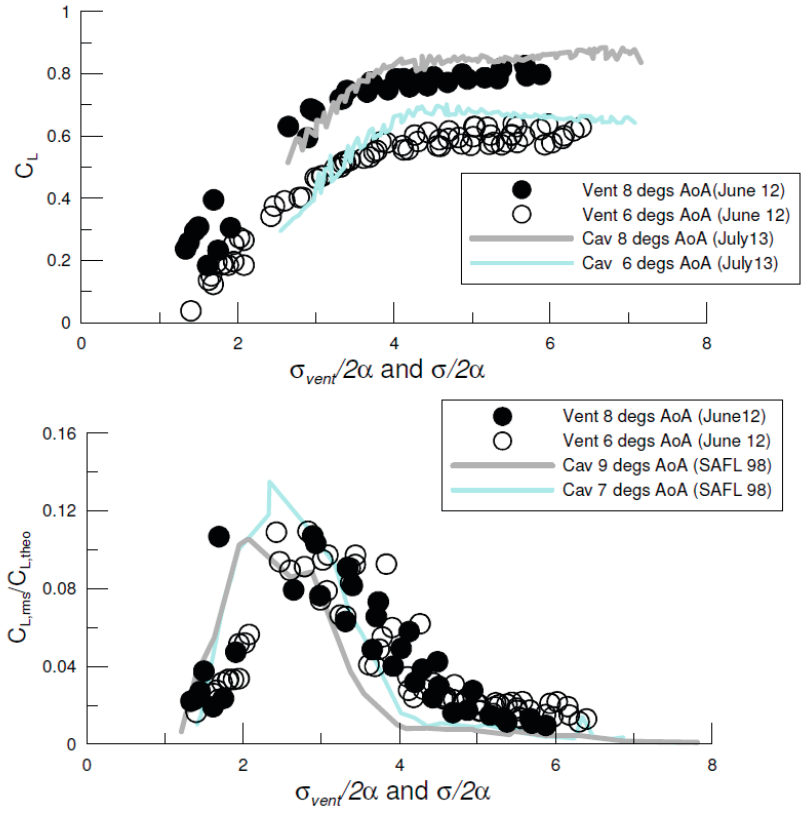

Figure 2.5: *Studies of blade loading of both ventilated and cavitating foil [23]. Notice the similarities to figure 2.4.*

calculated to $2000MPa$ and $35MPa$. The former pressure was only limited by the speed of sound in the liquid, here water. The solution served to demonstrate the influence of a bubble's gas content on the intensity of its collapse.

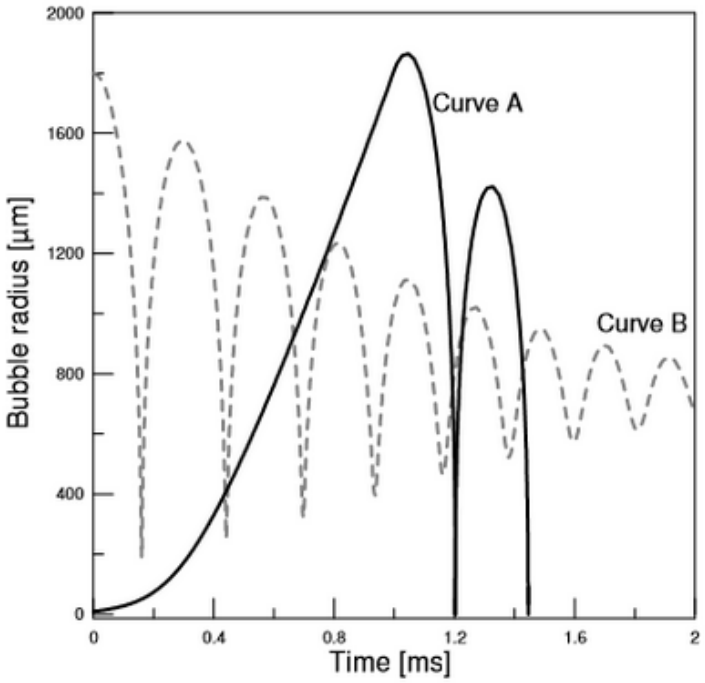

Figure 2.6: *Sample solution of a cavitation collapse for two bubbles with varying gas content. Curve A - Equilibrium for* $R = 10\mu m$ *at* $10kPa$ *ambient pressure, partial pressure of non-condensable gas within bubble* $P_{partial} = 25kPa$*. The bubble traced in curve A is further allowed to grow for* $1ms$ *at* $10kPa$ *tension in order to reach a maximum size of* $1800\mu m$*. Curve B - Equilibrium for* $R = 1.8mm$*, and with a partial pressure of non-condensable gas within bubble* $P_{partial} = 2.3kPa$

The present work relates to the previous work mentioned above by continuing research at SAFL-UMN, but with less focus on shedding. In addition the role of particles in cavitation serve as a back-drop for the field studies. It is likely to find periods lacking suspended particles in the water used by Norwegian hydro power, e.g. running on reservoir water in the winter season, while rapidly increased particle counts should be expected following heavy precipitation and snow melting.

3

Research Design and Experimental Setup

Research Goal

The experiments must focus on answering the overall research question; ”Does water quality affect cavitation characteristics sufficiently to affect recommended turbine operation restrictions?“. The following chapter is a description and summary of the design of the research and its related experiments.

3.1 Research Topic Details

3.1.1 Research Topic 1: Water Quality Quantification

An experimental setup must be developed, that continuously quantifies the water quality in a power plant. As postulated in the introduction, the presence of cavitation nuclei is crucial to the tensional strength of the water. The concept was further explained in chapter 2.1. Consider the typical laboratory experiment were the tensional strength of the water sample is defined by the pressure at which the first nuclei grows to a cavity. In a continuous flow, such as in a turbine, the cavitation zone is analog to the test sample, but it is continually fed new water; e.g. a continuous flow of cavitation nuclei. It is therefore not only likely that the presence of such nuclei define the tensional strength, but also that the concentration defines the rate of cavitation events. Thus it will be investigated if water quality variations affect inception pressure, as well as cavitation intensity. This effect would be expected to be most profound at operation conditions in the transition between developed cavitation and cavitation free operation.

To investigate this research topic a detailed cavitation mapping must be executed along with the evaluation of water quality conditions. A test setup must be designed, that is capable of obtaining valid water samples from the head race conduit and subsequently determine the present water quality. A set of measurable properties that describe the particle and gas content of water at the present time must be concluded upon. Additional laboratory experiment options investigating the same variations should be explored.

3.1.2 Research Topic 2: Continuous Cavitation Measurements

As methods used to detect cavitation, and most importantly to map the cavitation mechanisms across the operation span of the turbine, has already been described the important contribution of the present research is how the methods can be developed further to be confidently used for long-term cavitation monitoring. The initial goal of experiments in this work has therefore been to familiarize with the methods, and thereby being able to suggest sensible automation algorithms for the analysis. The experimental setup must include sensors as well as algorithms for processing the data and storing relevant results for later, while discarding the bulk of the raw data. The setup should store enough relevant data to investigate all the expected effects of water quality variations and cavitation characteristics. Additionally other external factors that could affect the results should be logged.

The algorithms must be able to execute on hardware that is designed for and capable of running unmonitored for longer periods of time. It is expected that the foremost limitation in this regard will be number of vibro-acoustic channels and their buffering lengths. Challenges are expected to be encountered with regard to the frequency analysis parts of the processing of raw data, due to the resource requirements associated with frequency analysis of high sample rate signals.

3.1.3 Research Topic 3: Investigation of Effect of Water Quality on Cavitation

As methods described in research topics one and two are established, the resulting opportunities for long term investigations should be harnessed in order to provide some insight in to the effect of water quality during normal power plant operation. These experiments will most likely have to serve as both tests of methods from the previous research topics, as well as producing results for the present topic. A balance must be struck between data storage requirements and data loss in the analysis algorithms. It must be expected that the results of these tests could be more valuable as algorithm experience than for considering the effect of water quality of cavitation.

3.2 Milestones

The milestones of the project emerged quite naturally;

1. Creation of a cavitation detection hardware-software environment, designed for intrusion free installation in an operational power plant. The system should be capable of recording the required data for post-processing to determine the cavitation characteristics of the turbine/power plant.
2. Definition of water quality parameters that are relevant, and are also quantifiable for extended periods of time through affordable sensor investments.
3. Provision of "transitional lab results", that show in a controlled environment the effects of scenarios imaginable in prototype power plants.
4. Design and initial deployment of a system that once mature will be able to continuously monitor cavitation status and water quality by performing real-time analysis to high speed raw data streams.

The milestones reflect both the academic requirements of the project, and the stakes held by FDB in terms of eventual economic returns from the project.

3.3 Research Process

3.3.1 Defining Water Quality (contextual)

As stated in chapter 2.4 water quality is a generic term that is used across a wide range of scientific fields, each emphasizing different properties of the water. As such, there is need to define water quality within the context of this research. According to the current state of knowledge one should focus efforts on the nuclei availability in cavitation exposed zones, concentrating on how this should be quantified.

Solid Matter Content Quantification

As stated in chapter 2.1 solid matter particles can act as cavitation nuclei, but their effectiveness is affected by their shape. Specifically the presence of concave surfaces on the particles. Consequently, the most accurate method of solid matter content determination would be to acquire water samples and in some way visually inspect the sample in search of such particles, all the while quantifying their concentration. This would require optical equipment that has not been available to us. The obvious expense, combined with expected challenges towards applying a visual method for long term monitoring of water quality, called for a simpler quantification of the particle content. It is common to relate the particle content of water to its turbidity, i.e. its cloudiness or opacity. High content

	Very Good	Good	Less good	Bad	Very Bad
Turbidity [FTU]	<0,5	0,5 - 1	1 - 2	2 - 5	>5
Susp. matter [mg/L]	<1,5	1,5 - 3	3 - 5	5 - 10	>10
Secchi depth [m]	>6	4 - 6	2 - 4	1 - 2	<1

Table 3.1: *Classification of fresh water quality based on turbidity, suspended particles and Secchi depth. Source: www.vannportalen.no*

of miniature particles, that each might not be visible to the naked eye, causes the distance of water through which light can penetrate without scattering to be significantly reduced. Vannportalen provides a relation between turbidity, suspended matter and Secchi depth (Nor: siktedyp). The data is presented in table 3.1. Turbidity is easily quantified using a method that measures scattering of light in a control volume. One should keep in mind that the total light scatter will be a result of both particles and micro-bubbles present.

Gas Content Quantification

Ideally, one should measure the total pressure of all dissolved gas in the liquid (TDGP). This is conceptually simple, because it can be achieved by measuring the pressure in a container that is separated from the measured fluid by a gas-permeable membrane. Gas diffusion across the membrane will cause equilibrium between the gas in the sealed container and the partial pressure of the dissolved gas in the fluid. Consequently the membrane must have a mechanical design that handles the pressure difference between the water at the point of measurement and the partial pressure of the dissolved gases. This design challenge becomes increasingly difficult to meet as the hydrostatic pressure at the measurement point increases. A second significant issue occurs when the equipment must operate for long periods of time. A small amount of water vapor tends to cross the membrane to establish liquid-vapor equilibrium. Over time it has been found that this increases the risk of condensation on the dry side of the membrane, which obscures the measurement. Consequently, total dissolved gas pressure probes has proven to require a higher degree of customization than many other sensor types to be used in the current project. After correspondence [26] with experts at Pro-Oceanus Systems Inc.[1] about a possible solution suitable for this project it was found that a suitable custom probe is available, but at a price[2] that was not coverable by the project budget.

A more common mean of quantifying gas content is to measure dissolved oxygen (DO), and using this quantity as an estimate of dissolved air in the water. Availabilty of sensors designed for use at large hydrostatic pressures is better in the affordable price range.

[1] www.pro-oceanus.com
[2] $ 33,500

3.3.2 Defining a Cavitation Detection Algorithm

The analysis methods for cavitation detection employed throughout this process has been heavily influenced by the cooperation with Xavier Escaler and his previous work [13]. It is comprised of combining analysis of noise level in selected high frequency bands, considerations of modulation levels at several hydrodynamic frequencies and to some extent work with automated methods aimed at counting discrete impacts from collapsing cavitation bubbles. The manipulation of measured data that is necessary is illustrated in figure 3.1, in which a sample of data taken during a measurement is displayed graphically through the amplitude demodulation analysis process. Additionally, other key quantities can be calculated along the process. The analysis of modulation levels come forth through initially band pass filtering the vibration measurements, in a band that could e.g. be selected by considering the frequency spectra of the vibrations to identify regions of elevated magnitude at certain operation loads. The filtering yields a signal that is composed solely of high frequency content. That content is presumably related to cavitation in the instances where that was taking place. To determine the level of modulation of said cavitation, one subsequently determines the amplitude envelope of the filtered signal. While some level of modulation noise is to be expected, in the presence of cavitation the rotor-stator interaction frequencies and/or the other major hydrodynamic frequencies of the system, is expected to dominate. Calculating and investigating the frequency spectrum of the envelope provides the desired information about major amplitude modulation frequencies in the monitored system. By comparing the modulation levels at the known frequencies to nearby silent frequencies or to levels at known cavitation free conditions (such as the best efficiency point) one establishes an indication of the severity of cavitation during the measurement.

The following is a step-by-step qualitative algorithm used to produce data for further analysis (e.g comparison to water quality measurements).

1. Calculate $RMS(x_{raw}(t))$
2. Find $x_{BPF}(t)$ by applying a bandpass filter to the measured vibroacoustic signal $x_{raw}(t)$.
3. Calculate $RMS(x_{BPF}(t))$.
4. Calculate the amplitude envelope $x_{AE}(t)$ of $x_{BPF}(t)$ as described in chapter 2.3.1.
5. Calculate the single-sided amplitude spectrum magnitude of x_{AE}.
6. Determine the amplitudes of the frequency bins in the spectrum associated with the hydrodynamic frequencies of the turbine.

The algorithm is widely scoped, but focused on finally being implemented as a standalone algorithm capable of continuously analyzing the large amounts of data inherent in high-sample-rate recording of signals. It was for instance reported by Bajic in [7] that more than 40 GB of data was collected and analyzed during a single cavitation mapping session involving one turbine. Similar data amounts were recorded during experiments

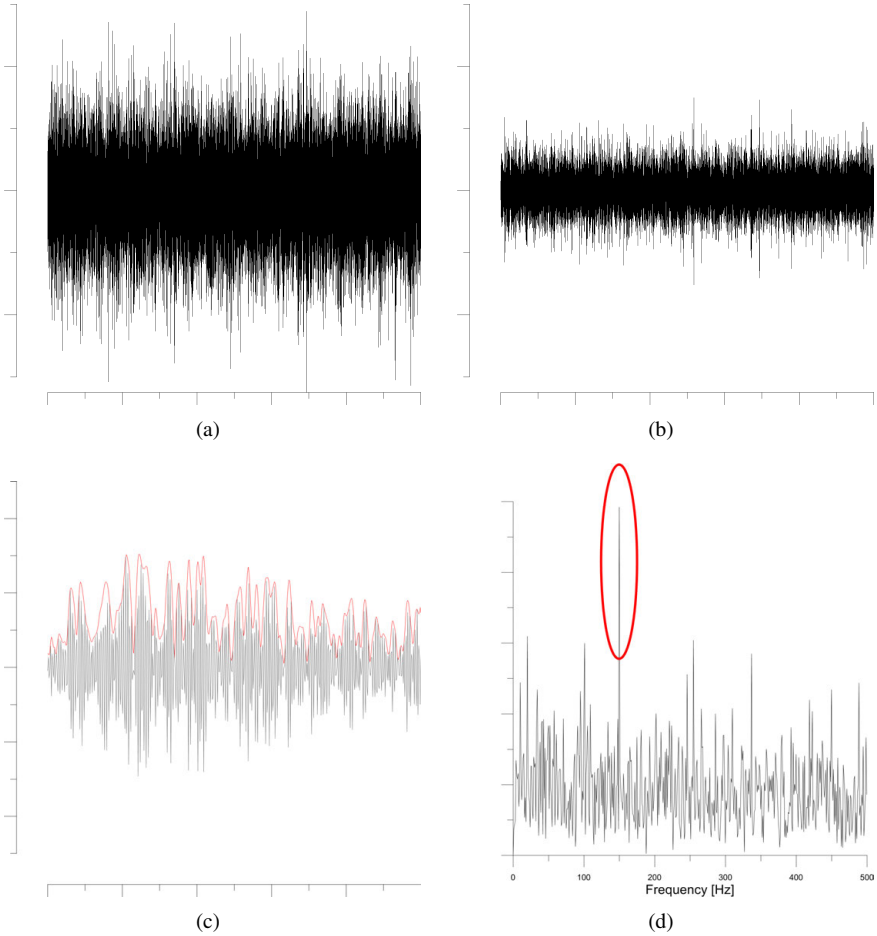

Figure 3.1: *The cavitation analysis process is based on use of high frequency time series of vibrations measured on the turbine housing (here: guide vane shaft top). The raw signal (fig. (a)) is initially filtered using a band pass filter that allows only high frequency content to remain. The resulting signal (fig. (b)) is somewhat attenuated to reflect the removal of low frequency content. Using a Hilbert transform the amplitude envelope of the filtered signal is attained. Figure (c) represents only a small fraction of the source signal, but illustrates the concept of amplitude envelopes very well. One assumes that a significant part of the observed amplitude modulation takes place because rotor-stator interaction causes cavitation prone zones to traverse shifting pressure fields. Figure (d) contains the RMS amplitude spectrum of the envelope, after the offset component was removed. One notes that the turbine blade passing frequency stands out as a particularly significant modulation frequency, which is in accordance with the expected observation when observing cavitation vibration from the guide vane shaft.*

within the herein presented work. Thus, it has been necessary to design an analysis algorithm capable of storing as much relevant data as possible, without saving the raw data.

Finite Time Field and Lab Measurements

During field and lab experiments over a finite period of time it is necessary to collect an amount of data that describe a sufficiently large number of turbine revolutions to gain a statistically sound sample. It has been the aim of this work to include at least 200 revolutions in each such sample. This was determined in correspondence with Escaler, and is more than the 100 revolutions that Bajic reports in [7]. As a consequence, experiments at Svorka generally involved 30-second samples at each operation point. The recorded data was recorded to files and analyzed at a later time.

Continuous Monitoring

Continuous monitoring is distinguished from finite time field measurements by a need to assess data storage requirements, and a much larger result array. It is likely that any operation point of interest for the system in question will be covered by at least one result set. Thus, the statistical validity of the results should be expected to increase. Also, depending on operation strategy at the monitored power plant, measurements across a more continuous spectrum of wicket gate settings may be obtained. However, because continuous recording of high sample rate vibration and acoustic emission sensor outputs generate large amounts of data (250-1000 kS/s), the analysis algorithm must be predetermined and only analysis results be stored for later inspection. Consequently, the option to return to the raw data later is eliminated. One should therefore expect to do preliminary finite time measurements to define an analysis and result storage algorithm.

3.4 Experimental Setup Overview

The following problems describe the initial experimental design stage, keeping in mind that a continuous monitoring system has been the final goal of the project with respect to measurements:

1. Identify what type of sensors are needed for the measurements, find suitable sensor models, determine sensor mounting. This includes a data recording system capable of acquiring signals from all the sensors.
2. Determine the amount of data samples needed for a single analysis "point", define the algorithm of analysis and decide which results to store. One inherently needs to identify the data processing requirements of the analysis algorithm, and ascertain that sufficient computing power is available.

3. Integrate sensors, data acquisition hardware and analysis computation devices as a system with a form factor that is suitable for both short- and long-term (temporary or permanent) deployment in a hydro-power plant or a lab.

An important point of this work is to move the research related to water quality induced variations of cavitation characteristics from the lab environment and in to operational hydro-power plants, as illustrated by the last point above. In order for this be successful additional design criteria regarding instrumentation and analysis were made for a final design proposal that should result from the experimental work. The criteria are:

- The sensors should not interfere with the process in any significant way; they should be non-intrusive.
- Sensor placement must be such that the measured quantities are valid for the analysis.
- Any analysis result should be based on simultaneously recorded data.
- Analysis results should be available in "real time".
- One must address the fact that the required raw data recording rate is too high to allow storage of all raw data.

3.4.1 Additional Benefits from the Experimental Work

As is the nature of hypotheses, it was not initially clear what conclusion could be drawn from the experimental work. However, successful completion of the experimental work implies that a viable method for cavitation monitoring, as well as water quality monitoring has been developed. Following rejection of hypotheses herein there are still reasons to map cavitation occurrence in turbines, or monitor gas content for environmental reasons.

A cavitation monitoring system running uninterrupted for long periods of time is able to more accurately map cavitation behaviour across the span of head that a turbine is subject to. A possible benefit is to set up qualified load restrictions based on turbine head, or even to investigate the impact of upstream and downstream head variations individually.

3.5 Sensors and Data Acquisition

3.5.1 Data Acquisition Tools

Data acquisition has consistently been solved using modular recording hardware and software from National Instruments(NI). National Instruments' solution provide a plethora of hardware components capable of conditioning and recording analog and digital signals from sensors, as well as controlling equipment. Their software, LabVIEW, provides a

graphical programming interfaces which allows the user to create "virtual instruments" for his/her tasks. Furthermore, within the NI scope two platforms were utilized:

1. **NI compactDAQ:** a modular system for data acquisition in which specialized c-modules are installed in a compactDAQ chassis according to the recording/output need of the current experiment. Each module is capable of input and/or output of specified signal types, e.g. a module will record analog milliampere signals, while another will record temperature from RTDs, etc. The cDAQ is solely an input/ouput device, and needs to be connected to a computer that records inputs and manages outputs. The capacity of such a system is to a large extent limited by computer power and interruptions from other applications. In most cases the author did not find it a viable solution to leave a PC to run data recording and analysis for longer periods of time. This is however the least resistance alternative for laboratory work and short-term field experiments.
2. **NI compactRIO:** these are compact *programmable* devices utilizing the same c-modules that are used on cDAQ systems. However, the cRIO devices have a built-in field programmable gate array (FPGA) and a CPU, as well as some RAM and non-volatile memory. The FPGA is a chip equipped with a number of input terminals, logical hardware components and re-programmable paths. They can perform a limited amount of processing, but with the benefit of running at extremely high rates and in true parallel. It has been a continuous process to migrate an increasing amount of processing/analysis to the FPGA. Both the FPGA code and the application running on CPU level is developed using LabVIEW. The real benefit of the cRIO lies in developing applications that are capable of running uninterrupted for long periods of time, and easily ensuring that the applications restart automatically after power outages. Nonetheless, cRIOs have considerably smaller CPU and RAM resources when compared to similarly priced PCs, and therefore require more effort to be put into writing efficient code.

Developing scientific data acquisition and analysis applications is a continuous process in which it takes time for the algorithms and analysis philosophies to mature and develop. The process is further fueled by the extensive attention given to results, but also existing publications, during the writing process. Furthermore one must consider the opportunities gained when developing a system that records data from a sensor every second of the day for (possibly) months or years, rather than recording a 30-second or 1-minute sample of each operation point, which is often the case in what the author would classify as "traditional field experiments".

3.5.2 Equipment for Cavitation Detection

The detection methodology is accurately described in chapter 2.3. This section concentrates on the acquisition of the signal needed for the analysis.

The collapse of cavitation bubbles excite vibrations and acoustic emissions [12] in the tur-

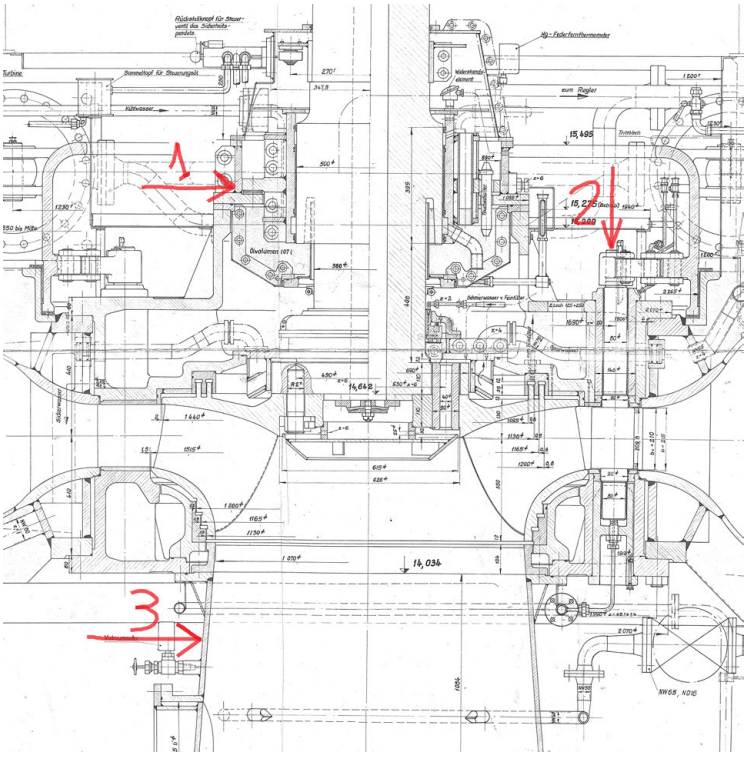

Figure 3.2: *Cavitation detection sensor placement*

bine and its enclosure. The vibrations propagate throughout the turbine, allowing sensors to be mounted on accessible surfaces on the turbine casing. Consequently, one needs to identify locations on the casing to where the vibrations may propagate with a minimum of attenuation. Considering that cavitation occurs on the runner and in the wicket gate, one needs to locate sensor positions that are as close to these, with respect to vibration propagation, as possible. The three most likely candidates are illustrated in figure 3.2, and are: the guide bearing pedestal, the guide vane shaft top and the diffuser inlet. The turbine shaft is also a good alternative, but the additional cost of telemetry and complicated power supply is inhibitive. In fact, the measurements at the guide bearing pedestal are chosen as the alternative, as the vibrations have been found to travel relatively well across the interface between the shaft and the bearing. The guide vane shaft tops have good connection to the quide vanes. However, as will be detailed in the results section, no cavitation signature could be detected in the vibrations recorded on the diffuser wall.

Many, or most, accelerometers work on the principle of a mass suspended on an arm or a material capable of being flexed to some degree. The rate of acceleration is then quantified as a function of the deformation of the material inflicted by the mass. This naturally applies some physical restrictions to the acceleration amplitude and frequency

range that a given accelerometer can sense. Generally, one needs to sacrifice sensitivity in order to detect high frequency vibrations such as those induced by cavitation.

All our experiments were performed using Brüel & Kjær 4397 CCLD Piezoelectric accelerometers. They were selected for their built-in preamplifiers and constant-current signals with voltage modulation[3]. These accelerometers were ideally suited due to the availability of modules specifically built to power and record that signal type being available for the NI cDAQ and cRIO system (the NI-9234), and their quick and easy installation. The accelerometers have a range of zero to 25kHz, and a sensitivity of about 10mV/g. Consequently, only the lower part of the amplitude range can be utilized. Nevertheless, this was a necessary sacrifice in order to make measurements. The accelerometers are mounted on threaded studs that are in turn either glued or screwed on to the measured surface.

While vibrations, defined as (mechanical) oscillations around an equilibrium point, is the most direct measurement of the effects of cavitation impacts we have seen that a threshold exist above which it becomes practically impossible to record the vibrations. Above this threshold one needs to apply different methods to detect effects of cavitation. During this work acoustic emissions, which are elastic waves emitted by deformation events in the material, has been measured at frequencies up to 50 kHz, using Kistler 8152B111 sensors. Together, the measurements provide a good base for cavitation detection analysis.

3.5.3 Equipment for Water Quality Evaluation

Turbidity

Turbidity has been measured using a Seapoint Turbidity Meter (STM) [4], which works on the principle of measuring light scattering in the measured fluid. This sensor was ideal due to its compact design and range flexibility. The STM has a linear response and was factory calibrated for output in FTU (Formazin Turbidity Unit). Two individual probes has been used;

- STM with standard connector: a "pelagic" probe, with a rubber sealed connector designed for measurements in free surface water bodies.
- STM with bulkhead connector: designed for mounting in a bulkhead wall, and thus ideal for measurements of turbidity in pressurized tanks or pipes.

The STM is rated for pressures up to 6000 mWc, can be set to ranges from 0 - 25 FTU to 0 - 4000 FTU.

[3]This signal conditioning methodology is known by many names, including IEPE, ICP, CCLD, Isotron, Deltatron, Piezotron, etc.

[4]www.seapoint.com/stm.htm

3.6 Description of Conducted Experiments

3.6.1 Transition from Laboratory to Field

The transition from laboratory to field experiments involves considerable alterations in experimental strategy. Many laboratory tools become effectively unavailable in most field experiment settings. E.g. it would not be realistic to install camera equipment capable of quantifying bubble sizes in a turbine conduit. Likewise, it would be difficult to determine presence of micro-bubbles acting as cavitation nuclei. One needs to depend on more "global" measurands, such as wicket gate position, inlet and outlet pressures, and water temperature to determine the state at which cavitation occurs in the turbine. Likewise, the actual cavitation is detected by indirect measurements rather than in-situ sensors or visual inspection. In the context of this project, and especially with regard to the water quality and continuous monitoring aspects of the experimental work, compromises were made, and measurement equipment had to be designed in some instances from little initial experience.

With regard to quantification of water quality, correspondence and discussions with Professor Knud Aage Mørch of DTU (Technical University of Denmark) has been very helpful. For the continuous monitoring experiment it was decided that measurement of turbidity and dissolved oxygen was a viable, and affordable, method considering the scarce availability of referenced similar experiments. It was considered unlikely that turbidity changes significantly through the turbine, while it was expected that DO levels would be significantly affected by processes within the turbine (namely cavitation and degassing due to reduced pressure). It was therefore decided that DO, and hence by convenience also turbidity, should be measured at the inlet of the turbine, as close to full inlet pressure as possible.

With regard to cavitation detection it was not necessary to "move from lab to field" as methods for cavitation detection in hydro turbines are already published, as referenced in chapter 2.3. In this regard, experiments in lab was more to be considered as a controlled method of familiarizing with the algorithms.

Finally, standard methods for pressure, and wicket gate position measurements could be applied to determine the conditions during any given measurement series.

3.6.2 Experiments in the Cavitation Tunnel, SAFL, UMN

The Saint Anthony Falls Laboratory, at University of Minnesota in Minneapolis, allowed us to use their closed-loop cavitation tunnel for controlled cavitation experiments that included manipulation of water gas content through degassing of the tunnel water. The test section of this particular tunnel has a square $190mm$ x $190mm$ cross section, and a length of $1270mm$. The transparent walls of the test section also provided good opportunities for visual inspection of cavitation, thus allowing us to familiarize with sensor response to

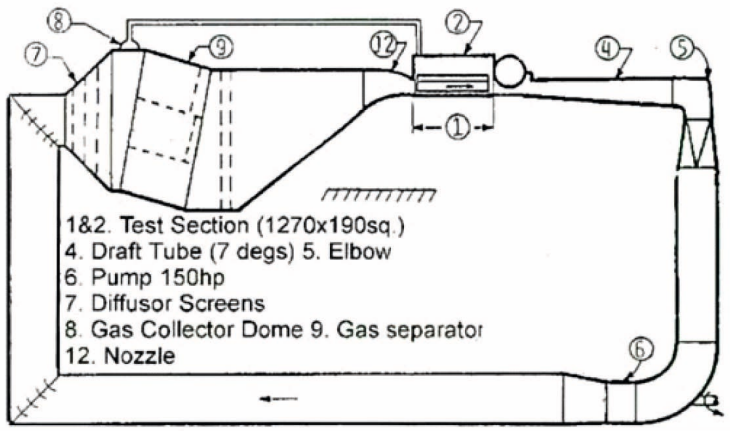

Figure 3.3: *The closed-loop cavitation tunnel at Saint Anthony Falls Laboratory, University of Minnesota, Minneapolis(MN)*

cavitation and investigation of results. The tunnel is illustrated in figure 3.3. The pressure in the test section is controlled by adjusting the air pressure above the water surface in the gas separation tank. By means of a vacuum pump, the pressure can also be reduced to below the ambient pressure. The flow velocity is controlled by the circulation pump speed.

2011 Experiments

The experiments conducted in November 2011 were the first during this project. Their two objectives were to test vibro-acoustic sensor equipment, and investigate the effect of dissolved gas content on cavitation characteristics.

Test Body and Equipment The experiments were conducted using a NACA0015 hydrofoil mounted to a base designed for use with a force transmitter. The setup has been used previously to measure lift oscillations induced by cavitation on the foil. The foil had a chord length of 81 mm and spanned the full width of the test section.

For the purposes of this experiment B&K 4397a uniaxial accelerometers were mounted on the base, using glued-on threaded studs, in alignment with the three major axes. Additionally a PAC R6α acoustic emission sensor was mounted on the test section wall using a magnetic clamp.

The vibro-acoustic sensor signals were recorded using NI compactDAQ, NI-9205 and NI-9234 hardware and a LabVIEW application developed by FDB.

Flow velocity, test section absolute pressure and dissolved oxygen content was recorded

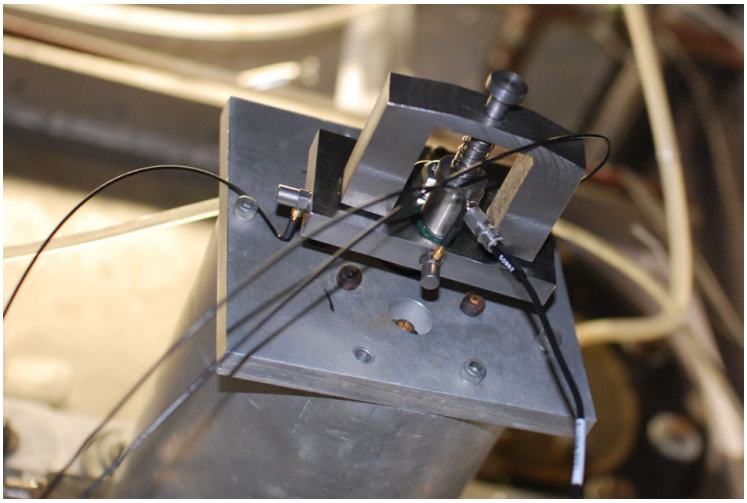

Figure 3.4: *Mounting of accelerometers and acoustic emission sensor. The acoustic emission sensor was moved to the test section wall (in the background), when the mounting illustrated here proved unfortunate.*

from the cavitation tunnel monitoring software, developed at SAFL.

Experimental Work During the experiments a series of tests were run where vibrations and acoustic emissions were recorded in 10-second intervals at test section cavitation numbers covering an interval from no cavitation to supercavitation on the foil. The cavitation numbers were normalized according to a standard method used at SAFL; $\frac{\sigma}{2\alpha}$, and ranged $\frac{\sigma}{2\alpha} \in [3, 12]$ The tests were repeated to cover a test matrix in which the following conditions were manipulated:

- The angle of attack of the hydrofoil was set to $2°$, $6°$ and $8°$.
- The pump drive was set to $22Hz$, $24Hz$, $26Hz$ and $28Hz$.
- Using first air saturated and then degassed water in the tunnel loop.

The degassing of the water in the tunnel loop was achieved by running the tunnel for an extended period at low a cavitation number, causing large scale cavitation to occur on the hydrofoil. The gas released during this process would subsequently be partially trapped in the gas separator (8 and 9 in figure 3.3) and removed from the system.

The data was recorded to file, and analyzed later. The accelerometers were recorded at a rate of $51,2kS/s$, and the acoustic emission sensor was recorded at a rate of $120kS/s$. Additionally, photographs of the foil's suction side were taken during each recording.

2014 Experiments

The return to SAFL in 2014 was made to rectify some doubts about numerical accuracy of some of the measurements that was performed in 2011. Specifically there were doubts about the numerical accuracy of the dissolved gas measurements, as well as non-ideal signal conditioning performed on the accelerometer recordings during the first experiment. A longer period was scheduled for the experiments, and most importantly for the preparations, instrumentation setup and quality assurance of the monitoring system for the tunnel. Some qualified[5] improvements were made to the LabVIEW monitoring application. After modification the application publish real-time measured values from the tunnel to the intranet, allowing other LabVIEW applications to read the current tunnel conditions. The instrumentation and signal conditioning prior to data acquisition was also reviewed and maintenanced in cooperation with SAFL staff.

Test Body and Equipment The experiments were performed on a NACA 0015 hydrofoil with a rigid mounting base that was produced specifically for this experiment. The foil was designed with a slot that allowed manipulation of the foil's suction side surface geometry. A smooth foil was obtained by installing an inlay flush with the NACA profile, while passive flow control could be achieved by installing an inlay with a 1mm tall triangular fence across the entire foil span. Like in the 2011 experiments the chord length was 81mm.

Like the 2011 experiments, the foil mount was instrumented with three uni-axial B&K 4397a accelerometer directed along the three major axes, and an acoustic emission sensor of type Kistler 8152B111 mounted on foil base. Additionally, a Seapoint Turbidimeter was used to measure the turbidity of samples of water extracted from the tunnel loop.

Vibro-acoustic sensor signals and the turbidimeter signals were recorded using NI compactDAQ, NI-9205 and NI-9234 hardware and a LabVIEW-developed recorder application. The recorder application also accessed the data from the tunnel monitoring application, and stored the information in the same files as the other recorded data.

Experimental Work The experiments conducted were conceptually the same as those in 2011. A structured test matrix was iterated through using saturated water, before the water was degassed and the same test matrix was re-iterated. Each test in the matrix consisted of measurements at a range of cavitation numbers from no cavitation on the foil to the minimum achievable. Contrary to the earlier experiments however, was the degassing process. A more effective de-gassing was achieved by a recently added auxiliary system in which the tunnel water was diverted through a spray nozzle in a vacuum tank before being returned to the tunnel. Running this diversion loop over night provided a far more effective de-gassing than previously achieved.

[5]The author is currently CLD (Certified LabVIEW Developer), which is the second highest NI certification level for LabVIEW development. Additionally FDB is an NI Alliance Partner.

3.6.3 Cavitation Mapping at Svorka Power Plant

FDB is in the lucky position that the owners; Statkraft AS and Svorka Energi AS, has granted us liberal access to conducting experiments at Svorka Kraftverk near Surnadal in Norway. Consequently many of the experiments during this doctoral work has taken place here.

The Svorka power plant is equipped with a Francis turbine with a nominal power of 25MW. The operation head is about 260m. The outlet is through a very short tunnel to a basin in the river Bævra, and as a consequence of this the outlet level may vary considerably. The draft tube is equipped with a water injection system designed to mitigate tangential velocity components that occur when the turbine is operated on part load, and their negative effects. The system was designed as part of the doctoral work of FDB colleague Håkon Hjort Francke.

2011 Cavitation Mapping

Instrumentation Uni-axial B&K 4397a accelerometers were mounted on the guide bearing pedestal housing at 0° and 270° angles (relative to the reference angle) in the shaft's rotational plane. The sensing axes of the accelerometers were oriented radially in reference to the turbine shaft axis. A third B&K 4397a accelerometer was mounted on the guide vane shaft that lies at 270° in the same plane. It's sensing axis was oriented parallel to the axis of the guide vane shaft (and turbine shaft). Finally, a B&K 5419 uni-axial accelerometer was mounted to the draft tube wall, at a 0° relative angular position in the rotation plane of the turbine shaft. Its sensing axis was oriented radially from the turbine axis. A PAC R6α acoustic emission sensor was also mounted on the guide bearing pedestal housing, at a 0° relative angle in the rotation plane. The angular position of the runner was monitored using a photo-detector that returned one pulse per revolution of the turbine shaft.

An instrumented hammer was used to determine the frequency-dependent propagation of vibrations from the runner blades to the external measurement positions described above. During these tests one accelerometer was also mounted to the runner blade using beeswax, and the instruments were recorded simultaneously during excitation of the runner.

Experimental Work A cavitation mapping of the turbine operating in a range from 7.7MW to 25MW was conducted. In addition, cavitation mapping was conducted at 10MW, 12.5MW and 15MW, while the draft tube water injection system was turned on. A 20-second data series was recorded during each measurement.

2012 Cavitation Mapping

The mapping in 2012 was conducted with a similar setup that was used the year before. However, the IEPE signal conditioning was improved to provide better signal-to-noise ratios and the water injection system was used in a wider operation range.

3.6.4 Cavitation and Water Quality Monitoring at Svorka Power Plant

The primary experiments served the purpose of building experience with implementation of signal recording and analysis in the available hardware-software environment. We were also able to investigate water quality influence by altering the gas content during the SAFL experiments. This experience was put to use to build a continuous water quality and cavitation monitoring system, with the aim of documenting the expected water quality variations and their influence on cavitation characteristics.

The measurements were conducted in the period from May 2014 to January 2015. During an inspection in August some bugs in the code were revealed, and the system was returned to the office for maintenance. The bugs proved non-critical for the results already produced, but increased the post-processing work load. The system was put back into operation in October. The vibro-acoustic equipment was dismounted and stored safely during the maintenance period. To prevent any small changes in vibration propagation characteristics between the two installations, results post and prior to the maintenance have been treated individually.

Water Quality Monitoring Solution

As previously stated (chapter 3.6.1), water quality would be monitored at the inlet conditions of the turbine. For this purpose a pressure tank was designed to be integrated in a bypass loop between the turbine inlet and the draft tube. The tank was designed to hold a turbidity probe and a DO probe, both of which were mounted bulkhead-style in the tank lid. The bypass flow was driven by the pressure difference, and limited by a throttling valve. The throttle was mounted at the bypass outlet (the return connection on the draft tube) to ensure maximum pressure in the test tank. This was done in order to perform the measurements in accordance with Prof. Mørch's recommendations (chapter 3.6.1). During the experiments the tank was connected downstream relative to the main head race conduit valve, and above the water level of the outlet. As a result the tank was drained, but most importantly de-pressurized, during turbine stops. To facilitate the evacuation of air from the tank during re-pressurization, the flow direction was from bottom to top.

Figure 3.5: *The pictures show the water hose connections at each end of the tank, and the dry side of the bulkhead-mounted sensors in the lid.*

Raw Data Analysis

A large amount of data was being recorded; in the order of 150000 30-second tests were completed, each returning around 50 numerical values. Additionally, the recording system was operational regardless of turbine operation condition. E.g. it has been necessary to filter results with respect to guide vane opening as well as detecting presumably erroneous results before starting the actual analysis of the data.

Data Collection Data was recorded at several rates, see appendix C.1.3. The data was recorded by a recording module and streamed to the analysis computer in chunks containing one second of recorded data. The analyzer appended the recorded data chunks, and performed continuity checks. Data was dumped and the data appendage was restarted if discontinuities were found. When a continuous 30-second sample was available the data was passed to the analysis algorithm. Operation condition data was collected from the installed nozzle injection control system; guide vane opening, draft tube pressure and injection system state.

Data Analysis and result handling Data was analyzed according to type, and the results stored as a single row of data in the log file. The results were grouped as conditions; time of measurement, turbidity, dissolved oxygen level, guide vane opening, tur-

bine outlet pressure and injection system state, and subsequently the results from analysis of the vibro-acoustic sensors were grouped according to source sensor. The raw data was dumped after the analysis.

Condition data and water quality The average measured value and the slope of the time series was calculated for each of the recorded measurements describing the operation conditions and the water quality.

Vibro-acoustic measurements Each signal was treated the same way. Initially, the raw signal was conditioned using the calibration values of the sensor. An RMS value of the signal was calculated before and after applying a bandpass filter that passed frequencies from $20kHz$ to $25kHz$ for the accelerometers and between $45kHz$ and $50kHz$ for the AE-sensor. Amplitude modulation (see chapter 2.3) levels were recorded at the following hydrodynamic frequencies: the Rheingans frequency, the rotation frequency of the runner, the guide vane passing frequency and the runner blade passing frequency. Additionally a baseline modulation level was recorded, which was defined as: the mean value of the lower 75th percentile of the demodulation levels between $0Hz$ and $1000Hz$.

4

Results

Chapter Summary

This chapter provides both overview and detail about the conducted experiments at SAFL and Svorka. In some cases the data is presented in graph clusters, to aid comparison between e.g. the different modulation frequencies. In these cases, a larger print of the graph is available in the appendix, chapter C.2.1.

4.1 Experiments conducted at St. Anthony Falls Laboratory

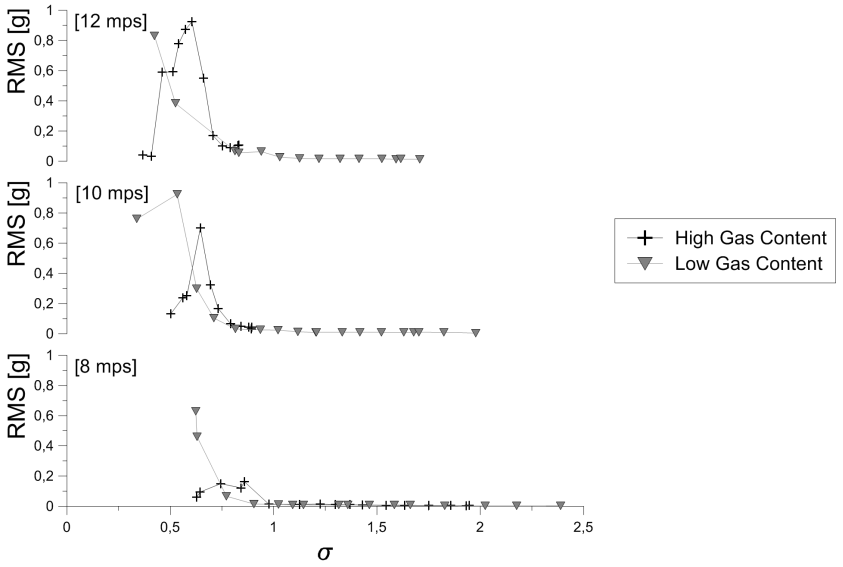

Figure 4.1: *A band pass filter has been applied to extract the high frequency components of the raw data, after which the RMS average of the signal was calculated. RMS values are plotted against cavitation number for high and low gas content cases, divided across three plots to account for different the flow velocities that was utilized. Here the angle of attack was* $2°$*. The source of the raw data is the accelerometer mounted in the X-direction.*

4.1.1 Test Matrix

The test matrix had five dimensions:

- Cavitation Number: 0.2 - 2.5 [-]
- Dissolved Oxygen Content: 4.75 - 12 [PPM]
- Angle of Attack, AoA: $2°$, $4°$ and $6°$
- Flow velocities in test section: $8mps$, $10mps$ and $12mps$
- Foil Flow Control: Smooth foil, or triangular fence installed.

Also indicated are the values of each variable, that was used or measured during the experiments. In the cases of angle of attack, flow velocity and foil flow control the different settings were set and used for several measurements, in which the cavitation number was

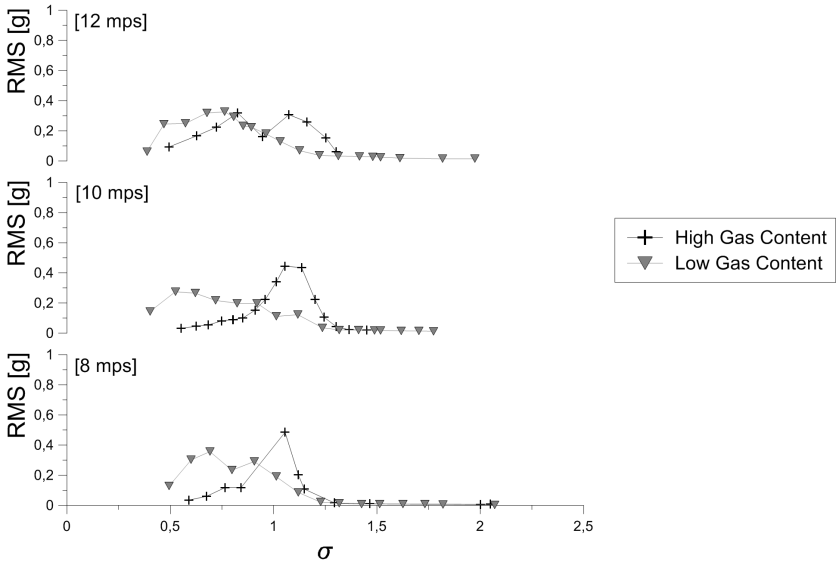

Figure 4.2: *A band pass filter has been applied to extract the high frequency components of the raw data, after which the RMS average of the signal was calculated. RMS values are plotted against cavitation number for high and low gas content cases, divided across three plots to account for different the flow velocities that was utilized. Her the angle of attack was* $4°$*. The source of the raw data is the accelerometer mounted in the X-direction.*

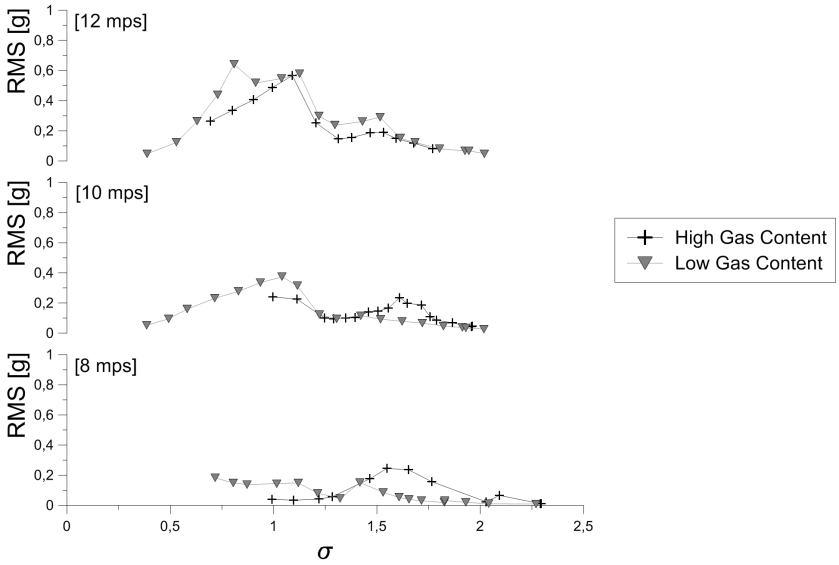

Figure 4.3: *A band pass filter has been applied to extract the high frequency components of the raw data, after which the RMS average of the signal was calculated. RMS values are plotted against cavitation number for high and low gas content cases, divided across three plots to account for different the flow velocities that was utilized. Her the angle of attack was* 6°*. The source of the raw data is the accelerometer mounted in the X-direction.*

manipulated. Finally the DO was manipulated once, through a lengthy degassing process. DO was measured continuously throughout the experiment, and it was confirmed that the levels were significantly reduced by the degassing. Within each permutation of the remaining matrix elements, results are treated as either having high or low gas content. Consequently, the results contain ranges of cavitation numbers within 36 permutations of the matrix.

4.1.2 Vibration Magnitudes

RMS values of x-direction vibration of the hydrofoil are plotted against the cavitation number σ in figures 4.1, 4.2 and 4.3. Each figure presents the results found at one angle of attack, and at all three flow velocities used. The corresponding results at high and low gas content is plotted together. It is found that the results vary to some extent between the angles of attack.

In figure 4.1, at 2° angle of attack one observes at $8mps$ that the vibrations increased only slightly, but it is still observable that the intensities decreased towards the lowest cavitation numbers achieved. In the case of low gas content, the vibrations were found to not increase until reaching a threshold significantly lower than that at high gas content. The corresponding vibration magnitudes were also significantly higher at the lower end of the range. At $10mps$ the vibrations at high gas content increase rapidly below $\sigma = 0.8$ and reaches a clearly defined maximum at $\sigma = 0.65$, the vibration levels then decrease rapidly as σ decrease further. At the same time, one observes that the vibrations measured at low gas content also start to increase around $\sigma = 0.8$, but at a much lower rate. The vibrations reach magnitudes comparable to the high gas maximum at $\sigma = 0.8$, but continue to increase at lower values of σ. Finally, at $12mps$, one finds that increased vibrations occur at the same threshold as the previous cases. However, the two gas content cases have similar patterns and magnitudes initially. At high gas content, a high level of vibration magnitudes is sustained in the range from around $\sigma = 0.6$ to $\sigma = 0.45$, upon which the vibrations subside quickly and return to non-cavitation levels at lower cavitation numbers. The low gas case increases rapidly to a peak level at around $\sigma = 0.7$, upon which further reduction down to $\sigma = 0.5$ sees a halving of the vibration levels. Further reduction of σ causes the vibration magnitudes to increase again, reaching the highest levels observed at this angle of attack and flow velocity.

At an angle of attack of 4°, found in figure 4.2, one finds less disparity between the flow velocities. At $8mps$ one observes that vibration magnitudes start to increase at around $\sigma = 1.25$. In the high gas saturation case, the magnitudes increase rapidly, and reaches a distinct maximum value around $\sigma = 1$, after which further reduction of cavitation number causes the vibrations to subside to close to non-cavitation levels. At low gas content the vibration levels start to increase at the same cavitation number, but only exhibit a gradual increase to a maximum at about $\sigma = 0.7$. This level is about a quarter of the magnitude found in the high gas content case. At the two remaining flow velocities, $10mps$ and $12mps$, the pattern is similar and the low gas content vibration levels measured

are of similar magnitudes. However, the high gas content cases exhibit significantly lower maximum levels. At $10mps$ the maximum level reached in the high gas content case is only about twice the magnitude of the low gas content case. In the final case, $12mps$, the maximum levels are the same at both gas contents.

Finally figure 4.3 presents the results of measurements with an angle of attack of $6°$. The vibrations start increasing when $\sigma = 1.75$. It is also generally noted that the vibration levels reach smaller maximum values than at the lower angles of attack. At $8mps$ the high gas content case reaches a maximum vibration level at $\sigma = 1.5$, after which the levels subside at lower cavitation numbers. At the same time, the vibration levels at low gas content are found to increase from around the same point. The maximum levels of vibrations measured are similar in the two cases. The pattern found at $10mps$ is similar. However, the low gas content vibrations reach a maximal value that is larger than that of the high case. Furthermore, the high gas content vibrations are found to also increase in parallel with the low gas saturation case. At $12mps$ the two saturation levels caused very similar patterns. Both reach a maximum value near $\sigma = 1.5$, however, the levels are sustained across a larger cavitation number range in the low gas content case.

It is the general observation that the gas content does not significantly affect the inception point of detectable cavitation, but has a noticeable effect on the vibration levels as observed by the externally mounted sensors. In the high gas cases the vibration levels increase rapidly after inception, but quickly reach a maximum level after which the vibration magnitudes decrease at a rate comparable to their rapid growth. These reductions are in correlation with the experimental notes, which describe largely developed cavitation continuing to full super-cavitation in the range in question. The observations included visibly and audibly detectable reduction of foil oscillations, and cavitation collapse propagating to the free-stream. In the low gas content cases cavitation covering the entire foil suction side, let alone super-cavitation, was not achieved at the same values of σ.

4.1.3 Lift Oscillations and Amplitude Modulation Frequencies

It is of major interest to explore the effect of the hydrodynamics of the experimental environment on the cavitation dynamics, but also the effect of the cavitation on the lift oscillation of the foil. Analysis was conducted to explore the dynamics found in the low frequency interval from $0Hz$ to $500Hz$ of vibrations on the foil. Results are presented as scaled amplitude magnitude spectra, which return the $[g_{RMS}]$ value associated with the amplitude of each frequency bin. It is generally found that broadband noise is present at frequencies above $100Hz$ in the cavitating cases, while the non-cavitation cases display some distinct peaks at repeatable frequencies. It is of general interest to investigate the presence of distinct frequencies in the amplitude modulation of the high frequency ranges of the same raw signal.

Figure 4.4 illustrates frequency analysis results of the measurements of the $10mps$ case of figure 4.1, in which increased vibrations covered a similar interval of cavitation numbers.

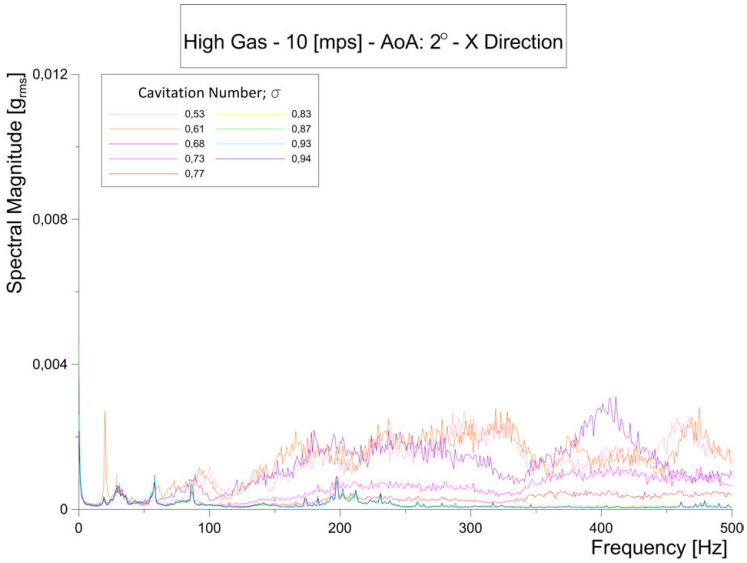

(a)

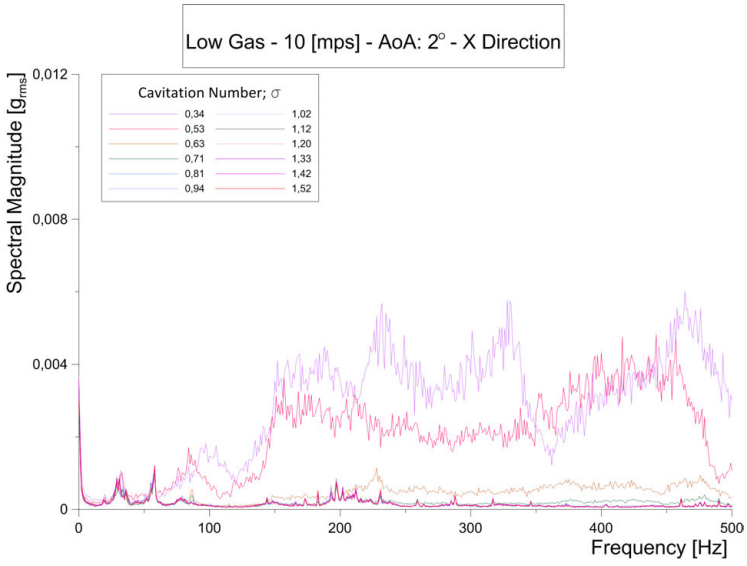

(b)

Figure 4.4: *Lift oscillations on the foil, expressed by the frequency analysis results of all measurements taken with high(4.4(a)) and low(4.4(b)) gas saturation, no fence installed,* $10mps$ *flow velocity and* 2° *angle of attack.*

It is evident that the two cases display similar patterns, and one also observes that cavitation and non-cavitation cases at both saturation levels are similar. For all non-cavitation cases two main peaks stand out, each spanning the small frequency intervals $45Hz$ and $205Hz$. In the low gas case there also appears to be a large degree of agreement between the cavitation cases in the $200 - 210Hz$.

Furthermore, the high and low gas saturation cases at $10mps$ and 4° angle of attack are compared in figure 4.5. Like in figure 4.5, one observes the peaks at/around $45Hz$ and $205Hz$. However, the peak around $205Hz$ has lost some significance. A series of new peaks (of diminishing magnitude) have appeared. In the high gas content case these peaks are discernible in a range spanning $0 - 100Hz$, while one can only find evidence of the peaks in the range from $0 - 60Hz$ in the low gas content case. A general increase of magnitude is found in the band above about $50Hz$, an approximate band spanning $100 - 125Hz$ exhibits reduced magnitudes compared to neighboring bands.

Figure 4.6 depicts the measurements at $10mps$ and 6° angle of attack. At these conditions, the aforementioned peak at around $45Hz$ is not evident. There are still traces of a peak at $200Hz$. The previously mentioned evenly spaced peaks found in figure 4.5 are indicatively present up to about $60Hz$. One notices at both high and low gas saturation that a relatively broad peak centered around $75Hz$ has appeared. Furthermore, even though the RMS levels are found to be higher in the low gas content cavitation cases, this is not reflected in the higher part of the plotted band.

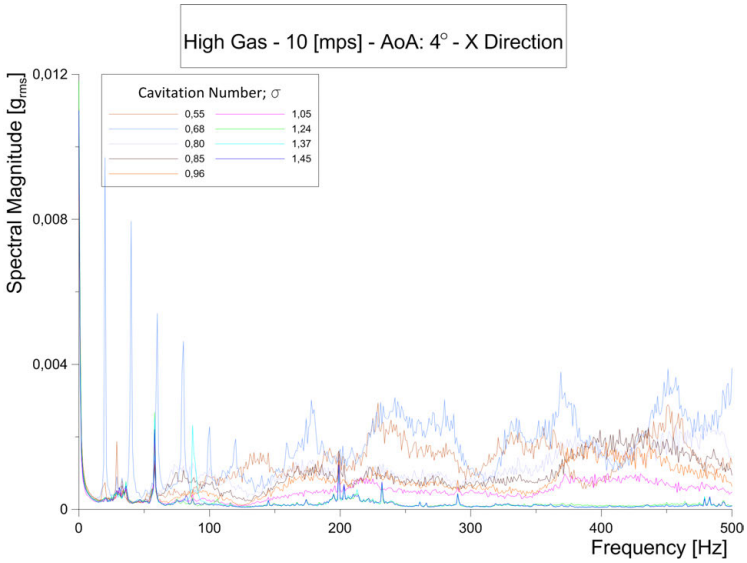

(a)

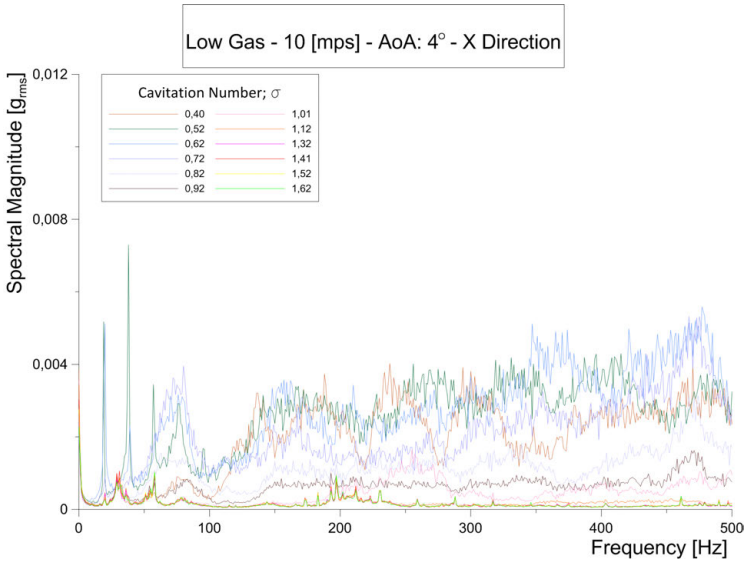

(b)

Figure 4.5: *Lift oscillations on the foil, expressed by the frequency analysis results of all measurements taken with high(4.5(a)) and low(4.5(b)) gas saturation, no fence installed,* $10mps$ *flow velocity and* $4°$ *angle of attack.*

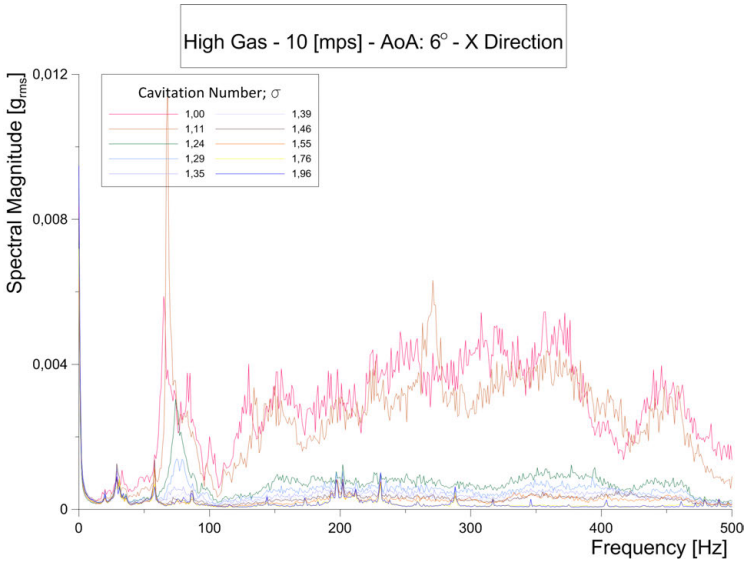

(a)

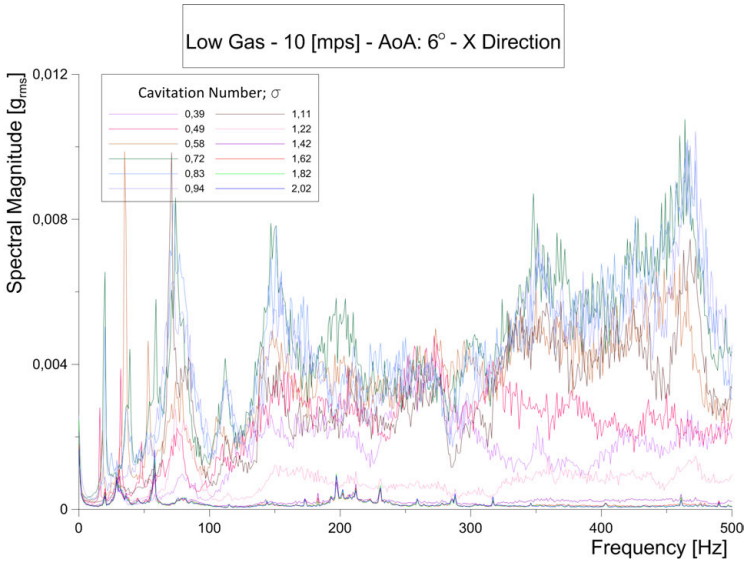

(b)

Figure 4.6: *Lift oscillations on the foil, expressed by the frequency analysis results of all measurements taken with high(4.6(a)) and low(4.6(b)) gas saturation, no fence installed,* $10mps$ *flow velocity and* $6°$ *angle of attack.*

4.2 Svorka Experiments

4.2.1 Cavitation Detection and Draft Tube Water Injection

A paper was published in the Journal of Fluids Engineering [30] that completely covers this topic, from which a summary is provided here.

The experiment intended to investigate the known issues of draft tube surge and cavitation erosion, in order to define restrictions that took both mechanisms into account. Thus, a full instrumentation of the machine was installed:

- Measurement of cavitation induced vibration and acoustic emission.
- Draft tube dynamic pressure measurement.
- Turbine efficiency measurement (IEC Thermodynamic).

The measurements reconfirmed the presence of pressure fluctuations at about one third of the runner frequency[1] during part and full load operation. The condition is known to occur in this plant and is covered in e.g [19]. The analysis of the vibrations included investigation of amplitude modulation by the Rheingans frequency as well as the remaining hydrodynamic frequencies of the machine. It was concluded that the main mechanism of cavitation modulation was linked to the guide vane passing frequency, and likewise it was concluded that the erosive capacity of the cavitation peaked at full load. The coherence studies indicated that the main propagation route of cavitation noise in the machinery is through metal and across oil films between rotating and stationary parts.

The results provided valuable experience regarding the cavitation analysis methodology, and this was put to use in the long-term monitoring tests described below. The full text of the paper is available in appendix A.1.

[1] The frequency commonly known as the Rheingans frequency.

4.2.2 Long-term Monitoring Results

The experiment was deployed in May of 2014, but had to be retrieved for maintenance during a routine inspection in July due to unstable execution. The system was redeployed in October, and ran uninterrupted until January 2015. It was unfortunately discovered upon review of the vibration measurement results from the second deployment period that some erroneous array operations had rendered the data unreliable. Thus only the results from the initial deployment period are presented herein.

Weather Data

Weather data from the measurement period was retrieved from the website of the Norwegian Meteorological Institute [2]. Precipitation and temperatures are available at 1-day resolution. The data is graphically presented in figure 4.7.

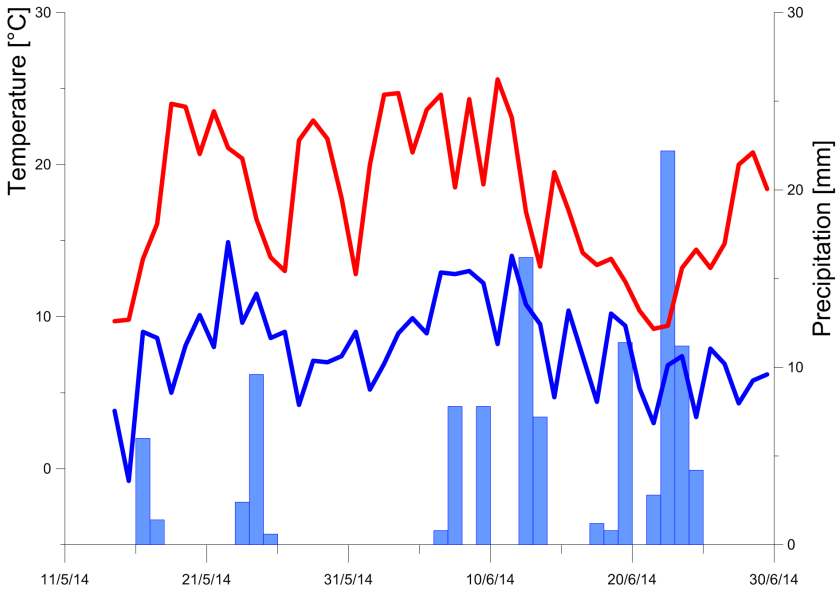

Figure 4.7: *Maximum and minimum temperatures are plotted in red and blue respectively. Furthermore, the precipitation is presented as bars.*

Results Overview

During this period the turbine was operated for extended periods at a specific guide vane opening, see figure 4.8, but reasonably spread operation periods (>30 mins) could be

[2] www.yr.no

found between 30% and 85% guide vane opening(GVO)/servo stroke.

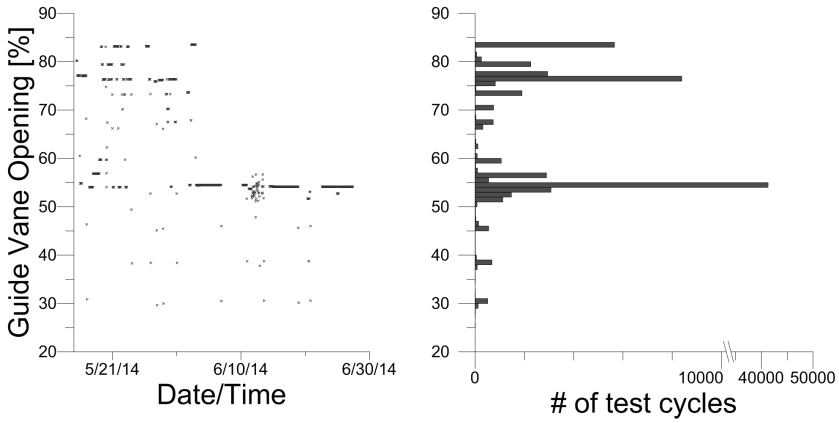

Figure 4.8: *(left) The graph chronologically illustrates the sample source that was used during analysis. The dots represent the guide vane openings registered for each individual analysis test cycle. (right) The histogram provides an illustrated overview of the number of test cycles performed within in each 1% interval of guide vane opening. This illustrates the significant variance of result availability in the operation range.*

An overview of the measured vibro-acoustic intensity is presented in figure 4.9; quantified by the RMS-levels of vibrations and acoustic emissions measured on the guide bearing pedestal and the guide vane shaft. Measurements are presented in filtered and unfiltered state. One observes a larger variance of intensity on part loads than is observed near the best efficiency point. The interval from 60% to 70% guide vane opening is proven to have higher levels of vibro-acoustic activity.

Modulation Levels Investigations were made on the modulation of the cavitation induced vibration amplitudes by known hydrodynamic frequencies; the Rheingans, rotational, blade passing and guide vane passing frequencies. The results are presented in figure 4.10 as a function of the guide vane opening. The presentation highlights the various mechanisms present as well the ability, or lack thereof, of sensors at certain placements to record the mechanisms. An example is the absence of blade passing frequency modulation picked up on the guide bearing pedestal. It should also be noted that levels at the guide bearing pedestal and guide vane shafts are not directly comparable, due to dissimilar propagation paths and difficulty in establishment of proper transfer functions [3].

The modulation levels related to the Rheingans frequency are generally one order of magnitude smaller than the remainder. They are however found to be two to three times larger

[3]While one could define transfer functions by use of an instrumented impact hammer or an accelerometer mounted to the runner, problems exist regarding induction of high frequency vibrations. Additionally the flexibility of the power plant owner was partially due to the flexibility of the installation, when not including emptying of the draft tube for transfer function establishment.

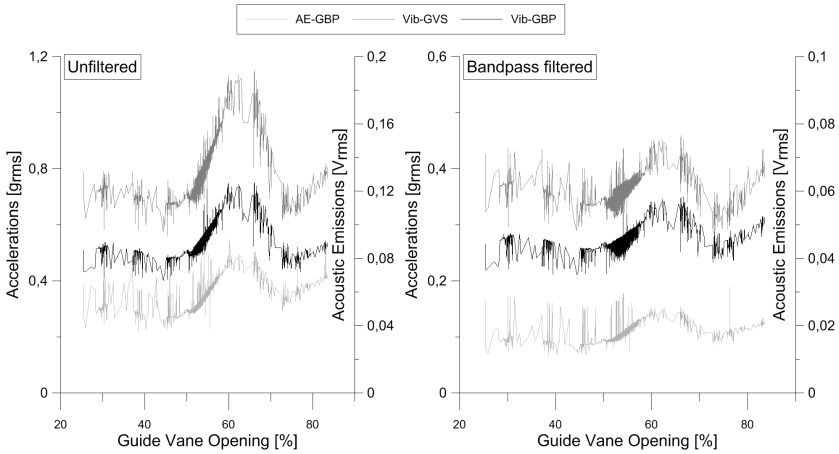

Figure 4.9: *RMS values of the measured vibrations are calculated before and after applying a band pass filter using the assumed frequency band of cavitation induced vibrations. The results are plotted against the guide vane opening at the time of measurement. RMS of (calibrated) raw signal from vibro-acoustic sensors (left), and the same signals after bandpass filtering (*$20 - 25kHz$ *and* $45 - 50kHz$*)(right).*

than the background noise modulation level. An increase by nearly fifty percent is observed around the best efficiency point, where it is noted that draft tube flow patterns associated with the Rheingans frequency are expected to be absent.

The rotational frequency has the largest modulation effect, as observed at the guide vane shaft accelerometer and by the acoustic emission sensor on the guide bearing pedestal. A rather large variance is observed in the measurements where the maximum occurs around about 77% guide vane opening, and this effect is illustrating the variance of cavitation even at relatively constant conditions. Below 50% the modulation is near equal to the Rheingans frequency modulation level.

Considerable modulation by the runner blade passing frequency is observed at the guide vane shaft, but also by the acoustic emission sensor, in the region from about 55% to 70% guide vane opening. In accordance with theory, blade passing frequency modulation is barely evident in the vibrations measured at the guide bearing pedestal (which is assumed to provide the most direct path of propagation from the runner). At the guide vane shaft the modulation levels are comparable to those found at the rotational frequency, but modulation takes place at lower loads.

Modulation at the guide vane passing frequency is found at both measurement points, and by all sensors. The levels are however lower compared to the background modulation, than is found at the rotational and blade passing frequencies. The effect is however more prominent in the acoustic emission measurements.

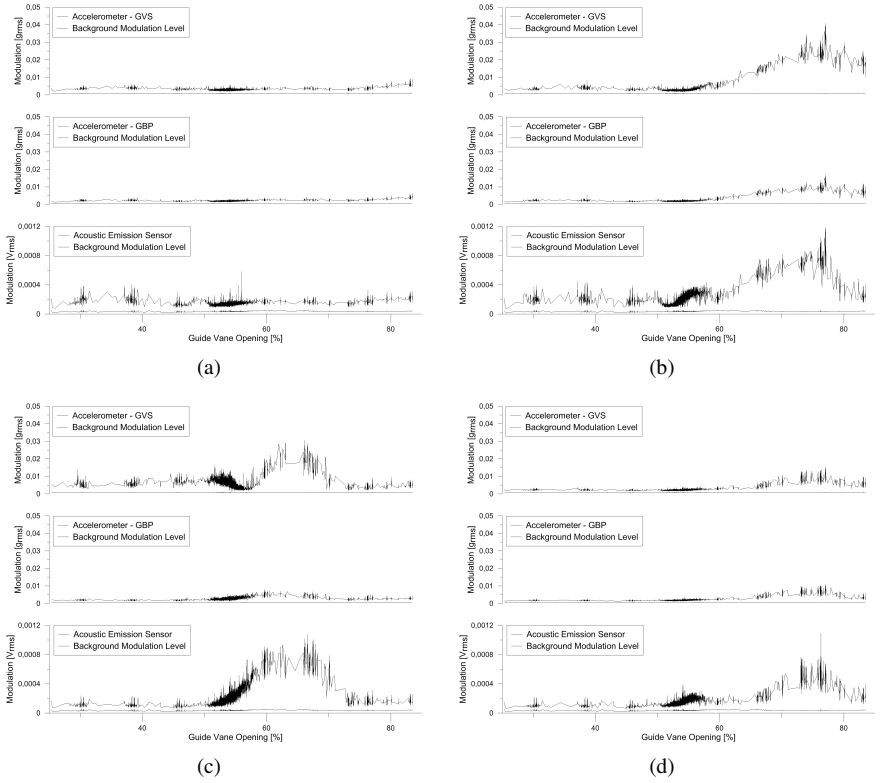

Figure 4.10: *Modulation levels at (a) the Rheingans frequency, (b) the rotational frequency, (c) the blade passing frequency, and (d) the guide vane passing frequency, plotted versus the guide vane opening. Modulation as recorded by the accelerometers at the guide vane shaft and guide bearing pedestal and the acoustic emission sensor at the guide bearing pedestal are plotted separately for each modulation frequency. In each plot, the recorded background level is plotted, appearing as a horizontal line below the main plot. Each set of graphs are plotted with the same axis limits, to illustrate the relative significance of each frequency on the overall modulation. Here it is seen that the blade passing and guide vane passing frequencies both modulate the cavitation in certain ranges of guide vane opening, that do not fully overlap. The graphs are available in larger size in appendix C.2.1*

Investigations at Specific Guide Vane Openings

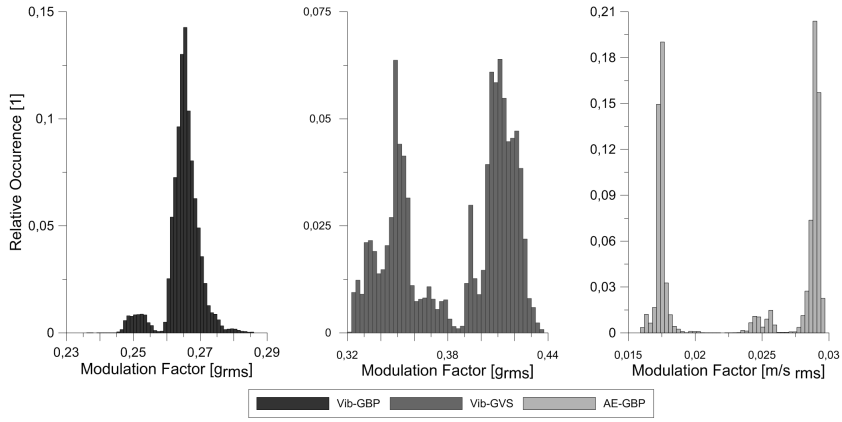

Figure 4.11: *Histographic representation of the variation found in RMS levels of the vibro-acoustic measurements at the* 54% *-* 55% *load interval. The printed histograms are from left to right: Guide bearing pedestal accelerometer, guide vane shaft accelerometer, guide bearing pedestal acoustic emission sensor. The intension of this graphical representation is to illustrate how all test cycles at a specific guide vane opening range are distributed. A bell curve would indicate that all measurements are near normal distributed around a mean value that is not significantly affected by external factors, while the multiple peak examples shown here indicate that some external factors caused the cavitation levels to change. The above example is of special interest because the amount of available data at this guide vane opening is very good. The remainder of the operation interval is illustrated in figure C.5.*

It is noted that operation points that are not in the main operation regions, i.e. not around 55% or 75% guide vane opening, have relatively small, but not insignificant amounts of results. These results have been obtained during ramped operation changes, with 30 minutes of operation at the given guide vane opening. That duration produces around fifty individual result samples. Accumulation during several start-ups has provided hundreds of data points to include.

The results from a selection of one-percent guide vane opening intervals have been considered. First, the RMS levels after band pass filtering has been used to create 50-bin histograms. The bin widths were adjusted to utilize the 50 bins as completely as possible, thus providing a comparable distribution within each range of results. The bin magnitudes are presented as relative occurrence, providing an indication of the dominance of the main bins.

It is evident from the distributions that cavitation intensities varied differently in the different load intervals. The interval up to around 60% guide vane opening (figures C.5(a)–C.5(d)) had a wide distribution, but the intensities were concentrated in (two) groups of bins across the intervals. This is especially evident in the acoustic emission measurements, where the samples are divided in two clearly separated and narrow bin groups.

One notices that, although the guide vane shaft accelerometer in figure C.5(e) disagrees,

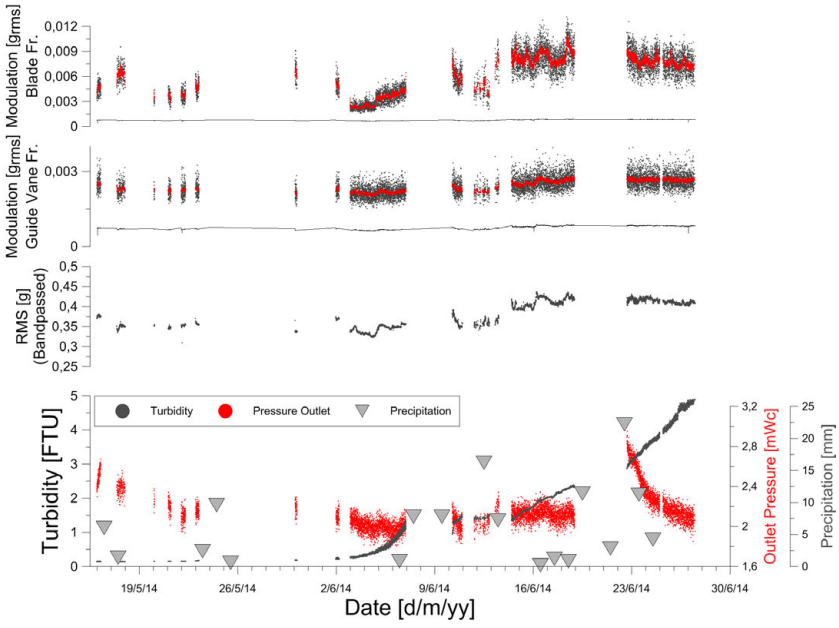

(a)

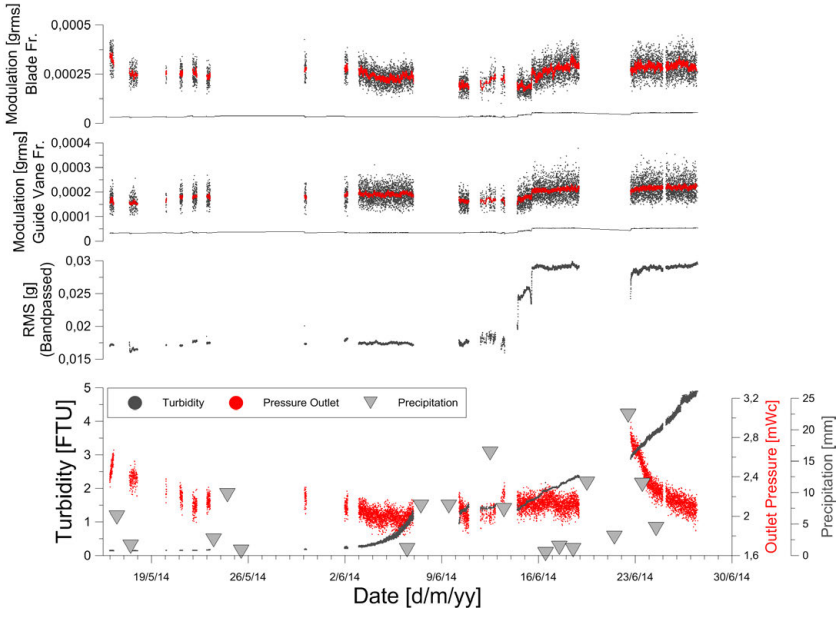

(b)

Figure 4.12: *4.12(a): Svorka R1* 54% *to* 55% *guide vane opening - GVS; 4.12(b): Svorka R1* 54% *to* 55% *guide vane opening - AE*

that the histograms appear to have normal distribution in figures C.5(e)–C.5(g). The cavitation intensities at these guide vane openings appear to be closer to normal distribution than is the case at the lower guide vane openings. This indicates that the guide vane opening is a more dominant factor for overall cavitation intensity in this range. This observation does however have to be cross-checked with the water quality variations during operation.

Turbidity Dependence With the aim of further comparison of recorded cavitation activity with recorded water quality variations several more graphical representations of the selected intervals were produced. In these graphs, modulation levels at guide vane and blade passing frequencies, RMS values after band pass filtering, measured turbidity, turbine outlet pressure, and precipitation recorded by the Norwegian Meteorological Institute were plotted against time. To aid comparability the time axis was kept at the same limits on all graphs. Thus, the relation between turbidity and cavitation intensity can be investigated, without ignoring the time distribution of the samples.

Figure C.6(a) presents the results from the accelerometer at the guide vane shaft for guide vane openings between 30% and 31%, which we see from figure C.5(a) is spread in a non-normal distribution. Similar variance is also found in the AE results in figure C.5(a), and one may look closer at this variation in figure C.6(b). Immediately it appears that the outlet pressure is a factor in terms of vibro-acoustic RMS-level magnitude. One also observes that the modulation levels have larger variance relative to mean values variability. However, one notices that at the end of the period, the levels reach higher magnitudes when the outlet pressure is not as high as in the first part of the period. During this period, however, the turbidity increased by one order of magnitude. When considering the AE measurements of figure C.6(b) there appears to be a turbidity threshold over which the vibration intensity increases, this being exceeded in the two last operation periods.

In the case of 38% to 39% guide vane opening, figure C.5(b) shows that scattering of RMS levels was found at all measurement locations during the period. The observations are clearly divided into two 'bins' at the guide bearing pedestal, but is divided into five 'bins' at the guide vane shaft. Like above, an increased level is observed for both modulation and RMS of the signal at the end of the period, starting around 13/06. It is also noted that the background modulation levels increase during this period. The increased turbidity could be caused by the precipitation during this period. A very similar pattern of events is observed in the 45% to 46% guide vane opening range, figures C.8(a) and C.8(b). However, there seems to exist a stronger correlation to the turbine outlet pressure here. Nevertheless, the increased cavitation activity measured towards the end of the period is clearly present here as well.

As is clearly evident in figure 4.8, 54% to 55% guide vane opening was operated for extended periods in the second part of the period. Thus a more detailed view of the dependency on turbidity is available here. One observes here too, that upon reaching a threshold of about $2FTU$ the cavitation intensity measured increase significantly. On the blade passing frequency modulation of the GVS, the effect is also visible before this

threshold is reached. However, the opposite is found in the blade passing frequency modulation of the acoustic emissions at the GBP. The observations confirms that a general increase of modulation and RMS levels of vibro-acoustic signals occured when the measured turbidity increased. This is in accordance with the distributions in figure C.5(d). One can also pin the date for the observed increase to between 12/06 and 13/06, which coincides with a comparably large rain-fall on the 12th. One also observes that precipitation on 23/06 presumably raised the outlet pressure by 40%; as it subsided the turbidity continued to increase. At the same time the observed cavitation intensity is sustained.

The remaining intervals, corresponding to figures C.5(e)–C.5(g), appear to be normally distributed. The time-depended plots, as well as figure 4.8, shows that none of the guide vane openings were in operation during the period of increased turbidity. Thus, the figures have been omitted from this chapter, but can be found in appendix C.2.1.

5

Evaluation and Discussion of Results

5.1 Experimental Outcome

5.1.1 SAFL Experiments

Initial Remarks

The experiments in the SAFL cavitation tunnel were designed to provide a transition to field experiments in hydropower plants, by providing a real flow environment in which the gas saturation and (potentially) other external factors would be controllable. It was indeed demonstrated that gas saturation studies could successfully be conducted in the facility. Figure 5.1 illustrates the known cavitation regimes on NACA0015 hydrofoils used in the tunnel. It is clear that different regimes were to be expected at the angles of attack that was utilized. While 2° is expected to solely produce bubble cavitation, conditions with more than 4° angle of attack initially experience patch cavitation, later transitioning to sheet cavitation. The cavitation number associated with inception has a higher gradient with reference to angle of attack, than the value associated with transition to supercavitation. Thus, a narrower span between no cavitation and supercavitation is experienced at 2° angle of attack, than at the higher angles. This affected the resolution of the cavitation characterization fingerprints.

The multidimensionality of the test matrix is an added resistance in the evaluation of the results. And it was necessary to clearly define the major demarcations between regimes before comparison of results. Thus, results were split between cases in which the foil had been a smooth NACA 0015 foil, and those in which the flowcontrol "fence" was

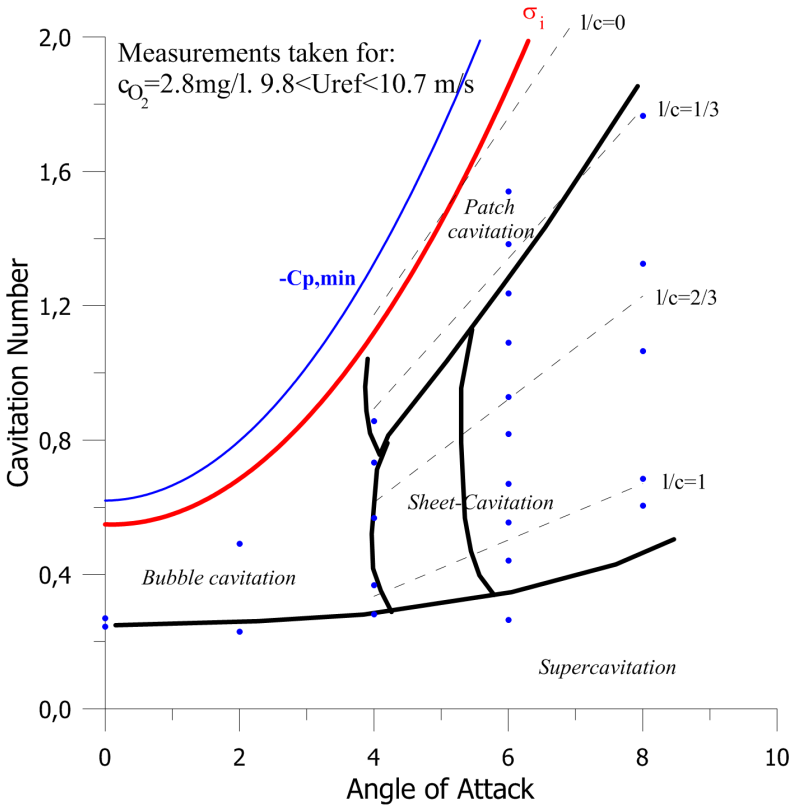

Figure 5.1: *A mapping of cavitation regimes on NACA-0015 hydrofoils in the SAFL cavitation tunnel with respect to variation of angle of attack and cavitation number. l/c is the time averaged relation between cavity length and chord length. Source: Kjeldsen et al [21].*

installed. Furthermore results were divided according to angle of attack of the foil. At this point what remained were the elements of highest interest; high and low gas content, effect on different cavitation mechanisms (governed by angle of attack), the necessary variation of cavitation number to determine inception, maximum vibration conditions, and the transition to super-cavitation.

Relation to research topics The experiments naturally did not add directly to the first research topic, as the on-site water quality instrumentation was used in place of equipment involved in the water quality measurement setup design. However, the experiments provided valuable results concerning the link between gas content of water and the characteristics of cavitation.

The experiments provided valuable data with regard to the effect of gas saturation levels on inception, intensity and supercavitation transition on flows across hydrofoils. This inspires further experiments in power plants were gas saturation levels would be expected to vary significantly through seasons and/or weather conditions. The experiments also provided more experience on use of vibration and acoustic emission sensing equipment and analysis of measured data to evaluate cavitation intensity and characteristics, including (in this setting) lift oscillations on the blade.

Smooth Foil Experiments

2° **Angle of attack** The obtained RMS values of the bandpass filtered vibration measurements presented in figure 4.1 provide the initial indication of the intensity of the cavitation. The use of high frequency bandpass filtered signals one focuses the attention on the modes vibration mostly induced by cavitation; providing a good initial indication of the erosion capacity. With exception of the high gas saturation case with the lowest flow velocity ,one observes that vibration levels increase significantly once $\sigma \leq 0.8$. The mentioned exception case exhibits a small increase of vibration levels around $\sigma = 0.9$, the levels reached are insignificant compared to the rest. The cavitation number at inception in the remaining cases are higher than indicated in figure 5.1, which is probably explained by the disparity of the methods used to identify cavitation. A most significant observation is that the high gas saturation cases all rise to a maximum vibration level before decreasing to near levels similar to cavitation free conditions once the cavitation number is decreased further. At low gas content cases the highest vibration levels were found at the lowest cavitation number achieved. The observation is attributed to the onset, or lack thereof, of supercavitation. This illustrates that while the achieved gas saturation variations did not significantly alter the inception pressure, the characteristic of the cavitation observed did indeed display significant alteration.

Considering first the two cases were flow velocity was $8mps$, the experimental notes show that visibly confirmed cavitation inception took place at $\sigma = 0.77$ and $\sigma = 0.86$ respectively in the low and high gas saturation cases. Additionally, the notes for the low

gas content case mention low buzzing and small ($1-2mm$) cavities on the flush inlay, that was used in place of the fence, when $0.9 \leq \sigma \leq 1.5$. This observation suggests that the small cavities here associated with surface imperfections induce much smaller vibrations, or vibrations in another frequency range, compared to pressure-field-induced cavitation. Furthermore, as is indicated both by the graphic presentation and the experimental notes, one enters the supercavitation domain at $\sigma = 0.65$ in the high saturation case, at which the low saturation case still only exhibits bubble cavitation on the suction side of the foil. From this latter observation, one also realize that the potential damage types are perhaps more susceptible to gas saturation variations than the restrictions one should apply to turbine operation.

For practical reasons the case of $8mps$ flow velocity is the one throughout the test matrix in which the minimum normalized cavitation number possible to achieve in the test section is highest. As the figure illustrates a full description of the possible cavitation conditions was not observed here. It is however notable that the low gas content case found increased vibration levels as the cavitation number decreased, while the high gas content case barely registers as increased when compared to the non-cavitation conditions. The two remaining cases in the figure both exhibit rapid increase of vibrations at high gas content, but the values decreased once the cavitation number dropped below a threshold of $\sigma \approx 0.65$. The experimental notes reports what was visually and audibly identified as nearing super-cavitation during the final stage of this level drop. However, before this the cavitation is described as increasingly covering the suction side of the foil, thus collapsing on the foil itself. It must be assumed that the sum of conditions caused cavitation bubbles to hold a significant portion of non-condensable gas (i.e. air), so that once collapse took place the final stage of implosion was dampened by an air cushion. This effect, previously explored by Kjeldsen (see chapter 2.5) would explain the significant reduction of cavitation induced vibrations. Both cases were recorded as approaching supercavitation when $\sigma \approx 0.5$, while the low gas saturation tests did not approach supercavitation until $\sigma \approx 0.4$. Moreover, the development of the cavitation vibration levels leading up to the supercavitation conditions did not involve a gradual level reductions, but rather continued to increase until the entire suction side and parts of the pressure side was covered by cavitation clouds and bubbles.

The load oscillation analysis, found in figure 4.4, show that a distinct and steady fingerprint exists for the foil when it is not exposed to cavitation. This remains virtually unchanged up to approximately $50Hz$ in the cavitation cases, over which the noise appears white with the exception of an apparent wide peak in the range $75 - 100Hz$. The levels are seen to rise at all higher frequencies once cavitation inception takes place.

4° **Angle of attack** The bandpass filtered RMS results are presented in figure 4.2. In the $8mps$ high gas saturation case the point density is somewhat sparse in the high cavitation vibration interval, due to elimination of low-quality measurements. The results are otherwise clearly indicating that cavitation inception takes place at $\sigma \approx 1.25$. Which, like the 2° angle of attack case, is slightly higher than indicated in figure 5.1.

The high gas content cases clearly increase more quickly than the low saturation cases, when the cavitation number is further reduced. The levels reach a maximum value at $\sigma \approx 1.0$ in the high gas cases, and subsequently subsides as cavitation number continues to decrease. At $\sigma \approx 0.5$ the magnitudes are reduced to non-cavitating levels. The notes on this range reveal that the cavitation covered area as expected increase when $1.0 \leq \sigma \leq 1.25$, where $\sigma \approx 1.0$ corresponds closely to the point in which cavitation coverage reaches the full span of the foil. Furthermore, the range $0.5 \leq \sigma \leq 1.0$ corresponds to when the cavitation on the foil increase towards full coverage in the chord direction as well. Interestingly, the large scale vibration of the foil was increasing in this range, more or less up to the point in which cavitation starts to appear on the pressure side of the foil. This confirms that while the erosive capacity of the cavitation is reduced at low values of σ, the risk of material fatigue is increased. In the $12mps$ case the intensity is sustained at lower cavitation numbers, that according to the notes probably originate from a shift from sheets starting on the leading edge to bubbles/clouds covering a larger parter of the suction side. An instability that could be predicted from the previous work in the tunnel.

The low gas saturation cases are seen to have slightly increased vibration levels from about the same value of σ as was the case in the high saturation cases. However, only the highest velocity case reach the same magnitude as its high gas content counterpart. The maximum levels are reached at $0.5 \leq \sigma \leq 0.75$, the same interval in which the high gas content cases approached supercavitation. The notes reveal that the highest vibration levels are associated with transition from bubbly cavitation to sheets or clouds and increased large scale foil vibration. Further reduction of the cavitation number causes gradual decrease of the high frequency vibrations, which finally recedes to cavitation free levels when supercavitation occurs.

One observes clearly throughout this experimental section that different cavitation mechanisms could be identified by looking at gradients and maxima of the RMS vs σ curve. One also observes the value of high frequency vibration measurements to identify cavitation impacts, while the sensor arrangement also detects low frequency shedding-induced oscillations of the blade. Indeed, a thorough investigation of figure 4.5(b) reveals that the $\sigma = 0.52$ and $\sigma = 0.62$ cases are the only ones to display peaks at $20Hz$ and $40Hz$, and coincidentally the only ones that were recorded to exhibit visibly and audibly confirmed foil vibrations. The free tip of the foil was observed to move $\approx 0.5cm$ perpendicularly to the flow, and the vibration was audible as a deep humming. In the other gas saturation case, figure 4.5(a), vibrations were found at $\sigma = 0.68$, while $\sigma = 0.55$ had supercavitation. At both gas saturations, one observes that supercavitation causes some white noise in the higher spectrum, but normally less than during partial cavitation coverage. But as can be seen it does not produce much vibration in the lower range, or any distinct tone. From an experimentalists point-of-view it is perhaps worth noticing that the relative calm achieved after traversing some heavy cavitation to reach the supercavitation conditions, is notably noisier than cavitation free conditions.

6° **Angle of attack** The bandpass filtered RMS results of the 6° angle of attack case find the vibration levels to start increasing once $\sigma < 2.0$. Like in the previously discussed cases, the high gas content instances experience the most rapid increase of vibration levels when σ is further reduced, except in the $12mps$ case. Here the two curves are generally of the same shape, but the magnitudes of the high gas content case are smaller. That is to say, similar cavitation mechanisms took place at a given σ value, regardless of the gas saturation. The foil started to vibrate when $\sigma = 1.1 - 1.2$, after which the high frequency gradually subside. The exception is low gas, $\sigma \approx 0.8$, were modulated shedding and foil vibration was recorded simultaneously. The question arises as to what causes the cavitation fingerprint to evolve towards gas saturation independence. It is noticeable that the supercavitation condition appears to be universally found in the interval $0.5 \leq \sigma \leq .75$, while the inception point has changed from $\sigma \approx 1.0$ to $\sigma \approx 2.0$ as the angle of attack was increased. This confirms that increasing amounts of tension is applied to the water by the increased angle of attack. It has been the working assumption of this work that water quality is at best/worst a secondary/tertiary factor in determination of the cavitation intensity. From that perspective one must assume that its effects are most visible when the primary factors are only marginally indicating cavitation risk. That is not the case at 6° angle of attack and $12mps$ flow velocity. As such, one might expect the effect of water quality to be less identifiable here. Nevertheless, the consistently lower magnitudes of the high gas saturation case indicates that the dampening effect of non-condensable gas prevails.

The $8mps$ cases retain the pattern found earlier, but the visual observations confirmed a mechanism transition taking place at $\sigma \approx 1.5$. Further reduction of σ caused the foil to achieve supercavitation. Supercavitation was not achieved in the low gas content case. The cavitation initially consisted of bubbles and patches, and the vibration level resided almost completely during the transition to sheet cavitation. Modulated shedding of the sheets caused heavy foil vibration when $\sigma \leq 1.2$.

Investigation of the lift oscillation analysis presented in figure 4.6(a) for the high gas content case reveal a vibration frequency in the range $0.65 \leq \sigma \leq 0.75$. The low gas saturation tests found the foil to be vibrating at all test points where $\sigma \leq 1.11$, but figure 4.6(b) reveals that the induced foil vibrations had different fingerprints depending on σ. When $0.72 \leq \sigma \leq 1.11$ the vibrations were similar to the high gas content case, but at the smaller σ values vibrations more closely resemble those found in the low gas saturation case at 4° AoA. The former interval is here associated with cavitation sheets collapsing mid-foil, and the latter saw collapse initiating nearer to the trailing edge. Finally, the vibration characteristics at $\sigma = 0.39$ resemble cavitation free conditions with slightly raised vibration levels above $100Hz$.

Practical Implications of the Results

Cavitation inception was found to be less affected by gas saturation than supercavitation occurence was. This implies that shifts or stretching, or both, of the σ intervals associ-

ated with different cavitation mechanisms must be present when the gas content changes. In cases of low gas saturation, a larger portion of the interval between inception and supercavitation was characterized as having cavitation noise, but not an erosive potential. However, once σ was sufficiently reduced the resultant cavitation intensity was found to reach larger magnitudes than was the case with a high gas saturation. When encountered in a turbine, one would find audible noise regardless of gas saturation, even if the actual strain on the turbine from the sum of impacts could be varying grossly.

The experiments provide strong indications that the pressure condition required for supercavitation is affected by the gas content. It was observed that supercavitation is occurring at significantly lower cavitation numbers when the gas saturation is low. However, this observation did not hold true in cases of large angles of attack and high flow velocities, in which the effect of gas content appears to be small significance. This transition was found when increasing flow velocity from $8mps$ to $12mps$ at 6° angle of attack.

The above mentioned exceptions at large angles of attack are relevant for cases of very low part, and full, turbine load in Francis turbines. Furthermore, these loads experience low and high flow velocities respectively, relative to the design conditions/BEP. From this one has to assume that gas saturation levels have less effect on cavitation intensity at full load than is the case at part loads. At part loads however, we found that changing gas saturation could bring the flow from cavitation noise to potentially erosive cavitation, or from fatigue inducing load oscillations and into the supercavitation domain. Both of the latter should of course be avoided at all costs. They are mechanisms that present themselves very differently in the audible spectrum. Keeping in mind that the magnitude of the induced vibrations, and hence the cavitation intensity, was generally found to be smaller at lower flow velocities one could argue to low gas saturation invites a certain release of operation restrictions. This should perhaps ideally be utilized through reduced NPSH, rather than operation at extreme part loads. One should also keep in mind that the expected penalty, should the restrictions be set too liberally, would the most severe encountered at these turbine loads.

We found that the periodically shedding cavitation taking place at low σ values gave a smaller fingerprint in the high frequency band associated with cavitation bubble collapse impacts. However, the low frequency vibrations originating from the induced load oscillations were clearly visible when investigating the $0 - 500HZ$ range. This is supported by conclusions from Bajic [7], [8] and [9], in which a general emphasis on the diversity of cavitation mechanisms, from a frequency fingerprint point of view, is emphasized. The results presented above, when investigated in this context, reveals the risk that cavitation mechanisms are neglected because they do not fall within the scope of a cavitation detection design. This confirms the need for local investigation before any long term cavitation detection scheme is installed, if the best possible results are to be expected.

5.1.2 Svorka Experiments

The dual nature of the experiments at Svorka, where some were traditional field measurements and some continuous collection of data from an automated measurement device proved quite successful. The initial experiments served as vital sources of both information and experience when the algorithm was designed for the continuous logging experiment. It was shown in the initial experiments, and results published in an article [30], that cavitation intensity could be estimated by analysis of vibration measurements and knowledge of the hydrodynamic characteristics of the turbine.

Relation to Research Topics

The work at Svorka contributed to all the research topics, but was also a small inhibitor to the fulfillment of research topic 3 given the simplicity of the head race system. Less variation of water quality was found than would have been expected in more complex water ways. However, the experiments has had to come to a conclusion and valuable experience and results have been obtained.

Cavitation Detection Experiments

The following involves the experiments that were conducted at Svorka HPP in the "classical" style; by setting up a sensor array and doing measurements while a predetermined operation schedule was followed. The method provides superb control over the conditions during each measurement, and one is able to make (subjective) notes on other observations during the experiments. How was the noise on the turbine deck? Did the noise alter its character at some time? Moreover, the predetermined schedule ensures measurements at all operation settings of interest. The data produced is stored in it's pure calibrated form, and one thus experiences a maximal degree of freedom when proceeding to the analysis phase. Nevertheless one produces results within a very limited period, often just a few hours, and ones opportunity to assess the present conditions compared to at other times is limited. However, the results are valuable when design of an analysis algorithm is required.

Continuous Cavitation and Water Quality Monitoring

The period had spells of warm and dry weather, interrupted by some heavy rainfalls. Thus one could hope to find that some variation of water quality had occurred. The observation is continuously increasing turbidity levels starting after nearly a week of precipitation free conditions. The first spells of rain after the increase does not appear to affect the turbidity. However, there appears to be a further increase of the turbidity following the heavy rains on 13.06.15 and 22.06.15. The author is not an expert of hydrology, but it stands to reason that the terrain in the catchment area of the HPP governs the reaction time we observe at

the turbine. In that context, one must be careful to remember that the hydrology of the outlet does not necessarily have similar time constants. Indeed it is clearly seen in figure 4.12 that only heavy precipitation affects the flow of the outlet river sufficiently to alter the outlet conditions in any significant way. The level is also seen to drop rapidly after the rain stops. However, it seems not unlikely that turbidity could continue to deteriorate in the inlet reservoir some time after the maximal inflow from the terrain.

It is clear from the data in figure 4.9 that the maximal overall vibration magnitudes are found in the $60\% - 70\%$ GVO range. The same was found after band pass filtering the raw signals. Furthermore, blade passing frequency modulation of the vibrations of the guide vane shaft, but also the acoustic emissions, is in accordance with the general level. However, it was found that similar magnitudes of modulation by both the rotational frequency of the runner and the guide vane passing frequency occurs around 75% GVO. It is therefore possible that several cavitation mechanisms exist at different part loads for this turbine. At the same time, one observes that the variance of the modulation increases in the elevated zones. Unfortunately the occurrences of operation in these interval took place early in the period, when the turbidity was constant.

The figures C.6, C.7, C.8, and 4.12 illustrates the span of loads that was operated during variation of turbidity. Some important variations, that are due to the physical realities of the turbine type can be seen if one studies these figures closely. One important such variation is the considerable difference in the outlet pressure. Some study of the axes reveal that the pressure at $54\% - 55\%GVO$ is only about a third of that at $30\% - 31\%GVO$, id est the cavitation number is lowered as one increases the load. One should therefore expect that the likelihood of cavitation is greatest in the upper part load region, even if the angles of attack also play an important role for the whole picture. This is also what we see, assuming that the modulation peaks mentioned above represents separate cavitation mechanisms. The most prominent, and promising, feature of the figures mentioned above, is the increased cavitation levels that manifest themselves from around the time of the initial turbidity increase. The full-page figures represent one vibration measurement at a guide vane shaft, and the acoustic emission measurement from the guide bearing pedestal. In accordance with the general observations in figure 4.9, the (relative abundance of) data recorded at $54\% - 55\%GVO$ show the blade passing frequency modulation of both measurements to most prominently increase in parallel with the turbidity rise. This is also the modulation level that was found to increase in general close to this GVO value. It stands to reason that the effects of cavitation intensity modifying factors would have the biggest impact here. While the modulation level of the vibrations is found to increase almost from the moment of turbidity rise, and only at a high turbidity level reach a "saturation" level, the acoustic emissions are seen to have a ramped increase that could be argued to be caused by the turbidity surpassing a threshold. From this several scenarios could be envisioned:

- The cavitation intensity slowly increase, as more nuclei seed ever more cavitation bubbles, until the cavitation zones have reached their potential for simultaneous occurrences. At the same time the acoustic emissions are initially low, because the

cavitation is much too weak to cause elastic waves or cracking. At some point the cavitation impacts reach a power that induces significant acoustic emission, causing a sudden rise in said measurement.

- The initial increase of vibrations have other explanations, and inception takes place where the ramp appears in the acoustic emissions RMS values. This correlates to a sufficient nucleus density to cause steady or continuous occurrence of cavitation bubbles.
- The increased cavitation intensity is not caused by turbidity alterations, but rather by reduced tensile strength of the water as a result of temperature change. Examples of tensile strength of water as a function of temperature is found in reference [24], where Mørch refers to work by Andreas Keller.

Regardless of these scenarios it is evident that cavitation activity varies at given operation settings/loads, and further investigations could shed more light on these processes. Having the opportunity to experiment in a power plant with a more complex waterway could perhaps have provided data that could more easily be analyzed, but we did indeed find cavitation variations even in a power plant with a very simple waterway.

Additional Notes and practical implications

The measurements at Svorka, though riddled by postponed startup and for a time interrupted by unexpected problems, produced somewhere between 150 000 and 200 000 measurement series, each analyzed and condensed into 47 separate result values. This data set needed to be analyzed per the aims of the study, but a quality check would also have to be performed. This is a challenging task, given that the raw data for the results one investigates is not available. One can still detect outliers quite easily, but systematic errors of data acquisition or pre-processing could disguise itself well. The most problematic error source in this regard was a systematic error that rendered the acceleration measurements from the second period invalid (and thus omitted from the results). However, we are certain that the results presented are valid.

5.2 Evaluation of Experimental Experiences

The execution of unmonitored continuous analysis and storage of raw data is evidently placed somewhere on the axis between solely storing measured data to a storage medium and automatic generation of an overall report[1]. The value of results that are stored would in the same interval vary according to the needs and capabilities of the end user. In the case of cavitation detection, we initially treated measurements as sequences that would be individually analyzed and averaged for given operation settings. As such, the field

[1] Which would be the final product of traditional experiments

measurement method would usually include a 30-second recording at a certain turbine load, that would be processed according to the algorithm described in chapter 3.3.2. This included recording a sequence of approximately 30 seconds followed by averaging frequency analysis results for a number of subsequences in order to amplify modulation frequencies of interest. However, in the context of continuous monitoring this is an element of data loss that perhaps should be avoided, as in contrast to the field measurement one does not store the raw data after analysis. From that perspective it would perhaps be more valuable to store results from every sub-sequence, rather than averaging an arbitrary number of successive sequences (as was done in the current experiment). There are several merits to this, including more efficient use of the (partly limited) computing resources available.

While the use of an automated test system provides large amounts of data, figure 4.8 serves to illustrate the potential for lack of access to certain operation regions. In the case of Svorka, a constant load of $54-55\%$ was operated for prolonged periods. This situation provided very good data at that specific load, but we are left with little to no knowledge of what would happen at other loads. This could be valuable from a local point-of-view; a very good data set is available at that load, but no actual base for evaluation of operation restrictions arise. nevertheless, any time distribution of the measurements provide some increased dimension compared to a one-day field measurement effort.

6
Conclusion

A vast body of experimental experience exists in the literature concerning the presence of cavitation nuclei and their effect on water's tensional strength. As one must perhaps expect the focal point of many of these experiments have been to establish the maximal tensional strength obtainable in extremely clean water samples. The fact that relatively high tensional strengths has been achieved, simply through pre-pressurization of ordinary tap-water, suggested that gas content of the water would have a discernible effect on the cavitation inception pressure in hydro-power contexts. Explanation given by e.g. Mørch on the significance of particles with regard to their cavitation inducing properties also suggested that the kind of particles expected to be found in hydro power contexts would significantly affect inception pressure. Furthermore, chapter 2.5 identified both particle and gas content as relevant factors when determining cavitation characteristics.

With the above mentioned experience in mind, an experimental course was laid out with the aim to test water quality effects on cavitation in hydropower and hydropower-mimicking flow regimes. Not an absolute premise for success it nevertheless quickly became evident that a cavitation quantification algorithm that didn't require storage of large amounts of raw data would greatly improve the outcome of the project. The experience needed was acquired through traditional field measurements at Svorka HPP and gas saturation effect studies at SAFL, allowing installation of a prototype system at the Svorka plant. An experimental high-pressure water sampling tank was intended to measure turbidity and dissolved oxygen at the inlet condition of the turbine. While the DO measurement had to be discarded, the remaining data indicated that increased cavitation intensity could be related to increases in turbidity of the produced water. Rather than finding a linear relationship between the turbidity and cavitation a thresholding effect was observed, where the intensity was found to increase when the turbidity exceeded a certain level. While it

is tempting to quantify the threshold, it is likely that it varies according to local conditions at the turbine in question. Interestingly, one could not observe a mitigating effect of increased outlet pressure caused by the same rain that presumably contributed to the turbidity increase.

The SAFL experiments revealed valuable results with regards to gas saturation dependence. It was found that the cavitation number at inception was near unaffected by gas content, but the cavitation mechanism/regime transitions were found to change significantly. Close to the inception pressure, one observed that the low gas content cavitation vibration level was lower than the corresponding high gas saturation case. Furthermore, transitions identified by changing vibration levels, as well as visible and audible changes, were found to shift towards lower cavitation numbers when the water was degassed. This is attributed to reduced concentrations of cavitation nuclei, and ultimately to lower air fractions in collapsing cavitation sheets when approaching supercavitation. It was therefore concluded that cavitation loads near the inception pressure are reduced following de-aeration of the water, while the opposite is true in cases of very low cavitation numbers.

At Svorka, field test defined to regions of cavitation activity where it was concluded that only the maximum load cases were found to have erosive potential. Furthermore, a continuous cavitation and water quality monitoring system was tested using an algorithm of data reduction in order to preserve only the results that would be used in further analysis. The experiment would have benefited from time to perform one or two more revisions during its deployment, but revealed some interesting results with regards to turbidity dependence of cavitation intensity. A significant increase of turbidity was found to occur during the latter part of the deployment period and a parallel increase of cavitation intensity levels was observed. It appeared that the turbidity needed to exceed a certain threshold before it affected the intensity, after which a close to linear response was observed.

6.1 Contributions

A dual obligation was imposed on the author in this projects. As a scientist and university-enrolled PhD candidate an obligation to contribute to the body of knowledge on cavitation and cavitation nuclei, specifically their impact on hydro power contexts. However, as an engineer in a small R&D company there were obligations to produce a product or service that add to the commercial basis of the same company. While it is not uncommon that some such duality occurs, after all most students eventually use their acquired skills in some sort of value production outside the university sphere, it is very direct in the scope of "PhD in Industry". While the company obligation has sometimes led to divergence from the scientific project, both have also served synergetically. A continuous monitoring system was developed, and it can be used both for further scientific investigation and to provide customers with required knowledge.

The experiments at SAFL and Svorka were facilitated by the co-supervisor, and initial ef-

forts with regards to signal recording and analysis was supported by Håkon Hjort Francke and Xavier Escaler respectively. As the project progressed this work was carried out by the author from the planning stage to paper drafts that were then finalized as team efforts with supervisors and research group. The continuous monitoring system was designed, built (signal recorder hardware), and programmed by the author, who also deployed and supervised the system during operation. Naturally, the post-processing of the results, and rejection of a significant part of them, was also performed by the author. This has put him in possession of knowledge that will be valuable to Flow Design Bureau as well as providing new knowledge through this publication. While the results herein are not conclusive, it has been shown that relatively cost-effective data recording/analysis systems can be built and deployed to provide new knowledge to the scientific community, but also to the end users of this knowledge; power production companies. Our cooperation with Statkraft AS also shows that interest in exploring new knowledge exists in the industry.

It seems clear that this thesis has contributed both to the concepts needed for water quality and cavitation measurements, and new knowledge towards the effect of water quality on cavitation. It was showed clearly in the SAFL experiments that the gas content affected the mechanics of cavitation after inception. The Svorka experiments indicated that turbidity above a certain threshold, which is here interpreted as a certain threshold concentration of particles in the water, increased the intensity of cavitation under otherwise similar conditions.

6.2 Future Work

The cavitation detection and data storage algorithm used during the continuous monitoring experiment was in many ways designed with too much likeness to the traditional field measurements from which experience was drawn for the design. The design did not properly distribute CPU load, and inflicted unnecessary loss of temporal resolution. Experience will be drawn from the post-processing of the results and an improved algorithm worked out. Key elements include a full elimination of the time series length dependency. The consideration of least time series period for validity of data will be addressed rather by combining consecutive result sets, rather than by analyzing 30 second bulks of measurements.

The water quality sampling system should be improved by moving the inlet to the side of the tank, as well allowing water to flow out through both the top and the bottom access holes. For prolonged operation the system should be fitted with automatic valves for regular flushing of inlet and outlet hoses, as well as pressure guards to ensure sealing of teh power plant water way in case of leaks. Ideally the DO measurement should be replaced by a total dissolved gas measurement[1], in which case the turbidity measurement may be moved to the draft tube outlet or a similarly accessible location.

[1] See chapter 2.4.2.

One should launch a study to better investigate the presence of variations caused by seasonal change or weather conditions in a suitably complex head race system. For this purpose an improved water sampling tank should be designed using experience from the initial experiment. The new design should to a larger extent take in to account potential for buildup of air and settling particles in the tank, this being a zone of strongly reduced flow velocity. While this experiment would not necessarily be too costly, it should be carefully planned and located, in order to provide the necessary insight.

It was clear that spending a single day of mapping cavitation characteristics could not reveal answers with regards to the effect of water quality. However, it has also been found that simply deploying a continuous measurement device could also prove to be insufficient. The inherent strength of the field measurement strategy proves to be found to a significant extent in the vertical integration of such a project in the power plant owner structure. Operation plans are produced and validated prior to the experiment, and in general a close cooperation is taking place with the local staff. This provides ample opportunity to perform measurements at all turbine loads of interest, but it is at the same time not possible to detect effects of changes that might occur on timescales of days or weeks. It is therefore a concluding remark from this work that production planning should take a continuously measuring system in to account, in order to maximize the value of the measurement project. According to the predetermined needs of the project, such action could be revision of load changing strategy by ramping any non-critical load change to provide steady operation for anything from two to five minutes at given intervals, especially in load regions of certain interest (such as lower load restriction). In the case of the current experiment, also to provide such data during periods of observed water quality variations.

6.3 Concluding Remarks

It seems unfeasible to design an affordable water quality sensor array that could quantify total dissolved gas content, gas bubble and particle occurrence, and providing knowledge of types and size distributions of said particles. This sort of system would involve extraction of water samples, and would most likely require microscope inspection of particles retrieved from these samples. The gas saturation measurement system needed to realize this was quoted by Pro-Oceanus Systems Inc. at close to $ 34000 and would include necessary assistance systems to prevent moisture from disrupting the quality of the measurements over time. The evaluation of particle properties would however require regular labor, continuity by having a trained person do all evaluations, and equipment to take samples, dry them, and inspect them.

Bibliography

[1] *Springer Handbook of Experimental Fluid Mechanics*. Springer.

[2] L. et al Alfayez. The application of acoustic emission for detecting incipient cavitation and the best efficiency point of a 60kw centrifugal pump: case study. 38:354–358, 2005.

[3] A. Andersen and K.A. MÃ¸rch. In situ measurements of tensile strength of water.

[4] Roger E. A. Arndt. From wageningen to minnesota and back: Perspectives on cavitation research. In *Sixth International Symposium on Cavitation, Cav2006*.

[5] Roger E. A. Arndt. Some remarks on hydrofoil cavitation.

[6] ASME. *The Non-Effect of Dissolved Air on Cavitation Erosion*, volume 88. ASME FED.

[7] Branko Bajic. Multidimensional diagnostics of turbine cavitation. 124:943–950.

[8] Branko Bajic. Methods for vibro-acoustic diagnostics of turbine cavitation. 40(1):87–96, 2003.

[9] Branko Bajic and Andreas Keller. Spectrum normalization method in vibro-acoustic diagnostic measurements of hydroturbine cavitation. 118(4):756–761, 1996.

[10] Hermod Brekke. *Pumper & Turbiner*.

[11] Christopher Earls Brennel. *Cavitation and Bubble Dynamics*. Oxford University Press.

[12] Xavier Escaler. A vibratory approach to cavitation erosion prediction.

[13] Xavier Escaler. Detection of cavitation in hydraulic turbines. 20:983–1007, 2006.

[14] J. C. Fisher. The fracture of liquids. 19, 1948.

[15] Francis E. Fox and Karl F. Herzfeld. Gas bubbles with organic skin as cavitation nuclei. *The Journal of the Acoustical Society of America*, 26(6):984–989, 1954.

[16] R. FÃ$\frac{1}{4}$rth. On the theory of the liquid state. *Mathematical Proceedings of the Cambridge Philosophical Society*, 37:252–275, 7 1941.

[17] Andreas P. Keller. Cavitation scale effects - empirically found relations and the correlation of cavitation number and hydrodynamic coefficients. In editor, editor, *Proceeding of CAV2001*.

[18] A.P. Keller. Influence of the cavitation nucleus spectrum on cavitation inception, investigated with a scattered light counting method. 94:917–925.

[19] Hǫn Hjort Francke. Increasing hydro turbine operation range and efficiencies using water injection in draft tubes, 2010.

[20] Pardeep Kumar.

[21] M. Effertz M. Kjeldsen, R.E.A. Arndt. Spectral characteristics of sheet/cloud cavitation. volume 122(3), pages 481–487, 2000.

[22] et al Marshall, H. B. Cavitation inception by almost spherical solid particles in water. 15(2), 2003.

[23] Roger E. A. Arndt Morten Kjeldsen. Blade load dynamics in cavitating and two phase flows. In *Proceedings of the 7th International Symposium on Cavitation, Cav2009*.

[24] K. A. MÃ¸rch. Reflections on cavitation nuclei in water. 20, 2004.

[25] Tomaz et al Rus. An investigation of the relationship between acoustic emission, vibration, noise and cavitation structures on a kaplan turbine. 129:1112–1122.

[26] Bryan Schofield. Correspondence regarding hgtd probe.

[27] C.E. Brennen S.L. Ceccio. Observations of the dynamics and acoustics of travelling bubble cavitation. 233:633–660, 1991.

[28] H N V Temperley. The behaviour of water under hydrostatic tension: Iii. *Proceedings of the Physical Society*, 59(2):199, 1947.

[29] D.H. Trevena. *Cavitation & Tension in Liquids*. Adam Hilger IOP Publishing Ltd., 1987.

[30] et al Xavier Escaler, Jarle Vikør Ekanger. Detection of draft tube surge and erosive blade cavitation in a full-scale francis turbine.

[31] David E. Yount. Skins of varying permeability: A stabilization mechanism for gas cavitation nuclei. *The Journal of the Acoustical Society of America*, 65(6):1429–1439, 1979.

A

Selected Papers

A.1 Detection of Draft Tube Surge and Erosive Blade Cavitation in a Full-Scale Francis Turbine

Is not included due to copyright

B

Secondary Papers

B.1 Cavitation Intensity Measured on a NACA0015 Hydrofoil with Various Gas Contents

The contents of this article was presented by the author at the Cav2012 conference in Singapore, and concerns the data recorded on the first visit by the author to SAFL in 2011.

Is not included due to copyright

B.2 Influence of Draft Tube Flow Control System on Cavitation Behavior on a Medium Pressure Francis Turbine

The contents of this article will be presented at the Cav2015 conference in Lausanne, and concerns the effects of a draft tube water injection system on cavitation behavior. The data was collected during several experiments at the Svorka HPP.

Is not included due to copyright

C Other

C.1 Technical Specification for Experiments

C.1.1 SAFL 2014

Recording Device

The sensors were recorded using a National Instruments cDAQ-9084 modular integrated controller, running NI's LabVIEW Real-Time operating system. An NI 9234 module was used to record the accelerometers, and an NI 9205 module was used to record the AE-sensor and turbidity probe. Data was streamed from the recorder to the analysis computer via an ethernet connection.

Analysis Device

The data was appended, validated and analysed; and results stored, using an NI 3100RT Single-Core Industrial Controller with LabVIEW Real-Time OS. Log files were stored locally.

Sensors

Accelerometers Two accelerometers of type B&K 4397a were used. One mounted radially (relative to rotational axis of turbine) on the guide bearing pedestal housing, and

the other mounted axially on a guide vane shaft end. Both sensors were located at angular location denoted as $270°$ relative to previously used reference. The accelerometers were mounted to the housing/shaft using cemented-on threaded studs. The data was recorded at a rate of $51.2kHz$.

Acoustic Emission Sensor The acoustic emission sensor of type Kistler 8152B111, connected to a Kistler 5125 preamplifier, was mounted on the guide bearing pedestal housing, using a magnetic clamp. Its angular position was like that of the accelerometers; $270°$ relative to the reference. The data was recorded at a rate of $100kHz$.

Turbidity Probe The turbidity probe used was a Seapoint Turbidity Sensor, set to a range of $0 - 25FTU$.

C.1.2 Svorka 2012

C.1.3 Cavitation and Water Quality Monitoring at Svorka Powerplant

Recording device

The sensors were recorded using a National Instruments cRIO-9076 modular integrated controller, running NI's LabVIEW Real-Time operating system. An NI 9234 module was used to record the accelerometers, and an NI 9205 module was used to record the AE-sensor and turbidity probe. Data was streamed from the recorder to the analysis computer via an ethernet connection.

Analysis device

The data was appended, validated and analysed; and results stored, using an NI 3100RT Single-Core Industrial Controller with LabVIEW Real-Time OS. Log files were stored locally.

Sensors

Accelerometers Two accelerometers of type B&K 4397a were used. One mounted radially (relative to rotational axis of turbine) on the guide bearing pedestal housing, and the other mounted axially on a guide vane shaft end. Both sensors were located at angular location denoted as $270°$ relative to previously used reference. The accelerometers were mounted to the housing/shaft using cemented-on threaded studs. The data was recorded at a rate of $51.2kHz$.

Acoustic Emission Sensor The acoustic emission sensor of type Kistler 8152B111, connected to a Kistler 5125 preamplifier, was mounted on the guide bearing pedestal housing, using a magnetic clamp. Its angular position was like that of the accelerometers; 270° relative to the reference. The data was recorded at a rate of $100kHz$.

Turbidity Probe The turbidity probe used was a Seapoint Turbidity Sensor, set to a range of $0 - 25FTU$.

C.2 Additional Results from Experiments

C.2.1 Cavitation and Water Quality Monitoring at Svorka Powerplant

R1: May '14 to August '14

Some text about the figures found here

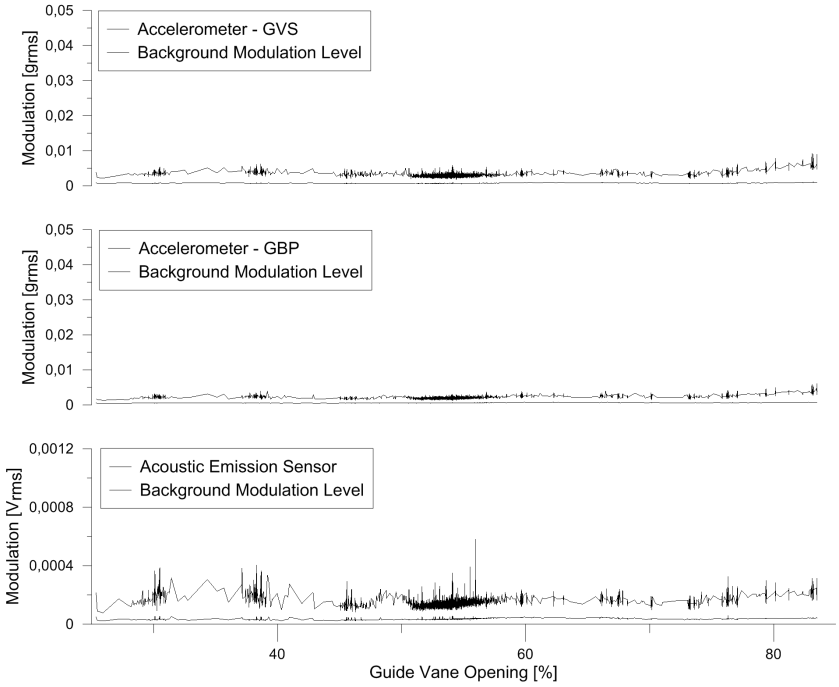

Figure C.1: *Modulation levels at the Rheingans frequency, plotted versus the guide vane opening. Modulation as recorded by the accelerometers at the guide vane shaft and guide bearing pedestal and the acoustic emission sensor at the guide bearing pedestal. In each graph, the recorded background level is plotted, appearing as a horizontal line below the main plot.*

Modulation Levels vs GVO Some text

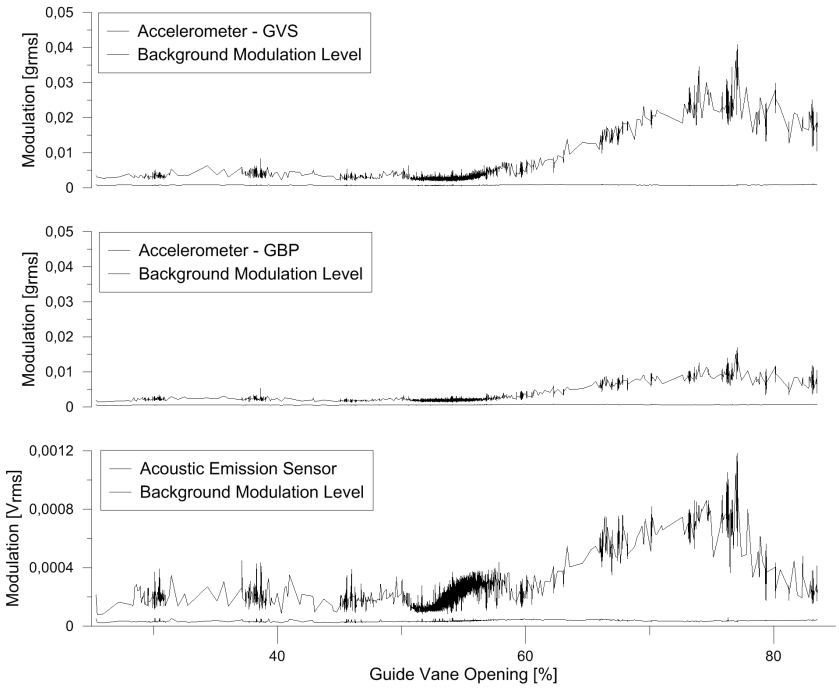

Figure C.2: *Modulation levels at the Rheingans frequency, plotted versus the guide vane opening. Modulation as recorded by the accelerometers at the guide vane shaft and guide bearing pedestal and the acoustic emission sensor at the guide bearing pedestal. In each graph, the recorded background level is plotted, appearing as a horizontal line below the main plot.*

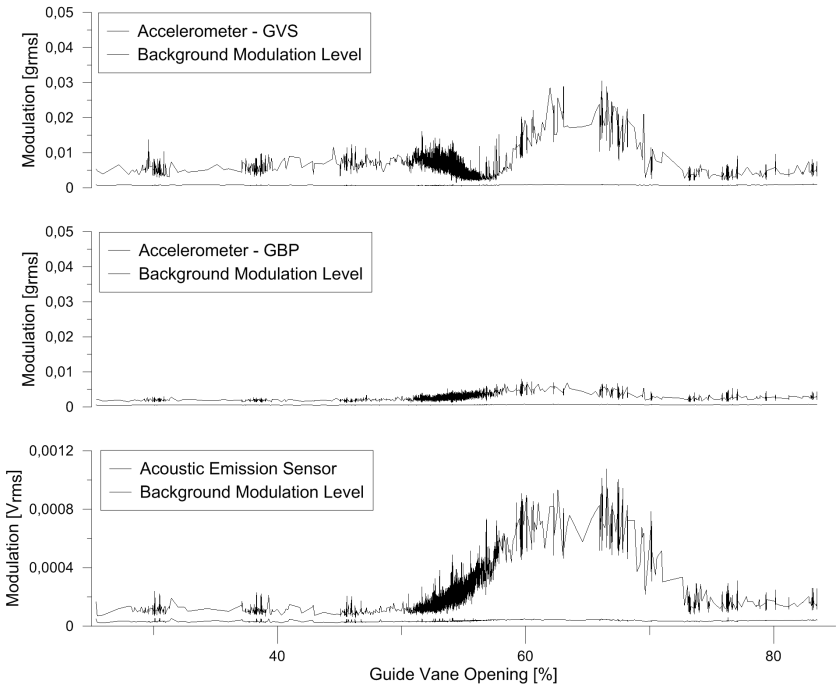

Figure C.3: *Modulation levels at the Rheingans frequency, plotted versus the guide vane opening. Modulation as recorded by the accelerometers at the guide vane shaft and guide bearing pedestal and the acoustic emission sensor at the guide bearing pedestal. In each graph, the recorded background level is plotted, appearing as a horizontal line below the main plot.*

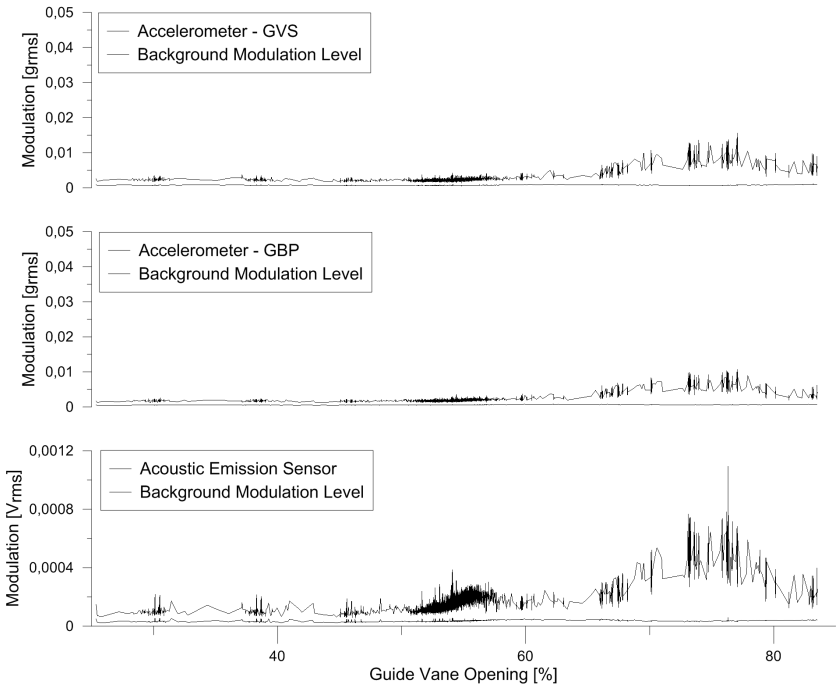

Figure C.4: *Modulation levels at the Rheingans frequency, plotted versus the guide vane opening. Modulation as recorded by the accelerometers at the guide vane shaft and guide bearing pedestal and the acoustic emission sensor at the guide bearing pedestal. In each graph, the recorded background level is plotted, appearing as a horizontal line below the main plot.*

GVO-specific Modulation Histograms

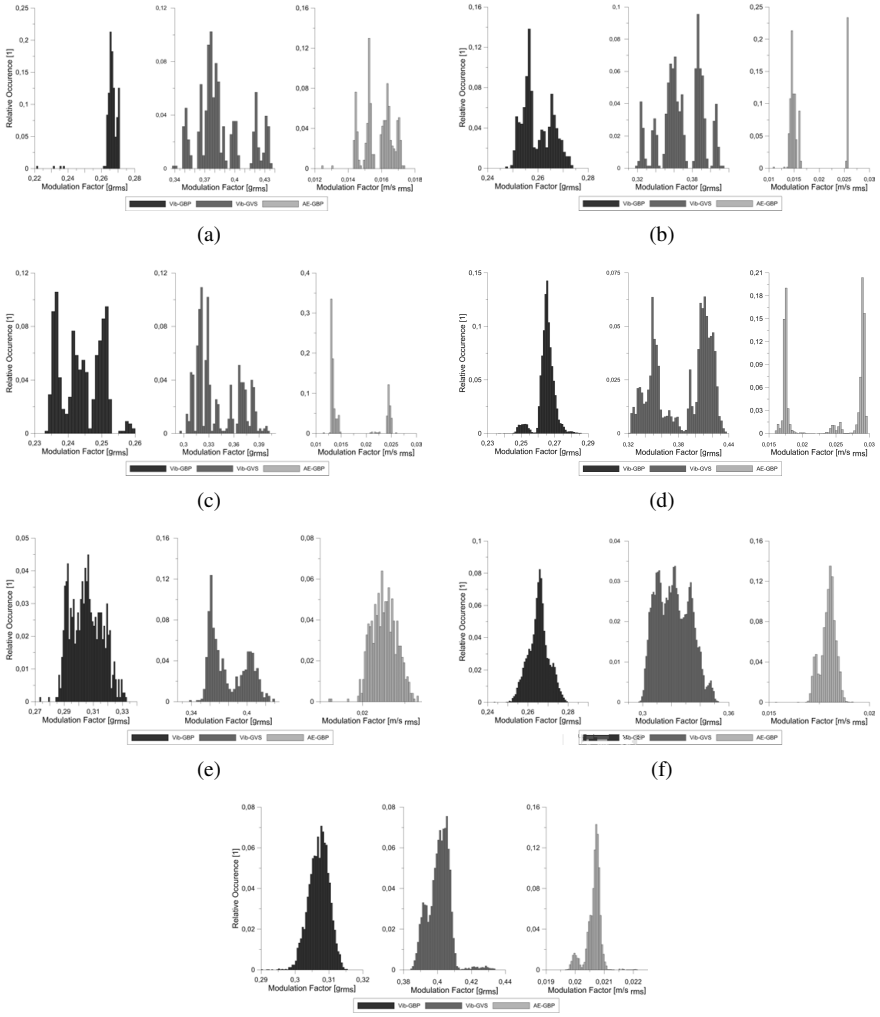

Figure C.5: *Histographic representations of the variation found in RMS levels of the vibro-acoustic measurements at the following intervals: C.5(a)* 30% - 31%*; C.5(b)* 38% - 39%*; C.5(c)* 45% - 46%*; C.5(d)* 54% - 55%*; C.5(e)* 67% - 68%*; C.5(f)* 76% - 77%*; C.5(g)* 83% - 84%*; Each set of histograms are from left to right: Guide bearing pedestal accelerometer, guide vane shaft accelerometer, guide bearing pedestal acoustic emission sensor. The figures are intended to illustrate the characteristics of variation found in the overall levels of cavitation induced vibrations. While a single-bell shape imply distribution around a mean value, multiple-bell shaped histograms implies that something has caused the cavitation conditions to change.*

GVO-specific Modulation Levels vs time and turbidity

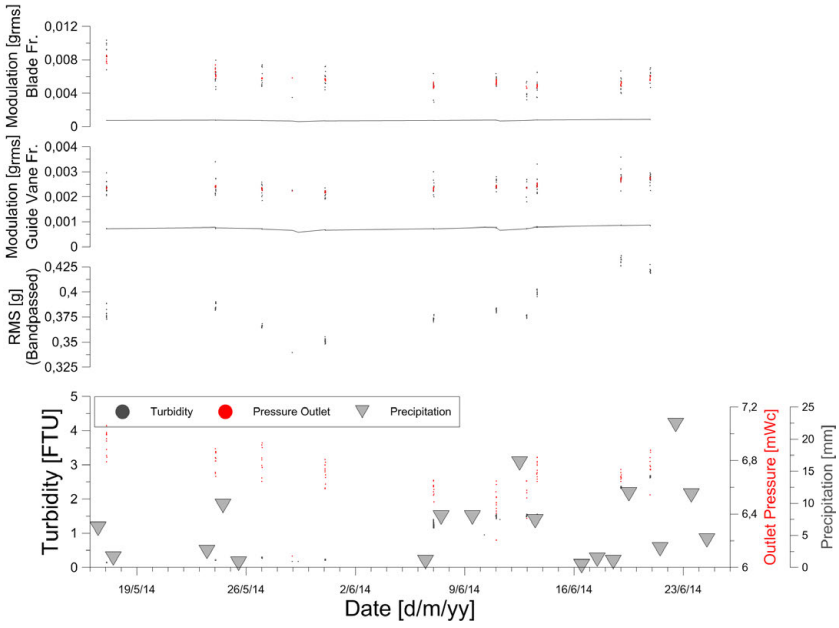

(a)

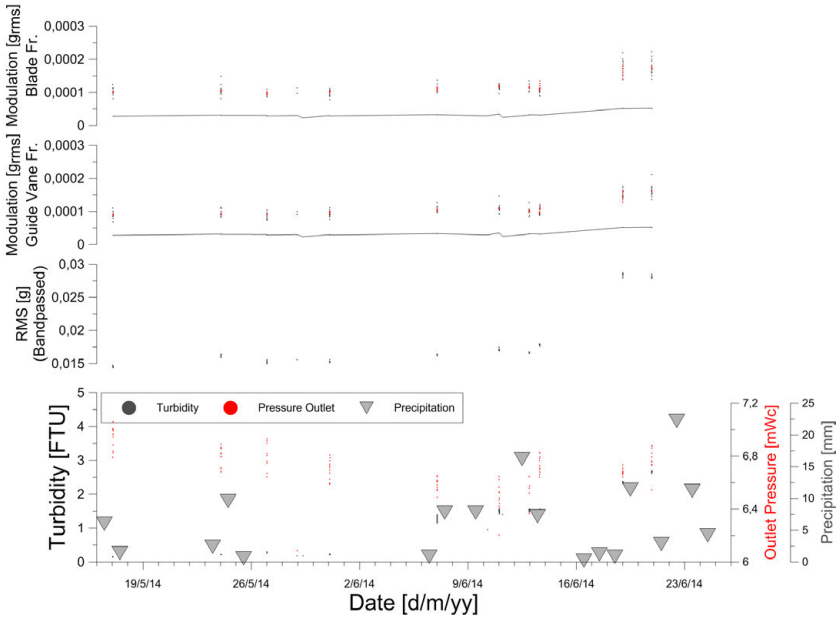

(b)

Figure C.6: *C.6(a): R1* 30% *to* 31% *GVO - GVS; C.6(b): R1* 30% *to* 31% *GVO - AE.*

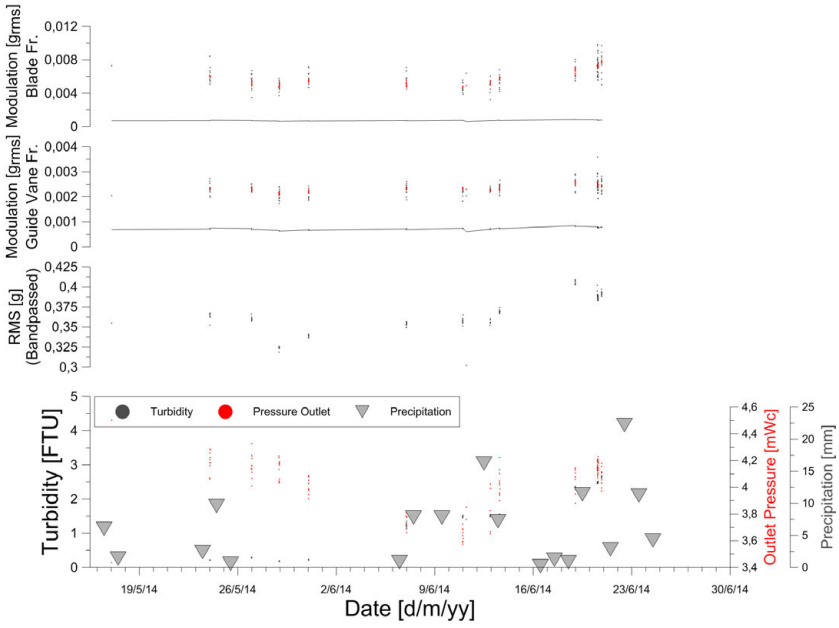

(a)

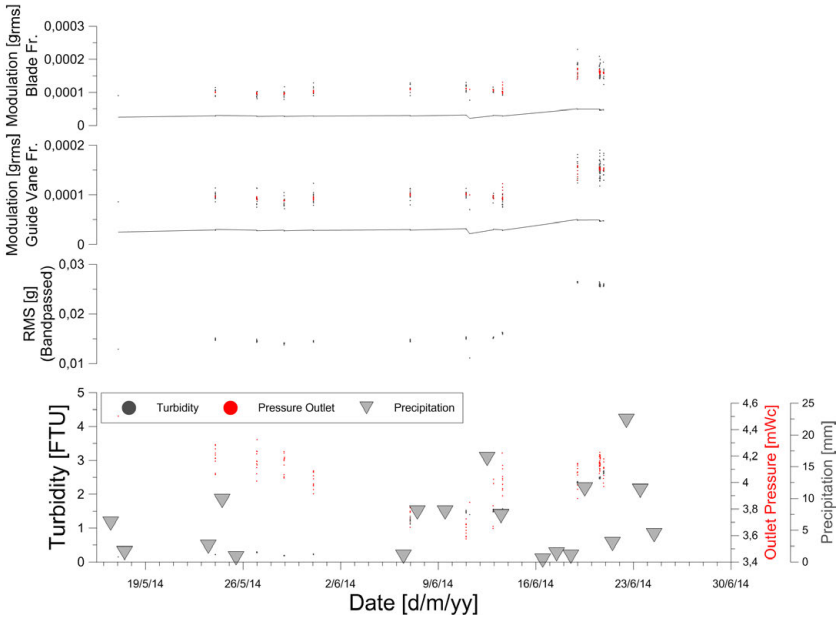

(b)

Figure C.7: *C.7(a): R1* 38% *to* 39% *GVO - GVS.; C.7(b): R1* 38% *to* 39% *GVO - AE.*

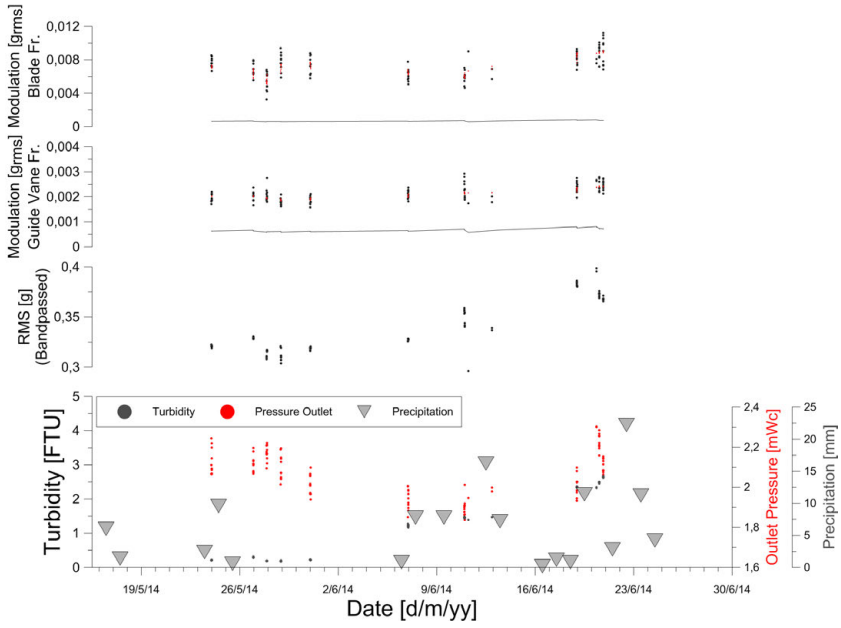

(a)

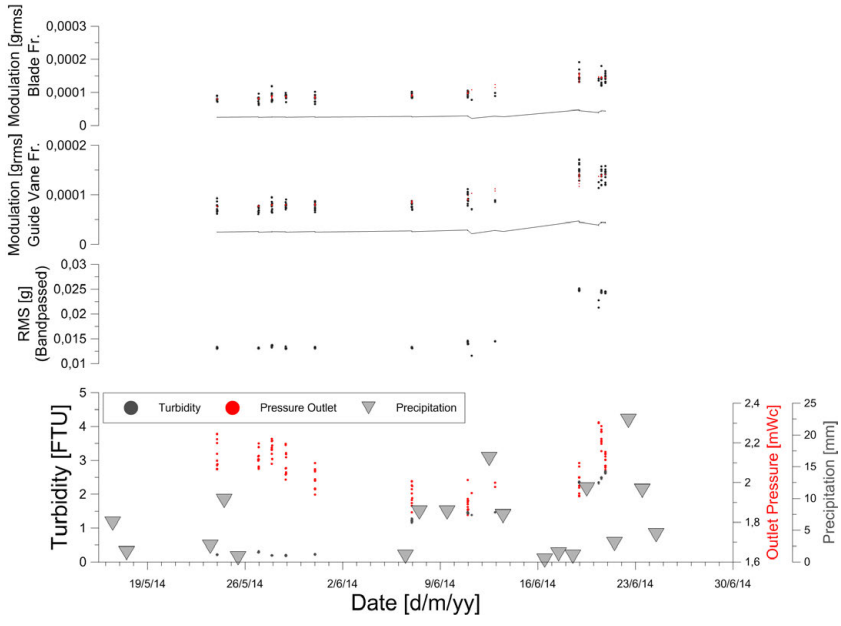

(b)

Figure C.8: *C.8(a): R1* 45% *to* 46% *GVO - GVS; C.8(b): R1* 45% *to* 46% *GVO - AE*

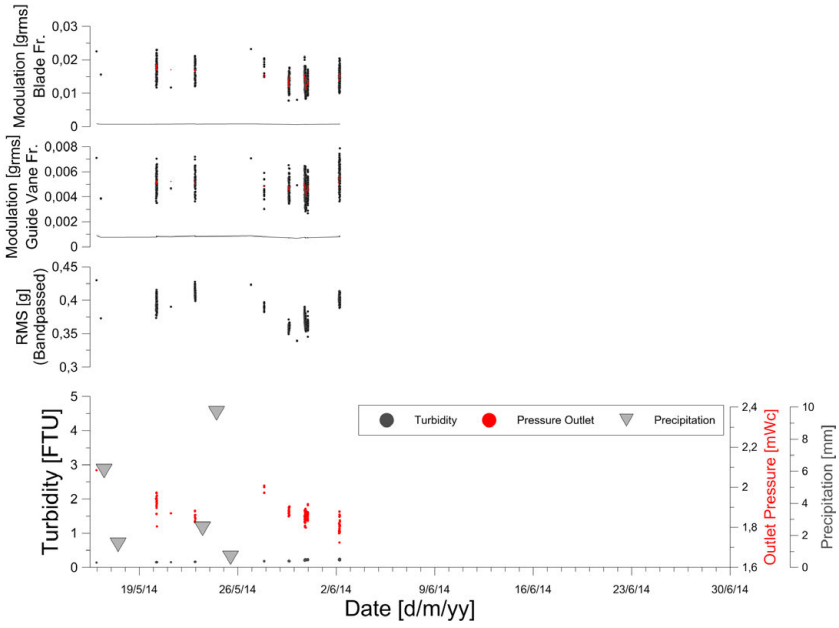

(a)

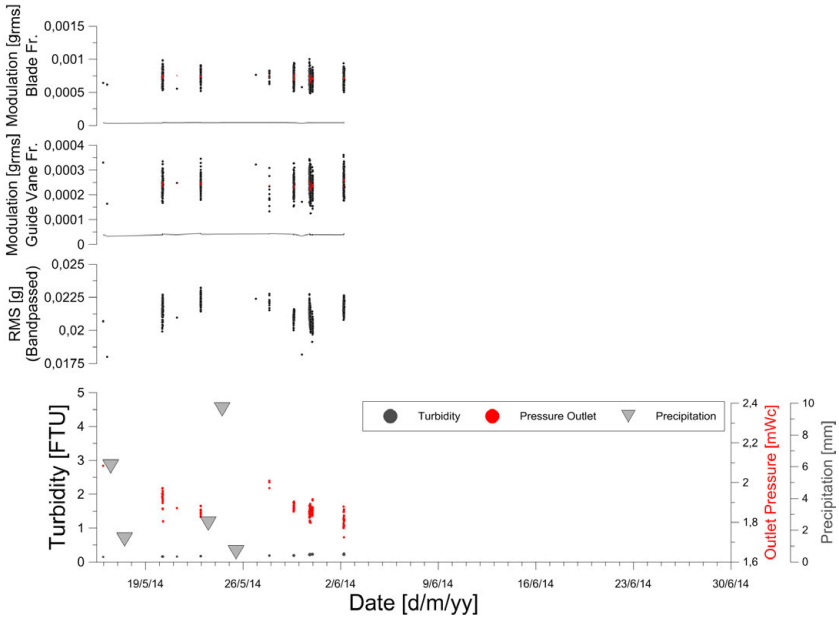

(b)

Figure C.9: *C.9(a): R1* 67% *to* 68% *GVO - GVS; C.9(b): R1* 67% *to* 68% *GVO - AE*

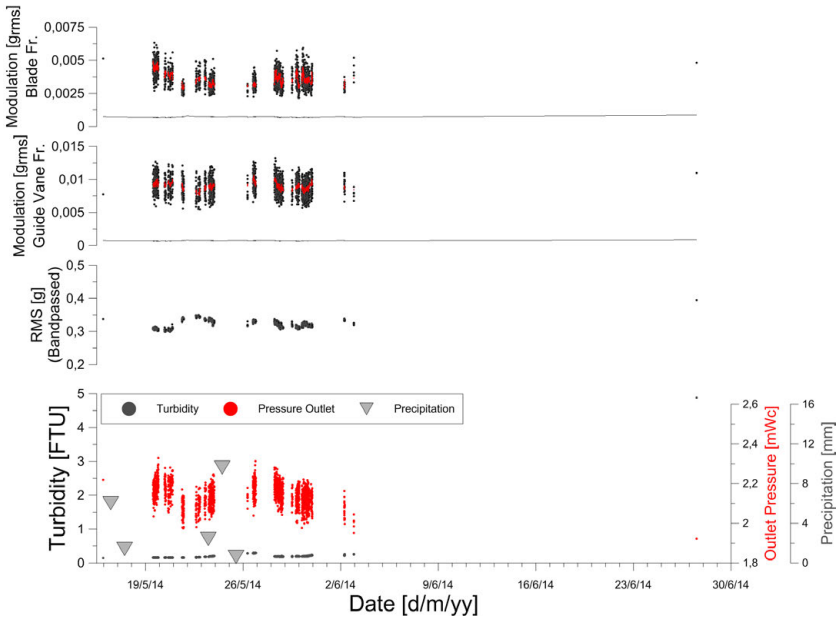

(a)

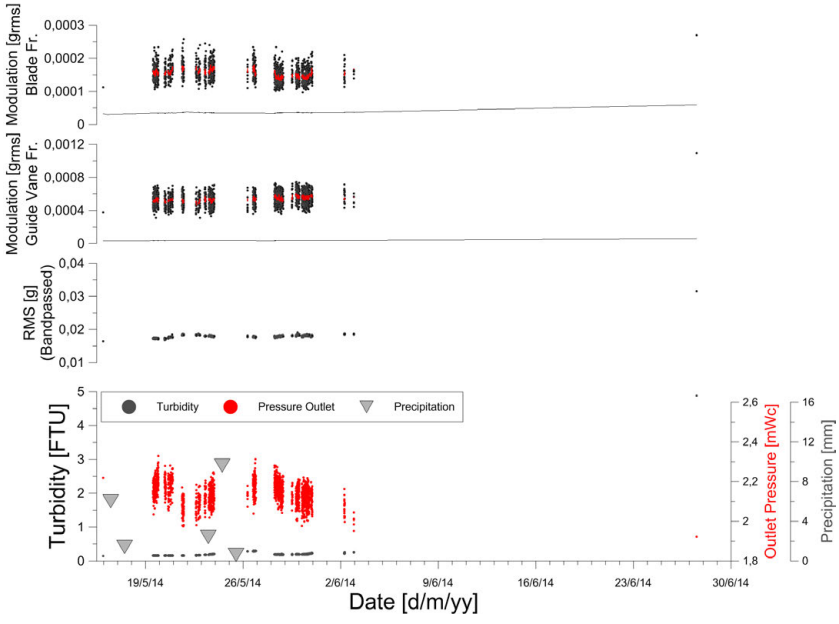

(b)

Figure C.10: *C.10(a): R1* 76% *to* 77% *GVO - GVS; C.10(b): R1* 76% *to* 77% *GVO - AE*

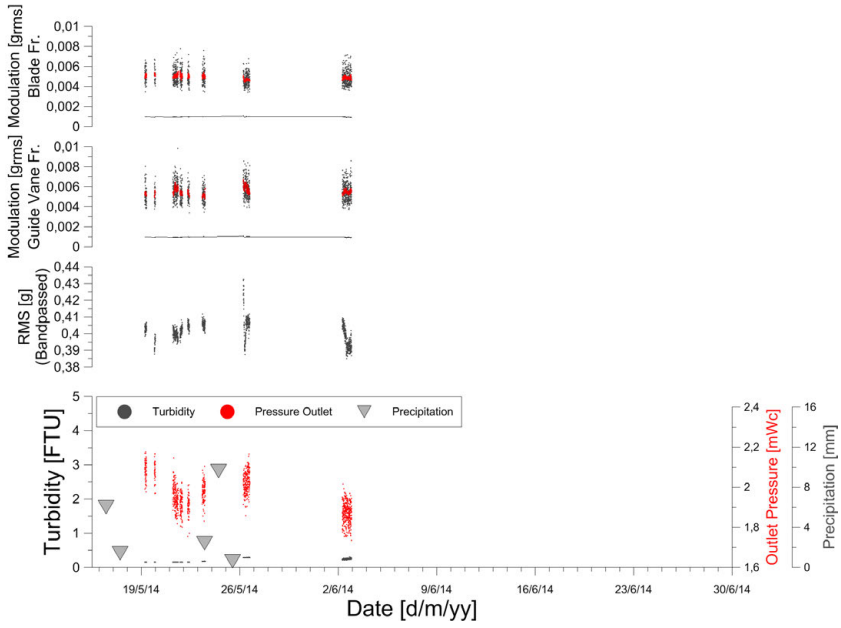

(a)

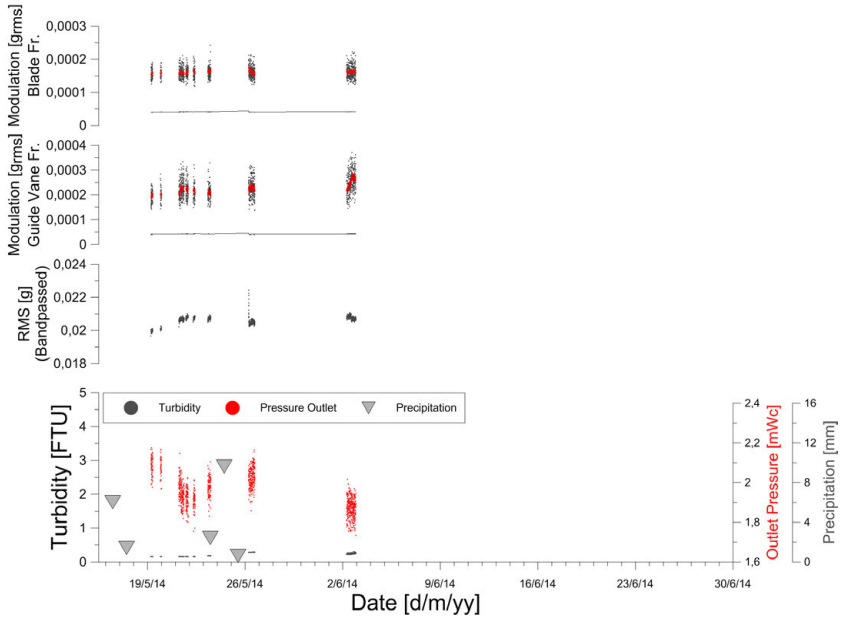

(b)

Figure C.11: *C.11(a): R1* 83% *to* 84% *GVO - GVS; C.11(b): R1* 83% *to* 84% *GVO - AE*